Functional Analysis of *INDETERMINATE DOMAIN 1* and *2* in Gibberellin Signaling in

Arabidopsis thaliana

by

Yuanjie Jin

Department of Biology
Duke University

Date:_____

Approved:

_____
Tai-Ping Sun, Supervisor

_____
Meng Chen

_____
David Sherwood

_____
Zhen-Ming Pei

_____
Gregory Crawford

Dissertation submitted in partial fulfillment of
the requirements for the degree of Doctor
of Philosophy in the Department of
Biology in the Graduate School
of Duke University

2015

ABSTRACT

Functional Analysis of *INDETERMINATE DOMAIN 1* and *2* in Gibberellin Signaling in *Arabidopsis thaliana*

by

Yuanjie Jin

Department of Biology
Duke University

Date:_____

Approved:

_____
Tai-Ping Sun, Supervisor

_____
Meng Chen

_____
David Sherwood

_____
Zhen-Ming Pei

_____
Gregory Crawford

An abstract of a dissertation submitted in partial fulfillment of the requirements for the degree of Doctor of Philosophy in the Department of Biology in the Graduate School of Duke University

2015

Abstract

Bioactive gibberellins (GAs) are phytohormones with various effects on plant development, from seed germination through fruit development. The signaling pathway of GA is centered on DELLA proteins (DELLAs), a group of growth repressors degraded upon perception of GA. Previous studies demonstrated that DELLAs administrate global regulation of gene expression. However, given that DELLAs do not contain any canonical DNA-binding domain and that DELLAs only have a moderate association to their target promoters, the nuclear-localized DELLAs are believed to interact with transcription factors for function. Indeed, quite a few transcription factors have been identified as DELLA interactors in the plant model *Arabidopsis thaliana*, some of which are well-known downstream transcription regulators involved in other signaling pathways. Nevertheless, the molecular mechanisms how DELLAs inhibit so many aspects of plant growth cannot be fully explained by the known DELLA interactors.

Recently, our lab discovered that INDETERMINATE DOMAIN 1 (IDD1), a C2H2 zinc-finger protein in *Arabidopsis*, and its closest homolog IDD2, have a strong physical interaction with DELLAs, revealing the potential involvement of these two *IDD* genes in GA signaling. Hence, the objectives of my doctoral research are (1) to evaluate the roles of IDD1 and IDD2 in GA-responsive phenotypes, (2) to investigate the genetic interaction between IDD1, IDD2 and DELLAs and (3) to identify the function of IDD1

and IDD2 and the significance of IDD-DELLA interaction in transcriptional regulation of IDD/DELLA targets. First, we found that both IDDs redundantly promote GA-induced hypocotyl elongation, and that they also play a positive role in stem elongation and floral initiation. Secondly, epistasis analyses exhibit that REPRESSOR OF *ga1-3* (RGA) and GA INSENSITIVE (GAI), two DELLAs with a predominant role in vegetative growth, antagonize IDD1 and IDD2 in hypocotyl elongation, and that GAI also opposes IDD2 in stem elongation and floral initiation. These results entail an antagonistic relationship between IDDs and DELLAs via protein-protein interaction. We then showed that IDD1 and IDD2 repress the expression of canonical DELLA direct targets, including *GA20ox2*, *GA3ox1*, *GID1b* and *SCL3*. IDD1 also inhibits transcription of *CAPRICE* (*CPC*) and *GLABRA2* (*GL2*), two crucial regulators of root epidermal cell patterning. Taking into account that IDD1 and RGA associate with the same region in *CPC* promoter, we conclude that *CPC* is a direct target of the IDD1/RGA complex. In addition, transient expression assays suggested that IDD1 and RGA counteract each other's effects on expression of *GA20ox2*, *GID1b*, *SCL3*, *CPC* and *GL2*, providing evidence that IDDs and DELLAs function antagonistically in transcriptional regulation of downstream genes in general. Although both IDDs bear a putative repression motif GLGLGL in their C termini, mutation of this motif did not affect the repressive activity of IDD1 in our transient expression system. On the other hand, fusion of the viral protein 16 (VP16) transcriptional activation domain to IDD1 seems to override the

original repressive activity of IDD1. Together, these results uncover a new branch of GA signaling pathway through IDD1 and IDD2, shed light on the interplay of the two IDDs and DELLAs in GA feedback regulation and give insights into the molecular mechanism underlying IDD-mediated GA repression of root hair development.

Contents

Abstract iv

List of Tables x

List of Figures xi

Abbreviations xiii

Acknowledgements xviii

Chapter 1 INTRODUCTION 1

1.1 Gibberellin function and significance 1

1.2 Gibberellin metabolism in plants 4

1.3 Gibberellin signaling and the role of DELLA proteins 8

1.4 DELLA-interacting proteins as part of a transcriptional network 16

Chapter 2 IDD1 and IDD2 (IDDs) antagonize DELLA's repression in GA-controlled phenotypes 22

2.1 Introduction 22

2.2 Materials and Methods 27

2.2.1 Plant materials. 27

2.2.2 Plasmid constructs and transgenic plants. 27

2.2.3 Plant growth conditions. 30

2.2.4 Hypocotyl elongation assay. 31

2.2.5 Immunoblotting. 31

2.2.6 Quantitative real-time PCR (qRT-PCR) analysis. 32

2.3 Results 34

2.3.1 IDD1 and IDD2 positively regulate GA-controlled hypocotyl elongation. 34

2.3.2 DELLAs counteract the effects of IDD1 and IDD2 in hypocotyl growth. 42

2.3.3 IDD1 and IDD2 play positive roles in flowering and stem elongation. 47

2.3.4 IDD2 antagonizes the role of GAI in flowering and stem growth. 54

2.4 Discussion 58

Chapter 3 IDD1 and IDD2 function antagonistically with DELLAs in transcriptional regulation of DELLA target genes 63

3.1 Introduction 63

3.1.1 Canonical DELLA targets and the potential role of IDD1 and IDD2 in transcriptional regulation of these genes. 63

3.1.2 Signaling network underlying root epidermal cell patterning and the role of IDD1 and IDD2 in GA-regulated root-hair development 69

3.2 Materials and Methods 74

3.2.1 Plant materials 74

3.2.2 Plant tissue growth and RNA analysis 74

3.2.3 Plasmid constructs for transient expression assays 75

3.2.3.1 Effector constructs for tobacco and *Arabidopsis* transient expression 75

3.2.3.2 Reporter constructs for tobacco and *Arabidopsis* transient expression 78

3.2.4 Transient expression assays in *Nicotiana benthamiana* by Agro-Infiltration 80

3.2.5 Transient expression assays in *Arabidopsis* Seedlings 81

3.2.6 Immunoblotting 82

3.3 Results 83

3.3.1 IDDs and DELLAs act antagonistically on transcriptional regulation of several GA pathway feedback genes 83

3.3.2 The inhibitory effect of IDD1 and IDD2 is not conferred by the putative repression motif GLGLGL 91

3.3.3 IDD1 and IDD2 antagonize DELLA activity in transcriptional regulation of CPC and GL2 97

3.4 Discussion 102

Chapter 4 Conclusions and Implications 107

4.1 IDD1 and IDD2 antagonize DELLA function in GA-responsive phenotypes and transcriptional regulation of DELLA targets 107

4.2 Insights into DELLA function and GA feedback 108

4.3 Mechanisms of repressive activity in IDD1 and IDD2 108

4.4 Potential future directions 109

4.5 Some inconsistencies with published studies 110

References 129

Biography 142

List of Tables

Table 3.1: Frequency of binding sites of known IDD homologs in promoters of promising AtIDD1 and AtIDD2 targets.....68

Table 3.2: Primers and restriction enzymes invovled in cloing of reporter constructs for transient expression.....79

List of Figures

Figure 1.1 Structures of bioactive GAs and GA-deficient phenotypes in *Arabidospsis*. 3

Figure 1.2 General GA biosynthetic pathway and feedback regulation in plants. 6

Figure 1.3 The domain structure of DELLAs. 11

Figure 1.4 Current model of early GA signaling pathway 15

Figure 2.1 The phylogenetic tree and domain analysis for AtIDD family genes. 26

Figure 2.2 Locations of T-DNA insertions in *idd1-1* and *idd2-1* and the wild-type transcript level of IDD2 in *idd2-1*. 37

Figure 2.3 The hypocotyl elongation assay of *idd1-1* and *idd2-1* single and double mutants. 38

Figure 2.4 *pIDD1:IDD1-cMyc* transgene complements defects of *idd1-1 idd2-1* in GA-responsive hypocotyl elongation in an IDD1-dose dependent manner. 39

Figure 2.5 IDD1 overexpressors enhance hypocotyl GA response in an IDD1-dose dependent manner. 40

Figure 2.6 IDD2 overexpressors enhance hypocotyl GA response in an IDD2-dose dependent manner 41

Figure 2.7 *rga-28* failed to rescue the defects of *idd1-1 idd2-1* in hypocotyl GA-dose response in Col-0. 44

Figure 2.8 *rga-28* failed to rescue the defects of *idd1-1 idd2-1* in hypocotyl GA-dose response in *ga1-3* background. 45

Figure 2.9 *rga-29 gai-t6* partly rescue the defects of *idd1-1 idd2-1* in hypocotyl GA-dose response. 46

Figure 2.10 IDD1 overexpression causes an earlier flowering time in Col-0. 49

Figure 2.11 *35S:cMyc-IDD1 #1* has a lower transgenic IDD1 protein level than *pIDD1:IDD1-cMyc/idds* 50

Figure 2.12 IDD2 overexpression causes an earlier flowering time in L*er* developmentally but not chronlogicallhy. 51

Figure 2.13 IDD1 overexpression promotes stem elongation in Col-0. 52

Figure 2.14 IDD2 overexpression promotes stem elongation in L*er*. 53

Figure 2.15 *35S:HA-IDD2_L* partially rescues the late-flowering phenotype in *gai-1* mutant 56

Figure 2.16 *35S:HA-IDD2_L* partially rescues the dwarf phenotype of *gai-1* mutant. 57

Figure 3.1 Current model of intercellular signaling network controlling the root epidermal cell patterning in *Arabidopsis*. 72

Figure 3.2 PAC treatment caused a mosaic pattern of *pGL2:GUS* expression (Zhong-Lin Zhang, unpublished data) 73

Figure 3.3 Relative mRNA levels of DELLA targets in 9-day-old seedlings in the Col-0 background. 87

Figure 3.4 Relative mRNA levels of DELLA targets in 8-day-old seedlings in the *ga1-3* background. 88

Figure 3.5 IDD1 and RGA antagonize each other in regulation of canonical DELLA targets from tobacco transient expression studies 89

Figure 3.6 Putative repression motifs in IDD1 and IDD2, and the mutations introduced in IDD1-m 94

Figure 3.7 The effects of IDD1, IDD1-m, IDD1-VP16 and IDD3 with or without RGA on SCL3 promoter activity in tobacco and *Arabidopsis* transient expression assays. 95

Figure 3.8 The protein levels of IDD3 and IDD1-VP16 are much lower than those of IDD1 and IDD1-m in tobacco transient expression assays 96

Figure 3.9 The effects of IDD1 and RGA on the expression of GL2 and CPC in the presence of WER and GL3. 101

Figure 4.1 A proposed model for antagonistic interaction between IDD1, IDD2 and DELLA in regulation of GA responses and GA feedback 111

Abbreviations

aa	amino acid
ABA	abscisic acid
ABRC	Arabidopsis Biological Resource Center
AGROBEST	*Agrobacterium*-mediated enhanced seedling transformation
ALC	ALCATRAZ
ARF6	Auxin Response Factor 6
At	*Arabidopsis thaliana*
A. thaliana	*Arabidopsis thaliana*
bHLH	basic helix–loop–helix
BLAST	Basic Local Alignment Search Tool
BME	β-mercaptoethanol
BOI	BOTRYTIS SUSCEPTIBLE1 INTERACTOR
BR	brassinosteroid
BRG1	BOI-RELATED GENE1
BZR1	BRASSINAZOLE-RESISTANT1
CaMV	Cauliflower Mosaic Virus
cDNA	Complementary Deoxyribonucleic Acid
ChIP	chromatin immunoprecipitation
coIP	coimmunoprecipitation

Col-0	Columbia-0
CPC	CAPRICE
CPS	ent-copalyl diphosphate synthase
CRC	chromatin-remodeling complexes
DLRA	dual-luciferase reporter assay
DNA	Deoxyribonucleaic Acid
E. coli	*Esherichia coli*
EGL3	ENHANCER OF GLABRA3
EHD1	EARLY HEADING DATE 1
EIN3	ETHYLENE INSENSITIVE 3
fLUC	firefly luciferase
GA	gibberellin
GAI	GA INSENSITIVE
GA2ox	GA 2-oxidase
GA3ox	GA 3-oxidase
GA20ox	GA 20-oxidase
GFP	green fluorescent protein
GGDP	geranylgeranyl diphosphate
GID1	GA INSENSITIVE DWARF 1
GL3	GLABRA3

GRAS	GAI, RGA and SCARECROW
HLS1	HOOKLESS 1
HRP	horseradish-peroxidase
H cell	hair cell
ID1	INDETERMINATE 1
IDD1	INDETERMINATE DOMAIN 1
JA	jasmonate
JAZ	JA ZIM-domain
KAO	*ent*-kaurenoic acid oxidase
KO	*ent*-kaurene oxidase
KS	*ent*-kaurene synthase
LD	long day
L*er*	Landsberg *erecta*
Luc	Luciferase
LPA1	Loose Plant Architecture1
mRNA	Messenger Ribonucleic Acid
MS	Murashige and Skoog
N. benthamiana	*Nicotiana benthamiana*
N cell	non-hair cell
OD	Optical Density

Os	*Oryza sativa*
Oligo	Oligonucleotide
PAC	paclobutrazol
PBS	Phosphate Buffered Saline
PCR	Polymerase Chain Reaction
pEG203	*pEarleyGate 203*
PIF3	PHYTOCHROME INTERACTING FACTOR 3
PIL5	PIF3-*like* 5
PRE1	PACLOBUTRAZOL RESISTANCE 1
qPCR	quantitative PCR
qRT-PCR	quantitative real-time PCR
rLUC	Renilla luciferase
RGA	REPRESSOR OF *ga1-3*
RGL1	RGA-LIKE1
RT-PCR	reverse transcription-PCR
SCF	SKP1-CULLIN-F-BOX
SCL3	SCARECROW-LIKE 3
SD	short day
SDS	Sodium Dodecyl Sulfate
SDS-PAGE	Sodium Dodecyl Sulfate Polyacrylamide Gel Electrophoresis

SE	standard error
SLY1	SLEEPY1
SPL	SQUAMOSA PROMOTER BINDING-LIKE
SPT	SPATULA
SWI/SNF	Switch/Sucrose Nonfermenting
T-DNA	transfer DNA
TTG	TRANSPARENT TESTA GLABRA
VP16	viral protein 16
WER	WEREWOLF
WT	wild type
Y2H	yeast two-hybrid
Zm	*Zea mays*

Acknowledgements

I would like to thank my thesis advisor Dr. Tai-Ping Sun. She is a great scientist as well as a nice person. She gave me the opportunity to work in her lab, provided me with her guidance and helped me through my research and writings. Thanks to her support and patience, I have grown a lot since I joined the lab, both scientifically and mentally. I also owe my thanks to my thesis committee members, Dr. Meng Chen, Dr. David Sherwood, Dr. Zhen-Ming Pei, Dr. Gregory Crawford and ex-committee member Dr. Xinnian Dong. During the past few years, they supported me whole-heartedly and offered numerous suggestions and critiques. I really appreciate their time and input to my thesis project.

I am grateful to all Sun lab members. Dr. Zhong-Lin Zhang has collaborated with me on part of my project. He is a kind-hearted guy and taught me a lot, from scientific theories to experimental techniques. Meanwhile, he generously shared his material, experience and unpublished results with me. Dr. Rodolfo Zentella is a great researcher and he joined Zhong-Lin and me in part of our study. Rodolfo is experienced in protein biochemistry and offered precious advice on that to me. He also has a good sense of humor and is ready to help whenever something went wrong. Dr. Xin Zhou, Dr. Jianhong Hu, Dr. Jonathan Dayan, Dr. Jeongmoo Park, Dr. Wen-Ping Hsieh and Ning Sui all helped me with material and experiments. We have been good friends

throughout my graduate career. Thank you all for participating in the discussions and maintaining a productive and joyful environment. In addition, I am thankful to people from Pei lab, Chen lab, Dong lab and Benfey lab for their sharing of seeds, facilities and experience.

I am fortunate to be enrolled in Duke Biology, a prestigious PhD program in the US. Anne, our administrative coordinator for graduate studies, is a great lady who is responsible, thoughtful and helpful and cares about us students. Interactions and activities with professors, staff and my fellow students make me feel at home, even though I am an international student. Being a teaching assistant for a few years, I have greatly improved my speaking English, teaching, management skills and most importantly, confidence. All these will be great memories in my life.

Last but not least, I cannot thank enough to my wife Junfei and my family back in China. Without their support and encouragement, I would not have had the courage and persistence to complete my long and tough PhD study. The past seven years of study is over, but a new expedition is just beginning. With invaluable experience and abilities gained from graduate school, I am confident to confront with any challenge through every stage in the rest of my life.

Chapter 1 INTRODUCTION

1.1 Gibberellin function and significance

Plants are sessile organisms that cannot move in response to environmental changes. Rather, they adapt their shape, growth and reproduction to the environment they live. This "plasticity" is largely achieved through modulation of their endogenous growth regulators, or plant hormones (Davies, 2004). In analogy with animal hormones, plant hormones are chemicals that take effect at a small amount. On the other hand, plant hormones differ from animal hormones in that plant hormones can be produced in many tissues instead of a small group of cells or glands, and they can function both within the cell producing them and be transported and work in other tissues. So far, there are eight major types of plant hormones that have been extensively studied: auxin, cytokinin, Gibberellins (GAs), abscisic acid (ABA), ethylene, brassinosteroids (BRs), jasmonates (JAs) and strigolactones.

Among known plant hormones, GAs are a large group of structurally similar diterpenoid compounds derived from the *ent*-gibberellane skeleton. The discovery of GAs dates back to the 1930s, when Japanese scientists discovered that *Gibberella fujikuroi*, the pathogenic fungus causing *bakanae* (foolish seedling) disease, produces a high amount of GA_3 such that the infected plant becomes extremely tall and sterile (Yabuta and Sumiki, 1938). Later it was found that GAs are actually endogenous plant growth regulators. 136 total different GAs have been identified in plants, bacteria and fungi;

however, only a few of them including GA_1, GA_3, GA_4 and GA_7 are biologically active, whereas other GAs are mostly biosynthetic intermediates or inactive forms (Hedden and Phillips, 2000). The bioactive GAs are involved in many physiological processes throughout plant life cycle, including, but not limited to, seed germination, stem and root elongation, leaf expansion, flower initiation, and flower and fruit development (Sun, 2008). In seedlings in particular, GA can strongly promote the elongation of embryonic stem, or hypocotyl (Alabadi et al., 2004). The majority of hypocotyl cells are formed in the embryo, and the increase in hypocotyl length during postgerminative growth is primarily through cell elongation rather than cell division (Gendreau et al., 1997). This unique feature and its simple morphology makes hypocotyl a convenient model commonly used in studying GA responsive cell elongation (Vandenbussche et al., 2005).

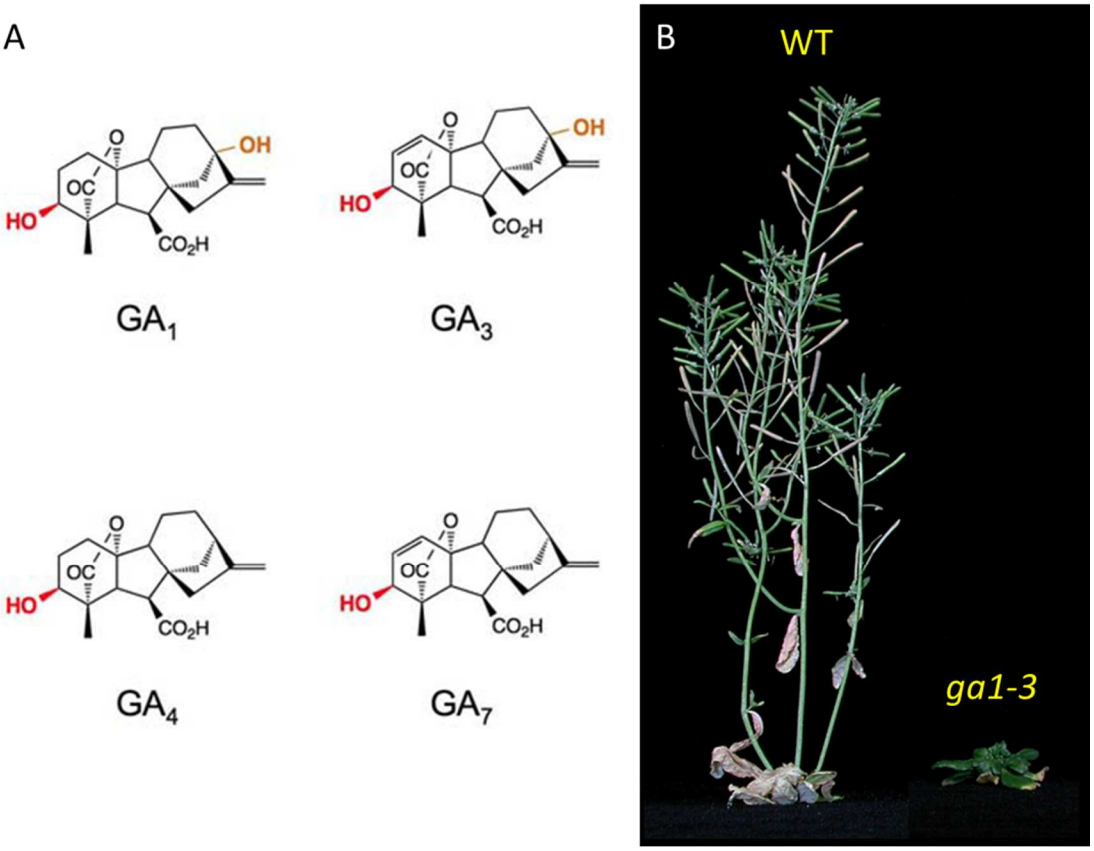

Figure 1.1 Structures of bioactive GAs and GA-deficient phenotypes in *Arabidospsis*.

A. Schematic structures of bioactive GAs GA_1, GA_3, GA_4 and GA_7. Among these bioactive GAs, GA_4 is the primary bioactive form in *Arabidopsis thaliana*, whereas GA_3 is produced from the fungus *Gibberella fujikuroi* for commercial use. Diagram modified from Sun, 2008.

B. Comparison of phenotypes between *Arabidopsis* wild-type (WT) and severely GA-deficient mutant *ga1-3*. These plants are in the Landsberg *erecta* (L*er*) ecotype background. The *ga1-3* mutant was treated with GA only for germination and left without further treatment. Compared with WT, *ga1-3* mutant is extremely dwarf, with a compact and dark green rosette.

GA plays a prominent role in agriculture. A majority of seedless grapes on the market have been treated with GA to promote their growth, which exemplifies wide commercial applications of GA (Silverstone and Sun, 2000). During the "Green Revolution" in 1960s and 1970s, many dwarf, lodging-resistant and high-yielding breeds were adopted for cereal crops including wheat, maize and barley (Conway, 1997; Peng et al., 1999; Silverstone and Sun, 2000). The traits of these new crop varieties reminiscent of partially GA-deficient phenotypes, turn out to be largely attributed to semi-dominant mutations in their corresponding DELLA genes, the key repressor of GA signaling (Hedden, 2003; Peng et al., 1999). Therefore, a better understanding of fundamental mechanisms underlying GA function is important for further improvements in crop yield and fruit quality via genetic modifications (Hedden, 2003).

1.2 Gibberellin metabolism in plants

During the past decades, there has been great advances in our understanding of GA metabolism in higher plants (Yamaguchi, 2008). GAs are synthesized from the linear molecule, geranylgeranyl diphosphate (GGDP). After two initial cyclization steps catalyzed by *ent*-copalyl diphosphate synthase (CPS) and *ent*-kaurene synthase (KS), GGDP is converted to *ent*-kaurene, which is then successively oxidized by two cytochrome P450 monooxygenases: *ent*-kaurene oxidase (KO) and *ent*-kaurenoic acid oxidase (KAO). A couple of further oxidations carried out by GA 20-oxidase (GA20ox) and GA 3-oxidase (GA3ox) finally lead to the generation of bioactive GAs, such as GA_1

and GA_4. Because bioactive GAs are very potent, plants also have catabolic pathways to deactivate them, an important example being 2β-hydroxylation of bioactive GAs catalyzed by GA 2-oxidases (GA2ox).

To maintain endogenous GA homeostasis, the expression of several genes encoding GA biosynthetic enzymes and catabolic enzymes is tightly regulated, through a GA signaling-mediated feedback and feedforward mechanism, respectively (Hedden and Phillips, 2000; Olszewski et al., 2002; Yamaguchi, 2008). For instance, in *Arabidopsis*, when GA content is low, the transcription of multiple *GA20ox* genes (*GA20ox1*, *GA20ox2*, *GA20ox3*) and a single *GA3ox1* gene are elevated, whereas upon GA treatment, their transcripts rapidly decrease (Hedden and Thomas, 2012). In contrast, several GA2ox genes are transcriptionally upregulated after treatment of exogenous GA (Hedden and Thomas, 2012).

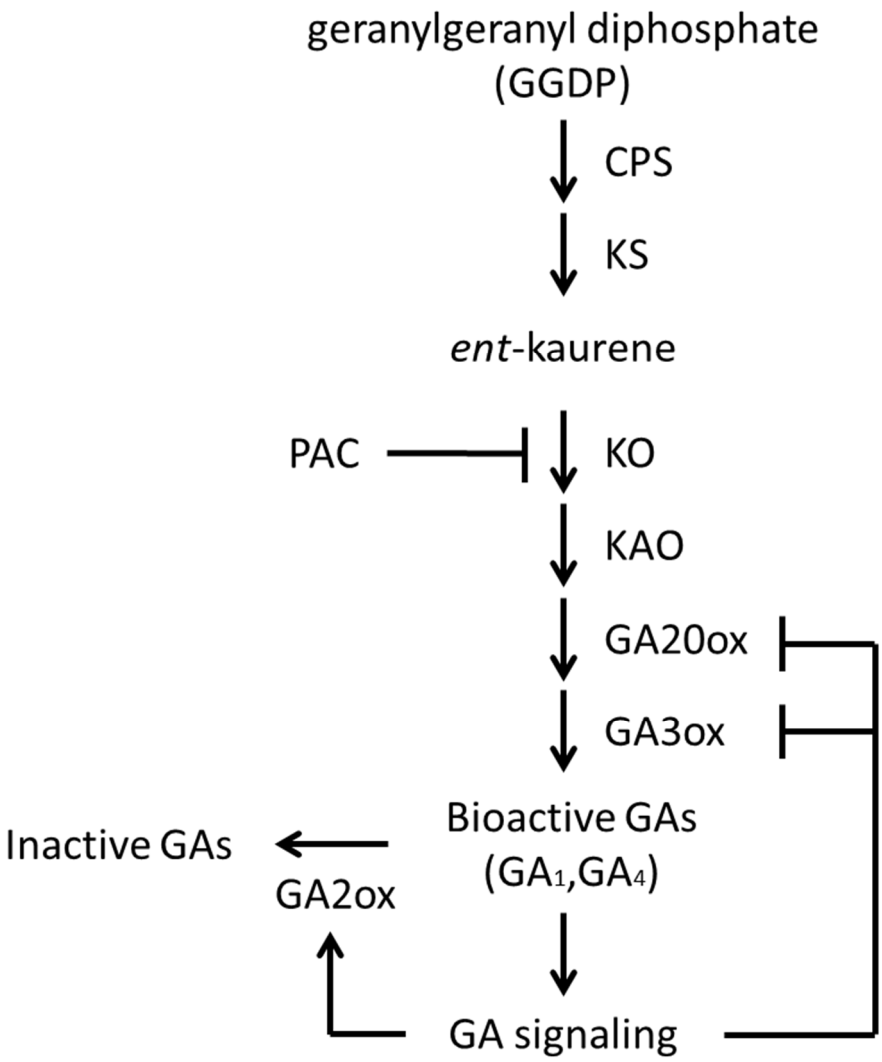

Figure 1.2 General GA biosynthetic pathway and feedback regulation in plants.

The GA precursor GGDP is first converted to *ent*-kaurene in steps catalyzed by enzymes CPS and KS. After a series of oxidation reactions carried out in order by enzymes KO, KAO, GA20ox and GA3ox, *ent*-kaurene is converted to bioactive GAs (e.g., GA1, GA4). Bioactive GAs can be inactivated by GA2ox. The bioactive-GA-triggered GA signaling in turn causes down-regulation of GA20ox and GA3ox and up-regulation of GA2ox, a mechanism that helps maintain GA homeostasis. The chemical PAC inhibits GA biosynthesis at the indicated step.

In addition to feedback and feedforward regulation, expression of GA metabolism genes is also subject to change under different environmental conditions. In *Arabidopsis* seedling hypocotyls, the transcripts of *GA20ox* and *GA3ox* genes accumulate more in the dark than in the light, while the transcripts of *GA2ox* genes display an opposite pattern, presumably contributing to differential GA levels and hypocotyl growth between dark and light (Achard et al., 2007b; Alabadi et al., 2004; Reid et al., 2002; Zhao et al., 2007).

In studies of GA biology, GA biosynthesis genes have been targets of genetic and pharmacological approaches to manipulate endogenous GA levels. One good example in genetics is the deletion mutant of CPS (encoded by the single gene *GA1* in *Arabidopsis*), *ga1-3*, which almost produces no GA and thus serves as a stable severely GA-deficient background (Sun et al., 1992). The extreme drawfism, dark green compact rosette, male sterility, late flowering (under long-day conditions), inability of germinate without GA treatment in *ga1-3* precisely depict major aspects of GA actions in plants (Koornneef and van der Veen, 1980). Another way to inhibit GA biosynthesis is by treating plants with paclobutrazol (PAC), a chemical that inhibits the activity of the KO enzyme (Rademacher, 2000). Easy and fast, the use of PAC treatments can circumvent time-consuming genetic crosses and can be finely adjusted to achieve different degrees of GA deficiency.

1.3 Gibberellin signaling and the role of DELLA proteins

It is amazing that bioactive GAs exert such drastic effects on a variety of plant growth and developmental processes. As such, how GA signaling works at the molecular level has been a central question of interest. A series of groundbreaking genetic and biochemical studies in plant model species *Arabidopsis thaliana* and *Oryza sativa (*rice) led to the discovery of early pathway in GA signaling (Sun, 2010), which, in brief, involves three major players: the soluble GA receptor GA INSENSITIVE DWARF 1 (GID1) (Griffiths et al., 2006; Ueguchi-Tanaka et al., 2005), the master growth inhibitor DELLA (Peng et al., 1997; Silverstone et al., 1998), and the F-box protein SLEEPY1 (SLY1) in *Arabidopsis* (McGinnis et al., 2003) or GID2 in rice (Sasaki et al., 2003).

GID1 was initially identified in rice and has a high affinity in vitro only to bioactive GAs (Nakajima et al., 2006; Ueguchi-Tanaka et al., 2005). Although it is homologous to hormone sensitive lipases from animals, it misses one essential catalytic His residue at its C terminus and has no detectable lipase activity (Ueguchi-Tanaka et al., 2005). Localized to both cytoplasm and nucleus, GID1 is a soluble GA receptor (Ueguchi-Tanaka et al., 2005; Willige et al., 2007). *Arabidopsis* has three GID1 ortholog genes, namely *AtGID1a*, *AtGID1b* and *AtGID1c* (Griffiths et al., 2006; Nakajima et al., 2006). These *AtGID1* genes share partially redundant functions, since none of their single mutants shows discernable phenotype, but their triple mutant phenocopies severely GA-deficient mutants and is GA insensitive (Griffiths et al., 2006; Willige et al., 2007).

Like some GA biosynthetic genes, *AtGID1* genes are also subject to feedback regulation. When GA is abundant, transcript levels of *AtGID1a*, *AtGID1b* and *AtGID1c* are all reduced, to different extents, and vice versa (Griffiths et al., 2006; Zentella et al., 2007).

The nuclear-localized DELLA proteins (DELLAs) are considered as master growth repressors that inhibits all types of GA responses (Hauvermale et al., 2012). In *Arabidopsis*, there are five DELLA isoforms, REPRESSOR OF *ga1-3* (RGA) (Silverstone et al., 1998), GA INSENSITIVE (GAI) (Peng et al., 1997), RGA-LIKE1(RGL1), RGL2 and RGL3 (Lee et al., 2002). The name DELLA comes from the fact that all these proteins share a common DELLA domain at their N termini, a domain containing DELLA and VHYNP as conserved core motifs (Peng et al., 1997; Silverstone et al., 1998). DELLA domain is indispensable for GA response. *rga-Δ17* and *gai-1*, both semidominant DELLA mutants whose corresponding gene products miss 17 amino acids in N-terminal domain, exhibit dwarf and late-flowering phenotypes similar to GA-deficient mutants (Dill et al., 2001; Peng et al., 1997). However, with production of stabilized RGA and GAI mutant proteins, respectively, *rga-Δ17* and *gai-1* have almost no response to exogenous GA (Dill et al., 2001; Peng et al., 1997; Willige et al., 2007). In contrast, DELLA loss-of-function mutations *rga-24* and *gai-t6* can partially derepress the GA-dependent signaling in *ga1-3* and the *rga-24 gai-t6 ga1-3* triple mutant phenotypically mimic wild-type plants with overdose GA treatment (Dill and Sun, 2001; Peng et al., 1997; Silverstone et al., 1998). Genetic analyses also indicate that different DELLA isoforms exhibit redundant

but also distinct functions in GA signaling. Overall, RGA and GAI play a predominant role in repressing floral induction and many aspects of vegetative growth, such as root and stem elongation (Dill and Sun, 2001). RGL2 is the major DELLA that inhibits seed germination (Lee et al., 2002; Tyler et al., 2004), RGL1 and RGL2 together with RGA regulate floral development (Cheng et al., 2004; Tyler et al., 2004), and RGL3 is implicated in stress responses (Achard et al., 2008; Wild et al., 2012).

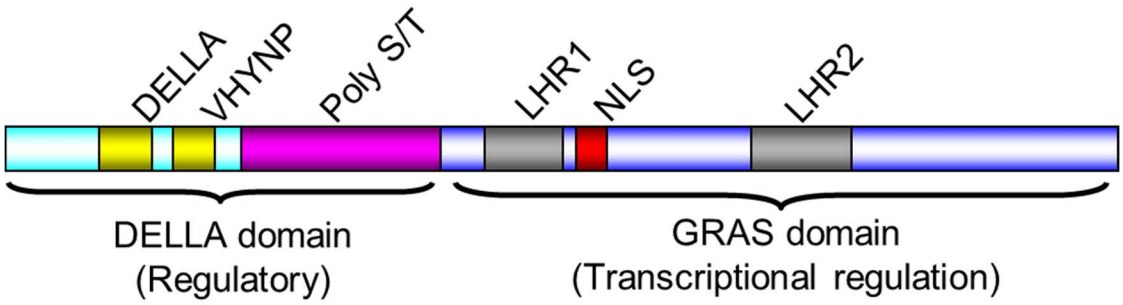

Figure 1.3 The domain structure of DELLAs.

DELLA proteins contain two common domains: the N-terminal DELLA domain and the C-terminal GRAS domain. DELLA domain has a regulatory role in GA signaling, whereas GRAS domain is important for transcriptional regulation. DELLA and VHYNP are two conserved motifs in DELLA domain, Poly S/T: serine/threonine rich region. LHR: leucine heptad repeat. NLS: nuclear localization signal.

.

The early GA signaling pathway is a process where GA triggers a rapid degradation of DELLA mediated through GID1 and SLY1 (or GID2 in rice) (Sun, 2010). As suggested by the crystal structure, the GA receptor GID1 contains a GA-binding pocket and a flexible N-terminal extension (Murase et al., 2008; Shimada et al., 2008). Upon binding to bioactive GAs, GID1 protein stabilizes its N-terminal extension which then functions as a lid to cover the GA-binding pocket (Murase et al., 2008). This conformational change enables GID1 to interact with DELLA N-terminal domain that comprises DELLA and VHYNP sequences (Griffiths et al., 2006; Ueguchi-Tanaka et al., 2007; Willige et al., 2007). The formation of GA-GID1-DELLA complex somehow facilitates the recognition of DELLAs by SLY1 (or GID2) as part of the SKP1-CULLIN-F-BOX (SCF) E3 ubiquitin ligase, which targets DELLA for polyubiquitination and subsequent degradation through the 26S proteasome pathway (Dill et al., 2004; Fu et al., 2004; McGinnis et al., 2003; Sasaki et al., 2003). Note that the DELLA domain is responsible for DELLA's interaction with GA-bound GID1, which explains why the DELLA domain deletion alleles *rga-Δ17* and *gai-1* produce stabilized GA-resistant DELLA mutant proteins (Dill et al., 2001; Willige et al., 2007).

Although the early GA signaling seems straightforward, the later stages downstream of DELLA still remain elusive today. An important question yet to address is, how DELLA inhibits so many processes of plant growth? Structural features have shed some light on the functions of DELLA. Sequence alignment of DELLAs suggests

that apart from N-terminal DELLA domains, DELLAs also share a high homology in their C-terminal GRAS (GAI, RGA and SCARECROW) domain (Lee et al., 2002; Peng et al., 1997; Pysh et al., 1999; Silverstone et al., 1998). The GRAS domain is exclusively identified among GRAS family transcription regulators in plants (Bolle, 2004; Pysh et al., 1999), implicating a potential role of DELLAs in transcription regulation. Consistent with this potential role, several microarray studies reveal that induction of DELLA activity causes global gene expression change in various tissues and a large fraction of GA-regulated genes are DELLA-dependent (Cao et al., 2006; Gallego-Bartolome et al., 2011; Hou et al., 2008; Zentella et al., 2007). Interestingly, among the most responsive and immediate DELLA target genes in shoots of *Arabidopsis* seedlings are GA biosynthetic genes *GA20ox2* and *GA3ox1*, and GA receptors *GID1a* and *GID1b*, suggesting that DELLA is involved in feedback regulation for GA homeostasis (Zentella et al., 2007). Despite their significant role in gene transcription regulation, DELLAs do not possess any canonical DNA-binding domain. Neither do DELLAs have a strong association with most of their target gene promoters based on chromatin immunoprecipitation (ChIP) (Zentella et al., 2007), indicative of a possibility that additional factors are necessary to mediate the association. Thus, instead of being a DNA-binding transcription factor, DELLAs affect downstream gene expression most likely through forming transcription complexes with transcription factors or

intermediate components. Indeed, a recent wave of discoveries of DELLA-interacting proteins seems to support this hypothesis (Daviere and Achard, 2013; Xu et al., 2014).

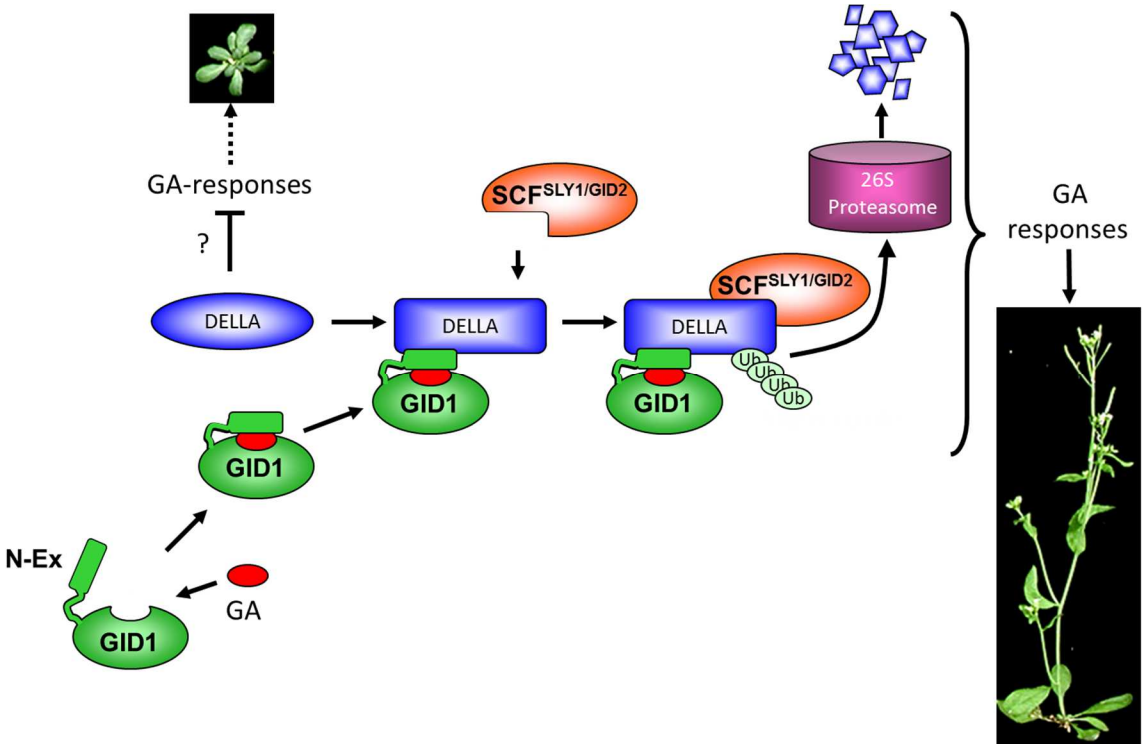

Figure 1.4 Current model of early GA signaling pathway.

Upon GA binding, the GA receptor GID1 has a conformational change such that its N-terminal extension is stabilized, which allows GID1 to interact with DELLAs. The GID1-DELLA interaction triggers the recognition and polyubiquitination of DELLAs by $SCF^{SLY1/GID2}$, leading to subsequent destruction of DELLAs via the 26S proteasome pathway and plant growth response to GA.

1.4 DELLA-interacting proteins as part of a transcriptional network

The two basic helix–loop–helix (bHLH) transcription factors, PHYTOCHROME INTERACTING FACTOR 3 and 4 (PIF3 and PIF4), are the earliest identified DELLA-interacting transcription factors (de Lucas et al., 2008; Feng et al., 2008). It is well established that PIF3 and PIF4 repress photomorphogenesis at seedling stage, e.g., promote hypocotyl growth, largely through inducing growth-related genes (de Lucas et al., 2008; Feng et al., 2008). By interacting with PIF3 and PIF4, DELLA sequesters the two transcription factors from their target gene promoters to inhibit their transactivity, resulting in a retarded growth of hypocotyls (de Lucas et al., 2008; Feng et al., 2008). Other than PIF3 and PIF4, yeast two-hybrid (Y2H) assay reveals that DELLA also interact with PIF3-*like* 5 (PIL5, or PIF1), SPATULA (SPT) and PIL2, three members from the same bHLH subfamily of PIF3 and PIF4 (Gallego-Bartolome et al., 2010). Interestingly, although SPT and DELLA have analogous roles in restraining the expansion of cotyledons, DELLA suppresses SPT protein levels possibly through their protein-protein interaction (Josse et al., 2011). ALCATRAZ (ALC), another bHLH protein required for separation layer differentiation in valve margin, is inactivated when interacting with DELLA, which provides a link between DELLA and fruit patterning (Arnaud et al., 2010).

DELLA interactors are not exclusive to bHLH proteins, though. A recent study identified interaction between DELLA and SWI3C, the core component of *Arabidopsis*

Switch (SWI)/Sucrose Nonfermenting (SNF)-type chromatin-remodeling complexes (CRCs), a finding that unravels a role of DELLA in epigenetic control of gene expression (Sarnowska et al., 2013). DELLA directly binds to the flowering-promoting transcription factor SQUAMOSA PROMOTER BINDING-LIKE (SPL), represses its transactivity and in turn delays floral transition (Yu et al., 2012). Through physically interacting with and presumably repressing ETHYLENE INSENSITIVE 3 (EIN3), a transcription factor activating *HOOKLESS 1* (*HLS1*) expression, DELLA negatively regulates *HLS1* transcription and HLS1-dependent apical hook development (An et al., 2012).

Some DELLA interactors are also DELLA target genes. The *Arabidopsis* RING domain protein *BOTRYTIS SUSCEPTIBLE1 INTERACTOR* (*BOI*) is one of DELLA early targets transcriptionally upregulated by DELLA (Zentella et al., 2007). *BOI* and its homologs *BOI-RELATED GENE1* (*BRG1*), *BRG2*, and *BRG3* (collectively referred to as BOIs) have been shown to associate with the same promoters of a subset of GA responsive genes as DELLA does, where BOIs and DELLA interact with each other and inhibit expression of these genes (Park et al., 2013). SCARECROW-LIKE 3 (SCL3), a GRAS family member and presumably transcription regulator, is another DELLA interactor and SCL3-DELLA interaction antagonizes each other's function in seedling growth and seed germination (Heo et al., 2010; Zhang et al., 2011) . Intriguingly, with a strong induction conferred by RGA on its transcription (Zentella et al., 2007; Zhang et al., 2011) and a relatively high enrichment of its promoter in ChIP using RGA (Zentella

et al., 2007), SCL3 is also considered as one of most convincing DELLA direct targets. The boosting of DELLA on transcription of its attenuator SCL3 serves as another example of DELLA-mediated feedback mechanism in GA signaling.

With more and more DELLA interactors identified, a question arises of what are the relations between different DELLA interactors. Several recent studies have started to address this question. For example, it has been shown that DELLA interacts with BRASSINAZOLE-RESISTANT1 (BZR1), a key transcription regulator in BR signaling, and Auxin Response Factor 6 (ARF6), a transcription factor controlling auxin-responsive genes, blocks their DNA-binding ability and consequently inhibits gene expression and hypocotyl elongation mediated by them (Bai et al., 2012b; Gallego-Bartolome et al., 2012; Li et al., 2012; Oh et al., 2014). Importantly, the three DELLA-interacting proteins BZR1, PIF4 and ARF6, interact with each other and synergistically control expression of a shared gene set underlying cell elongation in *Arabidopsis* hypocotyl (Oh et al., 2014; Oh et al., 2012). This DELLA-BZR1-PIF4-ARF6 regulatory module thereby illustrates a central molecular circuit that integrates GA, BR, auxin and light signals to coordinately administrate hypocotyl growth. Meanwhile, studies on crosstalk between GA and JA signaling identified another group of DELLA interactors which fall into JA ZIM-domain (JAZ) family, the central repressors of JA signaling. JAZ binds to the transcription factor MYC2 and inhibits its activation of JA-responsive genes. DELLA competes with MYC2 for interaction with multiple JAZ proteins, thus derepresses the transcriptional activity

of MYC2 (Hou et al., 2010; Yang et al., 2012). Further, MYC2 directly induces the transcription of RGL3, and the accumulation of RGL3 then renders more JAZ proteins inactive, which generates a positive feedback loop between DELLA and MYC2 (Wild et al., 2012). It was also discovered that JAZ proteins can interfere with the interaction between RGA and PIF3 (Yang et al., 2012). In spite of their antagonistic interaction in root and hypocotyl growth, flowering and resistance against necrotrophs (Hou et al., 2010; Wild et al., 2012; Yang et al., 2012), DELLA and JAZ collaborate in repression of trichome development (Qi et al., 2014). One mechanism underlying their synergy is that both of them repress the WD-repeat/bHLH/MYB transcription complex that is required for trichome initiation, through interacting with the major components of the complex (Qi et al., 2014). GA and JA can respectively induce degradation of DELLA and JAZ, thus releasing the WD-repeat/bHLH/MYB complex and coordinately promoting trichome formation (Qi et al., 2014). The context-dependent opposing and synergistic relationship between DELLA and JAZ illustrates the potential intricacy of the network involving DELLA and their interactors.

Although a number of DELLA interactors have been identified, the list is far from over. Recently, our lab isolated INDETERMINATE DOMAIN 1 (IDD1) as a new DELLA interactor through coimmunoprecipitation (coIP) in *Arabidopsis* (Zhong-Lin Zhang, unpublished data). The interaction between DELLAs and IDD1 or its closest homolog IDD2 has also been identified by yeast two-hybrid screens (Stephen Thomas,

unpublished data). As a homolog of INDETERMINATE 1 (ID1) in maize (Colasanti et al., 1998; Wong and Colasanti, 2007), IDD1 is a C2H2 zinc-finger protein which belongs to a large gene family consisting of 16 members in *Arabidopsis*. Several members in *Arabidopsis* IDD family emerge as important regulators in diverse processes of plant development. To name a few, AtIDD3 and AtIDD10 are involved in root cell patterning (Welch et al., 2007); AtIDD10 also regulates root hair formation (Hassan et al., 2010); AtIDD8 affects floral transition (Seo et al., 2011b); AtIDD14 plays a potential role in cold-responsive starch metabolism (Seo et al., 2011a); AtIDD14, AtIDD15 and AtIDD16 collectively control aerial organ morphogenesis and gravitropic responses (Cui et al., 2013; Morita et al., 2006). The functions of IDD homologs in rice have also been reported. OsID1, the rice homolog of ID1, upregulates transcription of EARLY HEADING DATE 1 (EHD1) and thus promotes transition from vegetative growth to floral development (Matsubara et al., 2008; Park et al., 2008; Wu et al., 2008). Loose Plant Architecture1 (LPA1), the rice ortholog of AtIDD15, acts to regulate plant architecture and influence shoot gravitropism (Wu et al., 2013). OsIDD10 is involved in ammonium uptake and assimilation in rice roots by directly activating expression of relevant genes (Xuan et al., 2013).

Coincidentally, a couple of recent studies have tied members of IDD family to GA pathway. AtIDD1 and AtIDD2 have been respectively shown to interact with DELLA and participate in DELLA-dependent GA feedback regulation, and their roles in

GA-controlled seed germination, hypocotyl elongation and flowering under short-day (SD) conditions were characterized (Feurtado et al., 2011; Fukazawa et al., 2014). Moreover, five other AtIDDs are found to physically bind to DELLA and the promoter of DELLA target SCL3, mediating DELLA's transactivation of SCL3 (Yoshida et al., 2014). On the other hand, SCL3 competes with DELLA for interacting with these IDDs to counteract the transcriptional activity of DELLA-IDD complexes (Yoshida et al., 2014). Together, these findings highlight IDD genes as a new class of DELLA-associated transcription factors. However, the roles of these DELLA-interacting IDDs in GA-related physiology are not fully understood, neither are their relationships with DELLA. In this study, I focus on the functional analysis of IDD1 and IDD2 in GA signaling in *Arabidopsis thaliana* (*A. thaliana*). Detailed characterizations of GA-regulated phenotypes in IDD1 and IDD2 mutants and their overexpression lines and analyses of their genetic interaction with DELLA are summarized in Chapter 2. The regulatory roles of IDD1 and IDD2 as transcription factors with or without DELLA are described and discussed in Chapter 3. Note that some parts are collaborative work, which are specified in the text. Finally, Chapter 4 contains the concluding remarks and a general discussion.

Chapter 2 IDD1 and IDD2 (IDDs) antagonize DELLA's repression in GA-controlled phenotypes

2.1 Introduction

As central negative regulators in GA signaling, DELLAs act to restrain many developmental processes during the whole plant life. For example, they inhibit seed germination and trichome initiation; they restrict hypocotyl and stem elongation; they impede flowering, especially under short-day (SD) conditions (Achard et al., 2007a; Alabadi et al., 2004; Blazquez et al., 1998; Lee et al., 2002; Penfield et al., 2006; Silverstone et al., 1998). Given that DELLAs do not possess a DNA-binding domain and the association between DELLAs and their target gene promoters is moderate (Zentella et al., 2007), current model of DELLA function proposes that DELLAs interact with other transcriptional regulators to control downstream gene expression. Up until now, there has been many DELLA interactors identified that support this model (Xu et al., 2014). However, like the tip of the iceberg, these verified interactions still do not account for all the developmental processes regulated by DELLAs. Thus, identifying and characterizing more DELLA interactors is necessary for a better understanding of mechanisms underlying DELLAs' function as a pivotal hub in integrating and coordinating various signaling activities to control plant growth.

The discovery of IDD1 as a novel DELLA interactor offers such an opportunity. In *Arabidopsis*, the IDD gene family contains 16 members that can be separated to two subfamilies based on their phylogenetic relationships (Figure 2.1; Miguel Moreno-

Risueno and Philip Benfey, unpublished data). Motif analysis by the MEME Suite (Bailey et al., 2009) shows that IDD proteins all share a conserved N-terminal domain that contains four zinc finger motifs (two are C2H2-type and the other two C2HC-type), whereas the C terminal of these proteins are more variable (Figure 2.1). Although several *IDD* family members have been characterized, the physiological and molecular roles of most *IDD* genes require further investigations. In this study, we mainly focus on IDD1, given the evidence that it can interact with all DELLAs (Zhong-Lin Zhang, unpublished data) and affects hypocotyl elongation and expression of GA feedback genes (Feurtado et al., 2011). Since IDD is a big gene family and *idd1* null mutant displays very subtle phenotypes (Figure 2.3), there likely exists functional redundancy among IDD members. We try to circumvent the genetic redundancy by also including IDD2 as our subject of study, because we speculate IDD1 and IDD2 may have similar functions for two reasons: 1) IDD2 is the closest paralog of IDD1 in *Arabidopsis* genome by BLAST search (http://blast.st-va.ncbi.nlm.nih.gov/Blast.cgi), with 85% identity in DNA sequence and 68% identity in protein sequence. Also, phylogenetic tree of IDD gene family suggests that IDD1 and IDD2 share the most recent common ancestor (Figure 2.1); 2) IDD2 was found to also interact with DELLAs by Y2H assay (Stephen Thomas and Zhong-Lin Zhang, unpublished data).

The interaction with DELLAs provides a link of IDD1 and IDD2 to GA signaling. As a first step in defining the roles of IDD1 and IDD2 in GA-related phenotypes, we

characterized mutants and overexpression lines for these two genes, in hypocotyl elongation, floral initiation and stem elongation. Hypocotyl is a common model in testing GA response, as its growth purely involves cell elongation (Gendreau et al., 1997), which is promoted by GA in a dose-dependent manner (Cowling and Harberd, 1999). Several DELLA interactors, including PIFs, SCL3, BZR1 and ARF6, have been characterized using this model (Bai et al., 2012b; de Lucas et al., 2008; Oh et al., 2014; Zhang et al., 2011). Flowering is also a well-known GA-dependent process. The GA deficient mutant *ga1-3* delays flowering under long-day (LD) conditions and does not flower at all under SD conditions (Wilson et al., 1992), a defect that can be fully rescued by knocking out RGA and GAI (Dill and Sun, 2001). Notably, ZmID1 and OsID1, IDD-related genes in maize and rice, respectively, and IDD8, an IDD family gene in *Arabidopsis*, all have been implicated in promoting floral transition(Colasanti et al., 1998; Matsubara et al., 2008; Seo et al., 2011b). It would then be interesting to see whether IDD1 and IDD2 also regulate flowering. As an important aspect of GA-stimulated growth, stem elongation is in the list of phenotypes to characterize because many GA signaling components that alter flowering time also affect stem elongation (Fleet and Sun, 2005)

If IDD1 and IDD2 are involved in GA signaling, then the next obvious question is, what is their relationship with DELLA? So far, the vast majority of DELLA-interacting transcription factors play opposite roles to DELLAs and are antagonized by DELLAs

(Xu et al., 2014). Would IDD1 and IDD2 serve as another example of DELLA-repressing transcription factors, or do they have an exceptional mode of function with DELLAs? We did epistasis analysis with combinations of their loss-of-function alleles or gain-of-function alleles to start to address these questions.

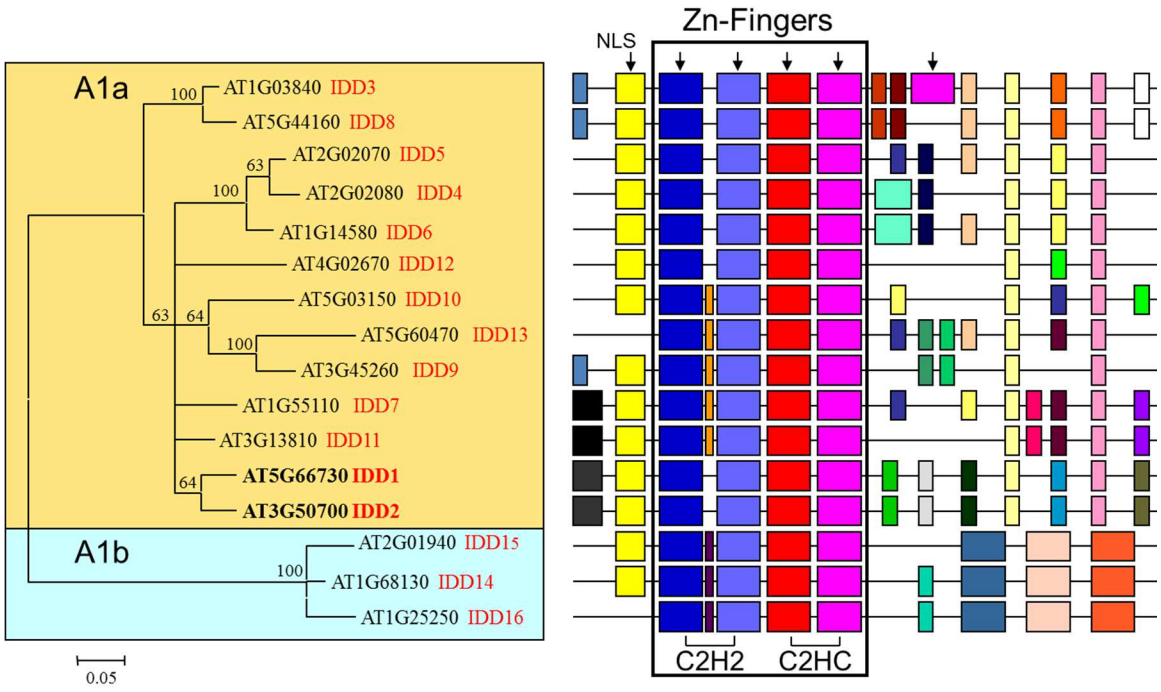

Figure 2.1 The phylogenetic tree and domain analysis for *AtIDD* family genes. The left panel shows the phylogenetic tree of *IDD* family genes in *Arabidopsis*. Based on the phylogenetic relations, IDD14-16 are clustered into a subgroup A1b, whereas the rest of IDDs are in the other subgroup A1a. IDD1 and IDD2 are closest IDD homologs in A1a group. The scale bar indicates 0.05 amino acid substitutions per site. The right panel shows the domains of corresponding left-side IDD proteins predicted by MEME (Bailey et al., 2009). All IDD proteins have four conserved Zinc-Finger motifs at N terminus. IDD1 and IDD2 also share a high homology in other putative domains. Diagram modified from Miguel Moreno-Risueno and Philip Benfey, unpublished.

2.2 Materials and Methods

2.2.1 Plant materials.

The mutants and transgenic lines for all experiments were derived from *Arabidopsis thaliana* ecotype Columbia-0 (Col-0) or Landsberg *erecta* (L*er*). The homozygous *idd1-1* and *idd2-1* transfer DNA (T-DNA) mutant lines in Col-0 genetic background was previously identified by PCR (Stephen Thomas, unpublished data). The *ga1-3* mutant in Col-0 was generated previously by crossing original *ga1-3* in L*er* to Col-0 six successive times (Tyler et al., 2004). The mutants *rga-28* in Col-0 and *gai-1* in L*er* have been previously described (Peng et al., 1997; Tyler et al., 2004). The *rga-29 gai-t6* double mutant in Col-0 (Oh et al., 2007) was the kind gift of Giltsu Choi (Korea Advanced Institute of Science and Technology). The homozygous mutants *idd1-1 idd2-1*, *rga-28 idd1-1 idd2-1*, *rga-29 gai-t6 idd1-1 idd2-1*, *ga1-3 idd1-1*, *ga1-3 idd2-1*, *ga1-3 idd1-1 idd2-1*, *ga1-3 rga-28 idd1-1*, *ga1-3 rga-28 idd2-1* and *ga1-3 rga-28 idd1-1 idd2-1*, all in Col-0 background, were obtained by genetic crosses and confirmed by PCR-based genotyping (Zhong-Lin Zhang, Yuanjie Jin and Stephen Thomas, unpublished data; see Appendix A for primer sequences).

2.2.2 Plasmid constructs and transgenic plants.

All the PCR amplifications were conducted with Phusion High-Fidelity DNA polymerase (New England Biolabs, Ipswich, MA) unless otherwise noted. The PCR-

amplified fragments in all constructs were checked by DNA sequencing to ensure that no mutations were introduced. Sequences of primers used are listed in Appendix A.

The plasmid *35S:cMyc-IDD1* [Cauliflower mosaic virus (CaMV) 35S promoter: cMyc-IDD1 open reading frame (ORF)] was made as follows (Zhong-Lin Zhang, unpublished data). A full-length coding region of *IDD1* cDNA was amplified by PCR from cDNA extracted from WT (Col-0) seedlings, using primers IDD1-CDS-5 and IDD1-CDS-3. The amplified DNA was first cloned into *pENTR/SD/D-TOPO* (Life Technologies, Grand Island, NY) and then transferred to the Gateway binary vector *pGWB418* (Nakagawa et al., 2007) by LR recombination (Life Technologies) to create an N-terminal fusion with 4-copy cMyc (4×cMyc) tag.

The plasmid *35S:HA-IDD2* was made with the following process (Rodolfo Zentella, unpublished data). The ORF of *IDD2* was PCR amplified with primers RIP2.23-BHI-F and RIP2.23-XbaI-R using the full-length cDNA clone U67269 obtained from the Arabidopsis Biological Resource Center (ABRC) as the template. The amplified DNA was first A-tailed with Choice Taq polymerase (Denville Scientific, Metuchen, NJ) and then cloned into *pCR2.1-TOPO* (Life Technologies, Grand Island, NY) by TA-cloning. The binary vector *p35S:HA-GFP* (with a *pCAMBIA1300* backbone) was digested with BamHI and XbaI restriction enzymes to remove the *GFP* gene and in its place the *IDD2* coding sequence was cloned, using the same restriction sites, to create an N-terminal fusion with HA tag.

The plasmid *pIDD1:IDD1-cMyc* was made as follows (Zhong-Lin Zhang, unpublished data). A 5.2-kb genomic DNA fragment carrying the full-length *IDD1* genomic coding sequence and its promoter region (2,711 bp) was amplified by PCR from genomic DNA extracted from WT (Col-0) seedlings, using primers IDD1-pro5-2 and IDD1-CDS-3-1. The amplified DNA fragment was first cloned into *pENTR/D-TOPO* (Life Technologies, Grand Island, NY) and then transferred to the Gateway binary vector *pGWB516* (Nakagawa et al., 2007) by LR recombination (Life Technologies) to create a C-terminal fusion with 4×cMyc tag.

All final constructs were transformed into *Agrobacterium tumefaciens* strain GV3101. *35S:cMyc-IDD1* was transferred to WT Col-0 plants by *Agrobacterium*-mediated transformation using the floral dip method (Clough and Bent, 1998), *35S:HA-IDD2* to both WT Col-0 and WT L*er* plants (referred to *35S:HA-IDD2_L* hereafter), and *pIDD1:IDD1-cMyc* to *idd1-1 idd2-1* double mutant in Col-0. Primary transformants (T1) were selected in media containing 1× Murashige and Skoog (MS) salts (Caisson Laboratories, North Logan, UT) 2% sucrose and 0.8% agar supplemented with the drug corresponding to the resistance marker of the plasmid transformed (50 μg/ml kanamycin for *35S:cMyc-IDD1*, 10 μg/ml BASTA for *35S:HA-IDD2* and *35S:HA-IDD2_L*, and 25 μg/ml hygromycin B for *pIDD1:IDD1-cMyc*). For each construction, transgenic lines with a 3:1 (resistant:sensitive) segregation ratio in their T2 generation were selected and at least two independent homozygous lines were identified in the T3 generation and

confirmed by immunoblot analysis. *gai-1 35S:HA-IDD2_L* lines was obtained by crossing *gai-1* to *35S:HA-IDD2_L*. The homozygosity of *gai-1* and *35S:HA-IDD2_L* is confirmed by PCR-based genotyping and BASTA resistance, respectively.

2.2.3 Plant growth conditions.

Plants were grown on MetroMix 200 soil (Scotts-Sierra Horticultural Products, Marysville, OH) at 22°C under long-day conditions (16 hour light/8 hour darkness). Wild-type seeds were imbibed in water at 4°C for 3 days prior to planting. Seeds in *ga1-3* background were imbibed in 100 μM GA_3 at 4°C for 3 days to promote their germination. For phenotypic characterization, the GA-deficient seeds were then rinsed thoroughly (at least 7 times) with water before planting and left untreated ever since; for seed propagation, these seeds were planted without rinsing and plants were sprayed with 100 μM GA_3 to restore WT-like growth. Flowering time was measured by both chronological and developmental ages. The chronological age was marked by the number of days needed after sowing the seeds for first clear appearance of a flower bud visible to the naked eye. The developmental age is measured by the number of rosette leaves formed when bolting stem reaches ~ 1cm high. The length from the root-shoot transition to the top of primary inflorescence stem was considered to be the final plant height. The length between 1st silique and 20th silique on the primary inflorescence stem was measured with a ruler and divided by 19 to obtain the internode length.

2.2.4 Hypocotyl elongation assay.

Seeds were incubated in 10% Clorox and 0.5% SDS for 20 minutes and rinsed five times with sterile water. After sterilization, seeds in WT background were directly plated on 0.5× MS media containing 1% sucrose, 0.4% phytogel and various concentrations of GA_4 in square plates, whereas seeds in *ga1-3* background were treated with 100 μM GA_4 for 3 days at 4°C in the dark before plating. Seeds of different genotypes were plated on the same plates to reduce random variations across the plates. After 4 days (or 3 days for GA-deficient seeds) at 4°C in the dark, the square plates were placed vertically in continuous light at 22°C. Pictures of the seedlings were taken on day 4 or 5 and hypocotyl lengths were measured with the aid of ImageJ software (http://rsbweb.nih.gov/ij/). At least 20 seedlings were measured for each genotype.

2.2.5 Immunoblotting.

The immunoblot analysis procedure was adapted from the protocol described before (Silverstone et al., 2001). 0.1g 8 to 10-day-old whole seedlings grown under continuous light at 22°C were harvested and frozen in liquid nitrogen. Total proteins were extracted by grinding the tissues in 150 μl 2x SDS sample buffer (4% SDS, 125 mM Tris and 20% glycerol, pH 8.8) supplemented with 5 μl/ml β-mercaptoethanol (BME), boiled for 5 min, and centrifuged in a microcentrifuge for 5 min at room temperature. The supernatant fractions were transferred to new tubes, and protein concentrations were determined by the Bradford assay (BioRad, Hercules, CA). Each sample then was

adjusted to be in 1× sample buffer and boiled again for 3 min. The proteins were separated by 8% SDS-PAGE and transferred onto nitrocellulose membrane (BioRad). Monoclonal anti-cMyc primary antibody from mouse (MMS-150P, Covance, Raleigh, NC; 1:2,000 dilution), monoclonal anti-HA primary antibody from mouse (MMS-101P, Covance; 1:2,000 dilution) and affinity-purified anti-RGA polyclonal primary antibodies from rabbit (1:500 dilution) (Silverstone et al., 2001) were used for detection of transgenic IDD1 protein fused with cMyc tag, transgenic IDD2 protein fused with HA tag, and endogenous RGA protein, respectively. The secondary antibodies horseradish-peroxidase (HRP)-conjugated donkey anti-mouse IgG (Jackson ImmunoResearch Laboratories, West Grove, PA; 1:5,000 dilution) and HRP-conjugated goat anti-rabbit IgG (Pierce; 1:10,000 dilution) were used to detect corresponding primary antibodies. The blots were then incubated in Supersignal Dura Reagent (Pierce), and the signals were detected by chemiluminescence. Ponceau staining was used to confirm equal loading.

2.2.6 Quantitative real-time PCR (qRT-PCR) analysis.

Total RNA was isolated from 9-day whole seedlings grown under continuous white light at 22°C using the RNeasy plant mini kit (Qiagen, Valencia, CA) and then treated with DNaseI using the DNA-free kit (Life Technologies), according to respective manufacturers' instructions. 0.5 μg of DNaseI-treated RNA was used to synthesize cDNA using Transcriptor First Strand cDNA Synthesis kit (Roche Diagnostics,

Indianapolis, IN). qRT-PCR was performed using Faststart universal SYBR Green Master (Rox) (Roche Diagnostics) with 50 ng cDNA and 0.5 μM primers (see Appendix A for primer sequences) in a Roche LightCycler (Roche Diagnostics). The housekeeping gene *Exp-PT* (At4g33380) was used as the normalization control of data from qRT-PCR, since *Exp-PT* has a stable expression level throughout plant development and under various environmental conditions (Czechowski et al., 2005). The relative mRNA level of tested genes is the mean ± SEM (the standard error of the mean) of two biological repeats including two technical repeats in each. A Student's t test was performed with the significance cutoff set to be 0.05.

2.3 Results

2.3.1 IDD1 and IDD2 positively regulate GA-controlled hypocotyl elongation.

A recent study suggested IDD1 promotes hypocotyl elongation in a GA-dependent manner (Feurtado et al., 2011). However, the transgenic plants (*2x35S:IDD1*) used for hypocotyl-length assays in that study may have produced some artifacts due to ectopic overexpression of IDD1. Meanwhile, the study only showed the difference in hypocotyl length with 10 μM GA_3, but did not analyze GA responses quantitatively. To avoid the possible artifacts and gain insight into how IDD1 and IDD2 affect overall GA response curve, we obtained two T-DNA insertion mutants, *idd1-1* and *idd2-1* in Col-0 background, and their double mutant *idd1-1 idd2-1* by crossing *idd1-1* to *idd2-1* (Stephen Thomas, unpublished data). DNA sequence analysis suggests that the T-DNA insertion site in *idd1-1* is located in 2nd exon of *IDD1* (370th nucleotide downstream of the start codon ATG), whereas in *idd2-1* the T-DNA is inserted in 3rd intron of *IDD2* (1156 nucleotide after translational start site) (Figure 2.2A; Zhong-Lin Zhang, unpublished data). To determine whether the T-DNA insertions interfere with wild-type transcript production, we performed reverse transcription-PCR (RT-PCR) using total mRNA extracted from 9-day seedlings of *idd1-1* and *idd2-1* as template and primers spanning the corresponding T-DNA insertions. No wild-type *IDD1* transcript was detected in *idd1-1* mutant, suggesting *idd1-1* is a null allele. Although some wild-type *IDD2* transcripts were detected by RT-PCR, *IDD2* transcript level is significantly reduced (by

more than 80 fold) in *idd2-1* mutant compared to WT according to qRT-PCR using the same set of primers and template (Figure 2.2B). Thus, *idd2-1* mutant largely abolishes the endogenous transcription of *IDD2*.

With *idd1-1* and *idd2-1* single and double mutants and Col-0 as a control, we did a hypocotyl-elongation assay where seedlings were grown on plates containing different concentrations of exogenous GA_4 under continuous white light for four days before measurement (Figure 2.3). Without GA_4, none of the lines showed any difference in hypocotyl length. However, in the presence of GA_4, the *idd* mutants showed a shorter hypocotyl phenotype than WT to varying degrees. At 0.1 μM concentration of GA_4 where the difference in GA response is most obvious, *idd1-1* (86.8% of WT) displayed a more reduced hypocotyl length than *idd2-1* (91.6% of WT), and the double mutant *idd1-1 idd2-1* (76.5% of WT) had the shortest hypocotyls. Using similar hypocotyl assays, a significant decrease in GA response was also seen in *ga1-3 idd1-1 idd2-1* compared with *ga1-3* (data not shown). These results suggest that IDD1 and IDD2 promote GA-induced hypocotyl elongation in an additive manner, and IDD1 is likely to play a more dominant role.

To confirm that the decreased GA sensitivity in *idd1-1 idd2-1* is caused by the mutations in *IDD1* and *IDD2*, we did a complementation experiment. The introduction of the fusion gene *IDD1-4×cMyc* driven by *IDD1* promoter in *idd1-1 idd2-1* genome (referred to as *pIDD1:IDD1-cMyc/idds* hereafter) rescued defects of the double mutant in

GA-responsive hypocotyl growth (Figure 2.4). An excessive expression of IDD1-4×cMyc protein even over-complemented the mutant hypocotyl phenotype (Figure 2.4). Consistent with these observations, the transgenic lines overexpressing IDD1 (*35S:cMyc-IDD1*) or IDD2 (*35S:HA-IDD2*) in Col-0 under the control of CaMV 35S promoter exhibited hypersensitive GA response in hypocotyl elongation (Figure 2.5A-B and 2.6A-B). Furthermore, among different independent lines of each overexpressor, the degree of GA responsiveness well correlates with the protein level of the corresponding transgene (Figure 2.5C and 2.6C). Together, these data support the hypothesis that IDD1 and IDD2 function as positive regulators in GA signaling where they play partially redundant roles.

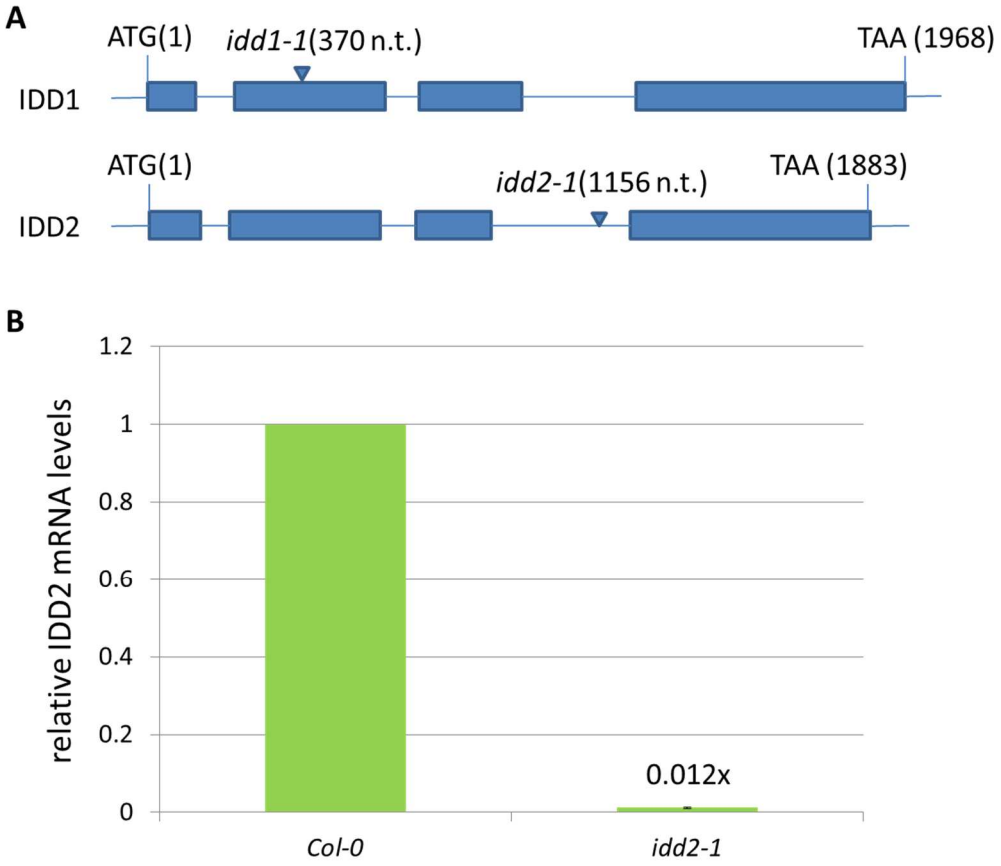

Figure 2.2 Locations of T-DNA insertions in *idd1-1* and *idd2-1* and the wild-type transcript level of IDD2 in *idd2-1*.

A. The schematic diagram depicting the genomic portions of IDD1 and IDD2. Rectangles represent exons and lines in between rectangles represent introns. Triangles mark the insertion sites of T-DNA for corresponding mutants. The numbers refer to start position and end position of gene sequences, and the position of T-DNA insertions relative to the gene translational start sites on the genome. n.t., nucleotide.

B. The relative mRNA level of wild-type IDD2 gene in *idd2-1* vs. Col-0. IDD2 transcripts are reduced by ~80 fold by *idd2-1* mutation.

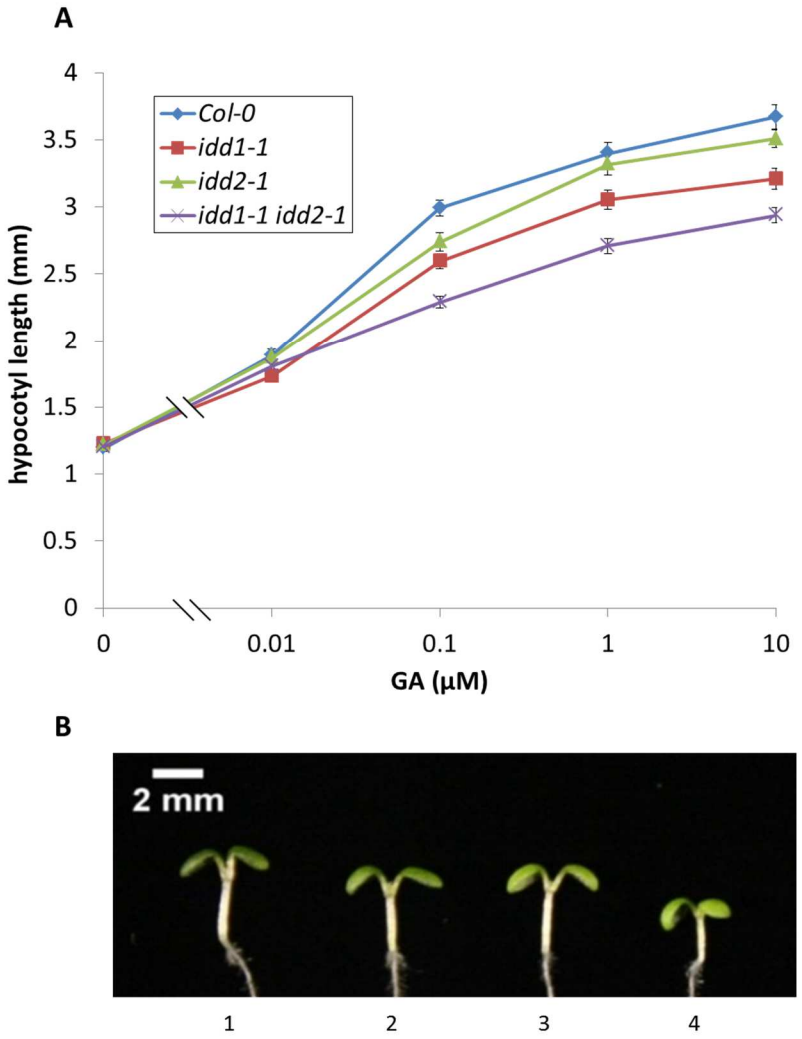

Figure 2.3 The hypocotyl elongation assay of *idd1-1* and *idd2-1* single and double mutants.

A. GA dose response curves of *idd1-1*, *idd2-1*, *idd1-1 idd2-1* and Col-0 by hypocotyl elongation assay. Seedlings were grown on plates containing specified concentrations of GA under continuous white light for four days before measurement. Without GA, all mutants have similar hypocotyl lengths to Col-0. As GA concentration increases, *idd2-1* showed a slightly lower GA response, *idd1-1* intermediate and the double mutant most insensitive, compared to Col-0.

B. The picture of seedlings representative of each line grown with 1μM GA. 1: Col-0. 2: *idd1-1*. 3: *idd2-1*. 4: *idd1-1 idd2-1*. Scale bar: 2mm.

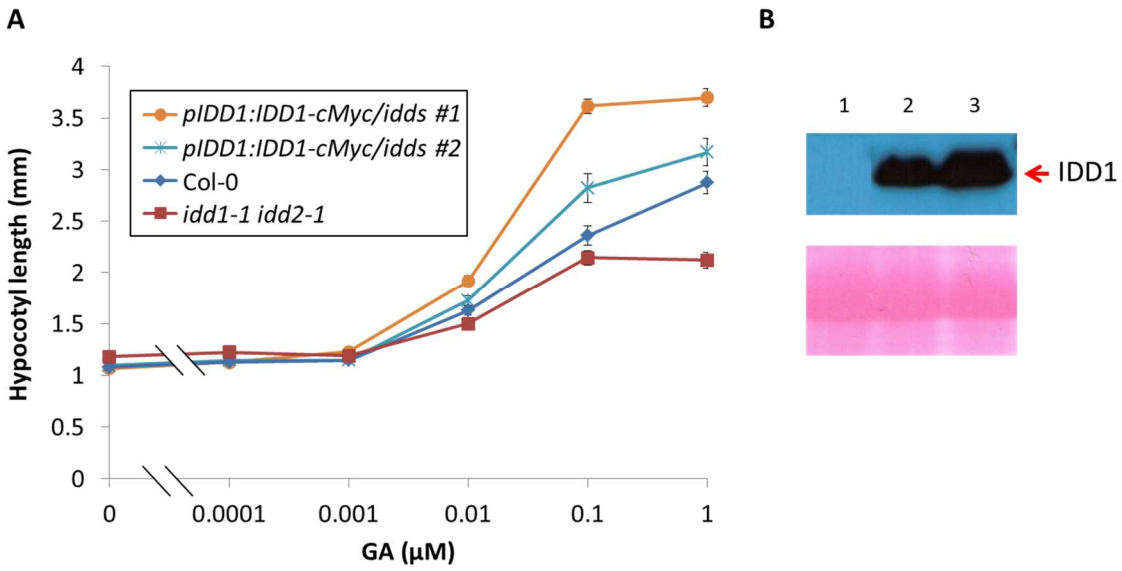

Figure 2.4 *pIDD1:IDD1-cMyc* transgene complements defects of *idd1-1 idd2-1* in GA-responsive hypocotyl elongation in an IDD1-dose dependent manner.

A. GA dose response curves of *pIDD1:IDD1-cMyc/idds* lines #1, #2, *idd1-1 idd2-1* together with Col-0 by hypocotyl-elongation assay. Seedlings were grown under continuous white light for four days before measurement. *pIDD1:IDD1-cMyc/idds* #2 has a near-normal GA response, while *pIDD1:IDD1-cMyc* overcomplements *idd1-1 idd2-1* in line *pIDD1:IDD1-cMyc/idds* #1, resulting in its hypersensitive GA response.

B. Western blot analysis for transgenic IDD1 protein in *pIDD1:IDD1-cMyc/idds* lines. 1: Col-0. 2: *pIDD1:IDD1-cMyc/idds* #2. 3: *pIDD1:IDD1-cMyc/idds* #1. Bottom: Ponceau Staining to check for equal loading of protein samples. Note the transgenic IDD1 protein level in different *pIDD1:IDD1-cMyc/idds* lines well correlates the hypocotyl phenotype.

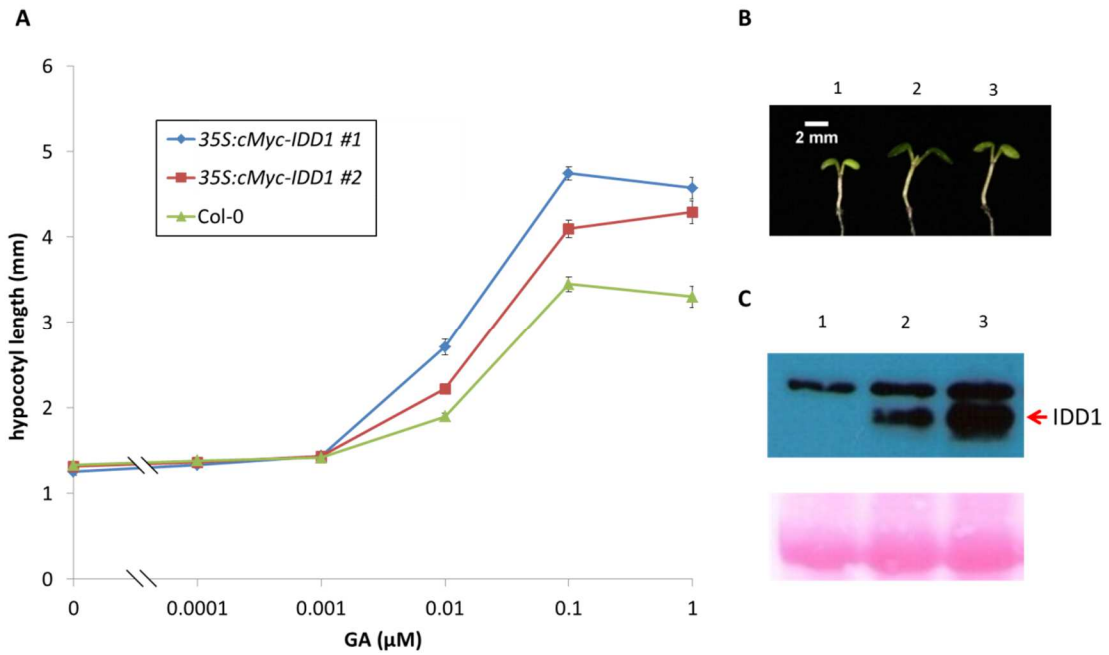

Figure 2.5 IDD1 overexpressors enhance hypocotyl GA response in an IDD1-dose dependent manner.

A. GA dose response curves of *35S:cMyc-IDD1* lines #1, #2 and Col-0 by hypocotyl-elongation assay. Seedlings were grown under continuous white light for four days before measurement.

B. The picture of seedlings representative of each line grown with 1μM GA. 1: Col-0. 2: *35S:cMyc-IDD1 #2.* 3: *35S:cMyc-IDD1 #1.* Scale bar: 2mm.

C. Western blot analysis for transgenic 4×cMyc-IDD1 protein in *35S:cMyc-IDD1* lines using monoclonal mouse anti-cMyc antibody. 1: Col-0. 2: *35S:cMyc-IDD1 #2.* 3: *35S:cMyc-IDD1 #1*. Bottom: Ponceau Staining to check for equal loading of protein samples. Note the transgenic IDD1 protein level in different *35S:cMyc-IDD1* lines well correlates the hypocotyl phenotype.

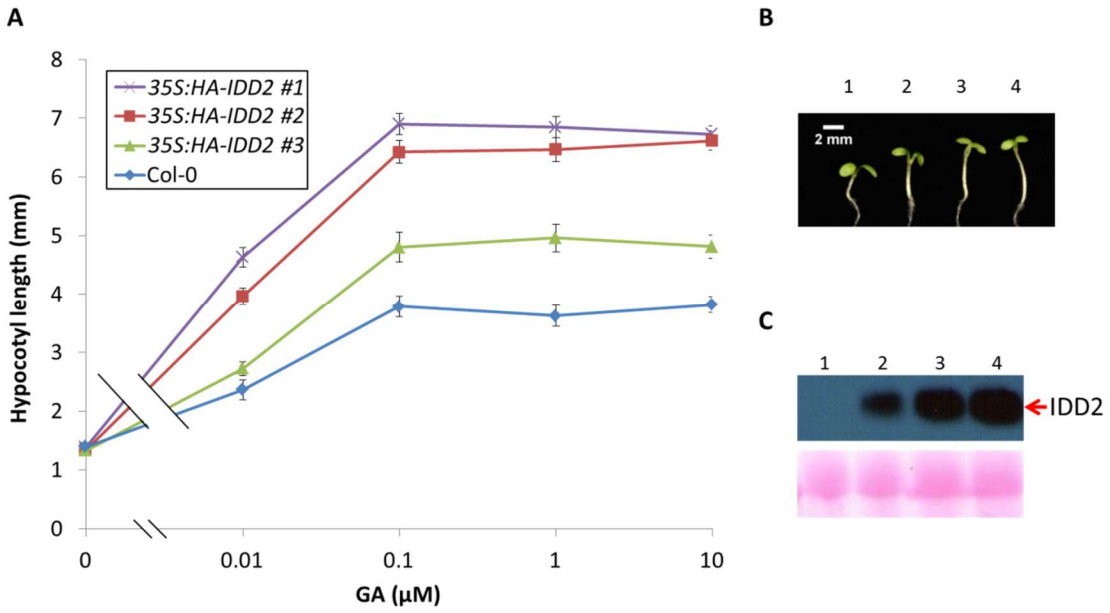

Figure 2.6 IDD2 overexpressors enhance hypocotyl GA response in an IDD2-dose dependent manner

A. GA dose response curves of *35S:HA-IDD2* lines #1, #2, #3 and Col-0 by hypocotyl-elongation assay. Seedlings were grown under continuous white light for four days before measurement.

B. The picture of seedlings representative of each line grown with 1μM GA. 1: Col-0. 2: *35S:HA-IDD2 #3.* 3: *35S:HA-IDD2 #2.* 4: *35S:HA-IDD2 #1.* Scale bar: 2mm.

C. Western blot analysis for transgenic HA-IDD2 protein in *35S:HA-IDD2* lines using monoclonal mouse anti-HA antibody. 1: Col-0. 2: *35S:HA-IDD2 #3.* 3: *35S:HA-IDD2 #2.* 4: *35S:HA-IDD2 #1.* Bottom: Ponceau Staining to check for equal loading of protein samples. Note the transgenic IDD2 protein level in different *35S:HA-IDD2* lines well correlates the hypocotyl phenotype.

2.3.2 DELLAs counteract the effects of IDD1 and IDD2 in hypocotyl growth.

The fact that IDD1 and IDD2 interact with DELLAs poses a question, what is the functional significance behind this interaction? Given the opposite roles between IDDs (IDD1 and IDD2) and DELLAs in GA-controlled hypocotyl elongation (King et al., 2001), we hypothesize that DELLAs and IDDs antagonize each other's function through direct protein-protein interactions. To test this hypothesis, epistasis analysis between DELLA mutants and *idd1-1 idd2-1* was conducted to see if the hypocotyl phenotype of *idd1-1 idd2-1* can be rescued by DELLA mutants. The double mutant *idd1-1 idd2-1* was used for epistasis analysis because IDD1 and IDD2 are partially redundant and *idd1-1 idd2-1* showed a more obvious hypocotyl phenotype than the single mutants *idd1-1* and *idd2-1* (Figure 2.3). Among the five DELLA proteins in *Arabidopsis*, RGA plays a primary role, and GAI a secondary role, in GA-regulated vegetative growth (Tyler et al., 2004). Thus, we first crossed the T-DNA mutant *rga-28*, a null mutant of *RGA* in Col-0 (Tyler et al., 2004), to *idd1-1 idd2-1*. As shown from hypocotyl-elongation assays (Figure 2.7), the GA response of triple mutant *rga-28 idd1-1 idd2-1* did not significantly differ from that of *idd1-1 idd2-1*, indicating that *rga-28* alone was not able to rescue the defects of *idd1-1 idd2-1* in GA-regulated hypocotyl elongation. Notice that *rga-28* single mutant showed a WT-like GA response, which raises a possibility that the effect of *rga-28* mutation is masked in Col-0 given the already low amounts of RGA proteins in most WT tissues due to high endogenous GA levels (Silverstone et al., 2001). The same experiments were then

repeated in *ga1-3* background. Still, *ga1-3 rga-28 idd1-1 idd2-1* showed a GA response closer to *ga1-3 idd1-1 idd2-1* than *ga1-3 rga-28* (Figure 2.8).

Although *rga-28* failed to rescue the defects of *idd1-1 idd2-1* in hypocotyl phenotype, it does not rule out the possibility is that *rga* single mutation is not sufficient for rescuing due to the redundancy between RGA and GAI (Dill and Sun, 2001). To test such a possibility, I crossed *idd1-1 idd2-1* with *rga-29 gai-t6*, a double loss-of-function mutant bearing a T-DNA insertion in RGA and a Ds insertion in GAI, respectively (Oh et al., 2007; Peng et al., 1997). I replaced *rga-28* with *rga-29* in this case because the combination of *rga-28* and *gai* null mutant lead to almost complete sterility of plants (Plackett et al., 2014), whereas *rga-29 gai-t6* is fertile (Jeongmoo Park, personal communication). As expected, compared to Col-0, *rga-29 gai-t6* has a longer hypocotyl without exogenous GA and a "flatter" response to increasing concentrations of exogenous GA (Figure 2.9). Although not identical, the quadruple mutant *rga-29 gai-t6 idd1-1 idd2-1* largely mimicked *rga-29 gai-t6*, rather than *idd1-1 idd2-1*, in GA responsive hypocotyl elongation (Figure 2.9). This suggests that the two major *Arabidopsis* DELLAs RGA and GAI partially antagonize the functions of IDD1 and IDD2 in hypocotyl growth, while additional factors, such as other DELLAs, are probably also involved.

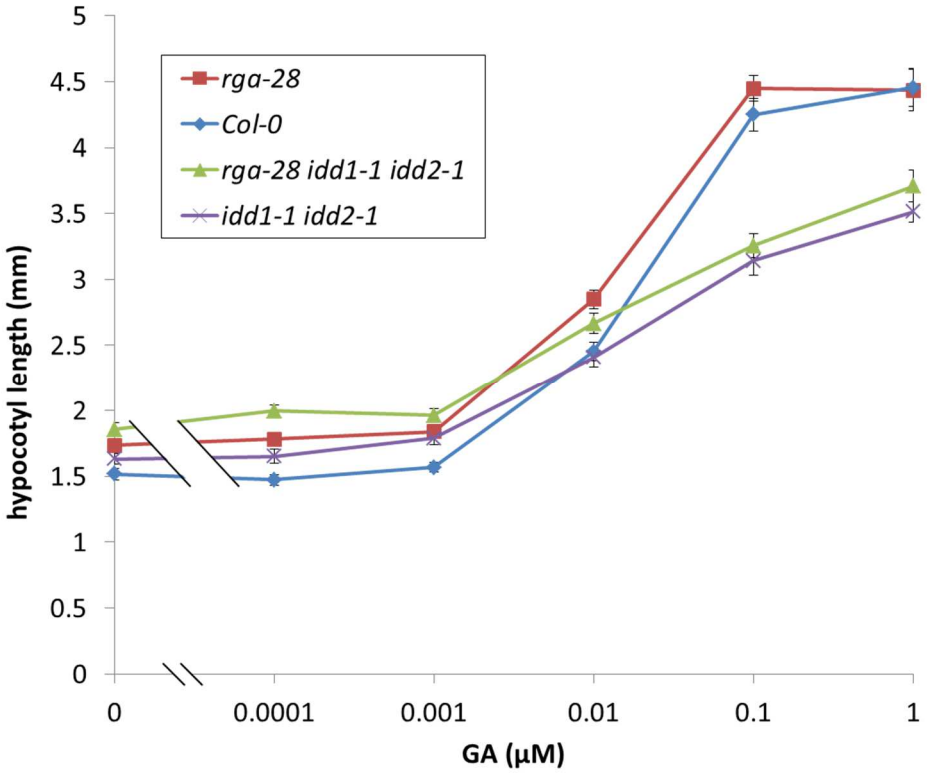

Figure 2.7 *rga-28* failed to rescue the defects of *idd1-1 idd2-1* in hypocotyl GA-dose response in Col-0.

Hypocotyl-elongation assays were performed with *rga-28*, *idd1-1 idd2-1*, *rga-28 idd1-1 idd2-1* and Col-0. Seedlings were grown under continuous white light for four days before measurement.

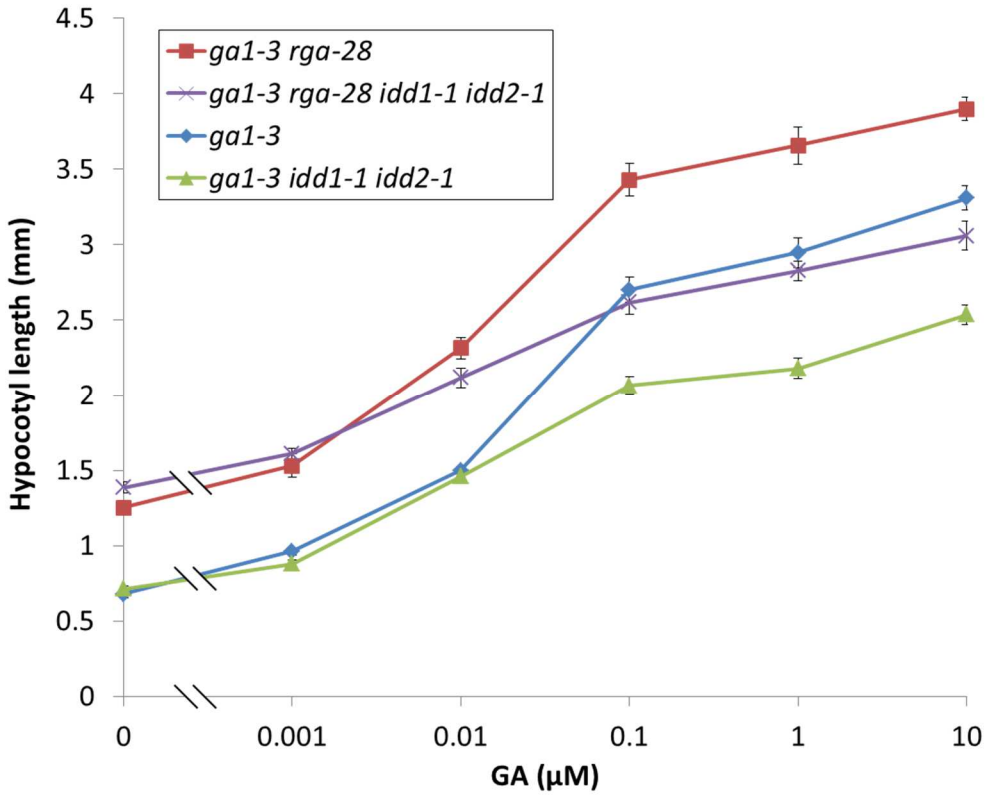

Figure 2.8 *rga-28* failed to rescue the defects of *idd1-1 idd2-1* in hypocotyl GA-dose response in *ga1-3* background.

Hypocotyl-elongation assays were performed with *ga1-3 rga-28*, *ga1-3 idd1-1 idd2-1*, *ga1-3 rga-28 idd1-1 idd2-1* and *ga1-3*. To promote germination, all seeds were treated with 100 μM GA_3 for three days and then washed before plating. Seedlings were grown under continuous white light for five days before measurement.

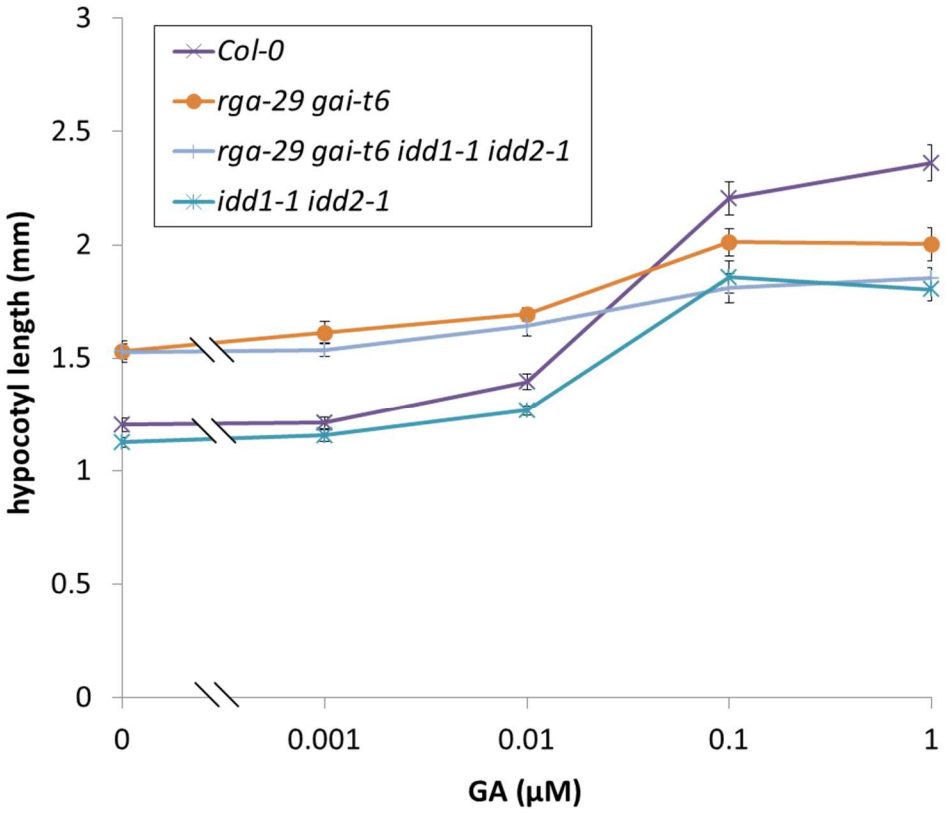

Figure 2.9 *rga-29 gai-t6* partly rescue the defects of *idd1-1 idd2-1* in hypocotyl GA-dose response.

Hypocotyl-elongation assays were performed with *rga-29 gai-t6*, *idd1-1 idd2-1*, *rga-29 gai-t6 idd1-1 idd2-1* and Col-0. Seedlings were grown under continuous white light for four days before measurement.

2.3.3 IDD1 and IDD2 play positive roles in flowering and stem elongation.

Apart from the role of IDD1 and IDD2 in hypocotyl growth, we also examined the effects of mutations and overexpression of the two genes in GA-promoted adult phenotypes including flowering and stem elongation. A few IDD homologs across different plant species have been implicated in flowering (Colasanti et al., 1998; Matsubara et al., 2008; Seo et al., 2011b). Although a previous study showed that none of the IDD single mutant in *Arabidopsis* causes a flowering time change except *idd8*, which delays the flowering (Seo et al., 2011b), it is possible that other flowering-regulating IDDs were not identified because of redundancy. To explore this possibility, I compared the flowering time of *idd1-1 idd2-1*, transgenic lines *35S:cMyc-IDD1 #1* and *pIDD1:IDD1-cMyc/idds* #1, to the flowering time of Col-0, under LD conditions. *35S:cMyc-IDD1 #1* and *pIDD1:IDD1-cMyc/idds* #1 were chosen because they have both the highest IDD1 expression and the strongest GA response, among *35S:cMyc-IDD1* lines and *pIDD1:IDD1-cMyc/idds* lines, respectively. Flowering time was scored in both chronological and developmental ages. *idd1-1 idd2-1* and *35S:cMyc-IDD1 #1* did not have a significantly altered flowering time, but *pIDD1:IDD1-cMyc/idds* #1 was slightly early-flowering, both chronologically and developmentally (2.8 days earlier, $p < 0.001$; 0.9 fewer leaves, $p < 0.05$; Figure 2.10). The discrepancy between *35S:cMyc-IDD1 #1* and *pIDD1:IDD1-cMyc/idds #1* in flowering time is not surprising, due to the fact that *pIDD1:IDD1-cMyc/idds* #1 has a much higher IDD1 protein level than *35S:cMyc-IDD1 #1*

(Figure 2.11). In addition, two independent transgenic lines overexpressing IDD2 in L*er* (*35S:HA-IDD2_L*, western blot data not shown) flowered slightly earlier than L*er*, developmentally but not chronologically (Figure 2.12). Together, these results indicate that IDD1 and IDD2 may play a positive role in floral initiation, although we could not rule out the possibility that the above-mentioned flowering phenotypes are caused by ectopic overexpression.

To find out whether IDD1 and IDD2 affect stem elongation, final bolting stem height and the average internode length were measured for plants of abovementioned lines. Again, *idd1-1 idd2-1* was not distinguishable from Col-0 in both measurements (Figure 2.13). However, *35S:cMyc-IDD1 #1* and *pIDD1:IDD1-cMyc/idds* #1 both are a little higher than Col-0 and their final heights correlate well with their average internode lengths, respectively (Figure 2.13), indicating that the increase in their heights is likely due to enhanced stem cell elongation instead of more internodes. A similar pattern of final height and internode length was observed for *35S:HA-IDD2_L #1* and *35S:HA-IDD2_L #2* as opposed to L*er* (Figure 2.14). By these data, we conclude that IDD1 and IDD2 are involved in promotion of not only hypocotyl elongation, but also stem elongation in *Arabidopsis*.

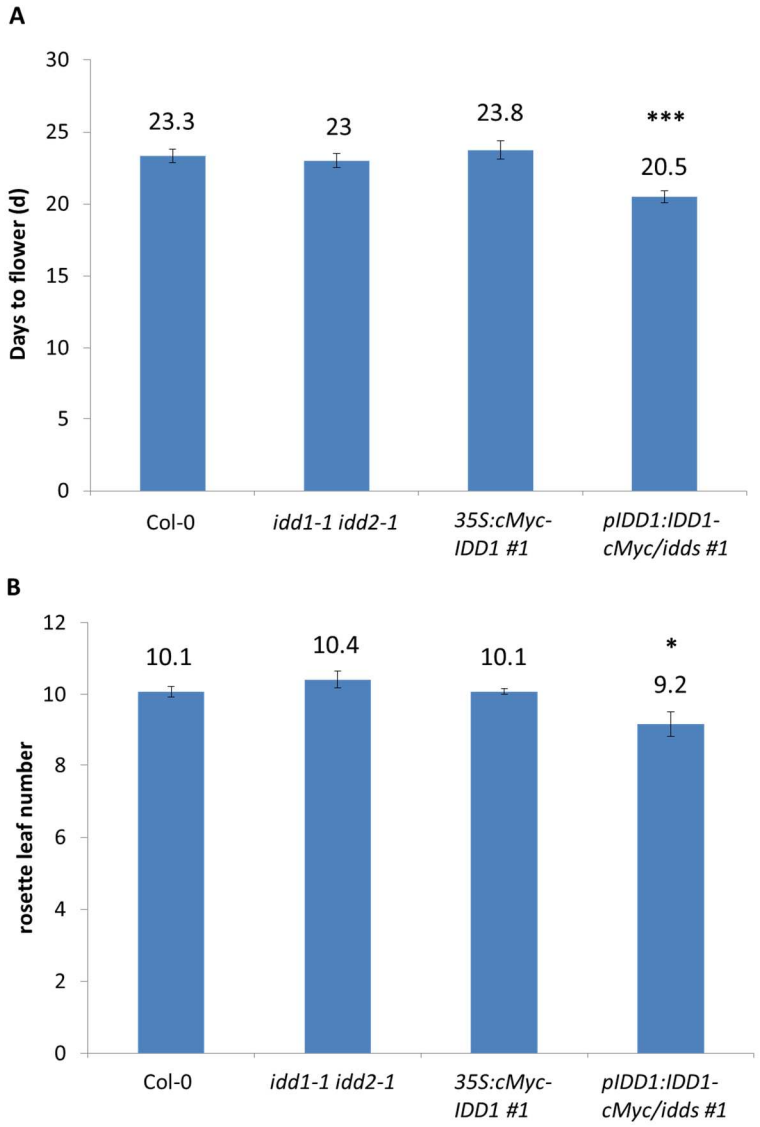

Figure 2.10 IDD1 overexpression causes an earlier flowering time in Col-0.

A. Flowering time of *idd1-1 idd2-1*, *35S:cMyc-IDD1* #1, *pIDD1:IDD1-cMyc/idds* #1 and Col-0 plants measured by days to flower. 12 plants were scored for each line. The numbers above bars represent the mean of measurements for each line. *pIDD1:IDD1-cMyc/idds* #1 showed a significantly earlier flowering than Col-0. ***: $p < 0.001$.

B. Flowering time of *idd1-1 idd2-1*, *35S:cMyc-IDD1* #1, *pIDD1:IDD1-cMyc/idds* #1 and Col-0 plants measured by the rosette leaf number when bolting stem reaches ~ 1cm high. 12 plants were scored for each line. The numbers above bars represent the mean of measurements for each line. *pIDD1:IDD1-cMyc/idds* #1 had a significantly fewer rosette leaf number than Col-0 as flowering initializes. *: $p < 0.05$.

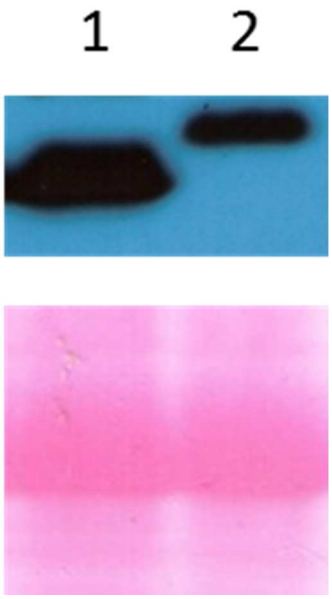

Figure 2.11 ***35S:cMyc-IDD1 #1*** **has a lower transgenic IDD1 protein level than** ***pIDD1:IDD1-cMyc/idds***

Transgenic IDD1-4×cMyc and 4×cMyc-IDD1 proteins were detected in western blot from whole-seedling extracts of (1) *pIDD1:IDD1-cMyc/idds* #1 and (2) *35S:cMyc-IDD1 #1,* respectively using monoclonal mouse anti-cMyc antibody. Bottom: Ponceau Staining to check for equal loading of protein samples.

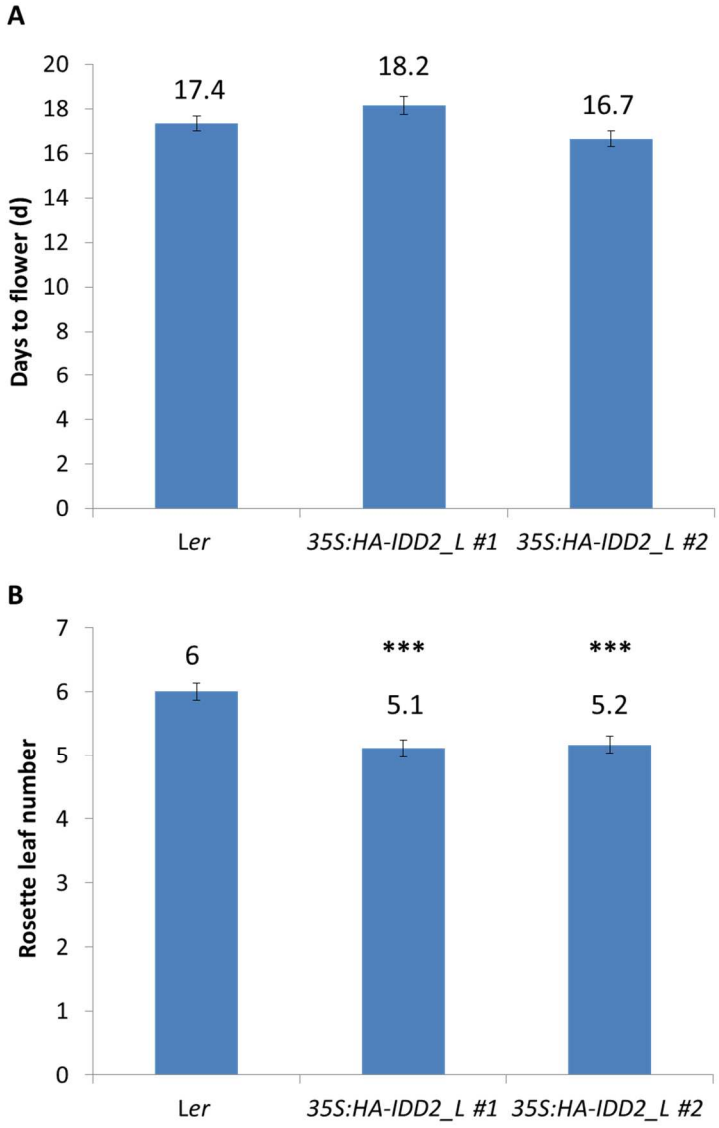

Figure 2.12 IDD2 overexpression causes an earlier flowering time in L*er* developmentally but not chronlogicallhy.

A. Flowering time of *35S:HA-IDD2_L* #1, #2 and L*er* measured by days to flower. 12 plants were scored for each line. The numbers above bars represent the mean of measurements for each line. Neither *35S:HA-IDD2_L* line showed a significant difference from L*er*.

B. Flowering time of *35S:HA-IDD2_L* #1, #2 and L*er* plants measured by the rosette leaf number when bolting stem reaches ~ 1cm high. At least 11 plants were scored for each line. The numbers above bars represent the mean of measurements for each line. *35S:HA-IDD2_L* line #1 and #2 both had a significantly fewer rosette leaf number than Col-0 as flowering initializes. ***: $p < 0.001$.

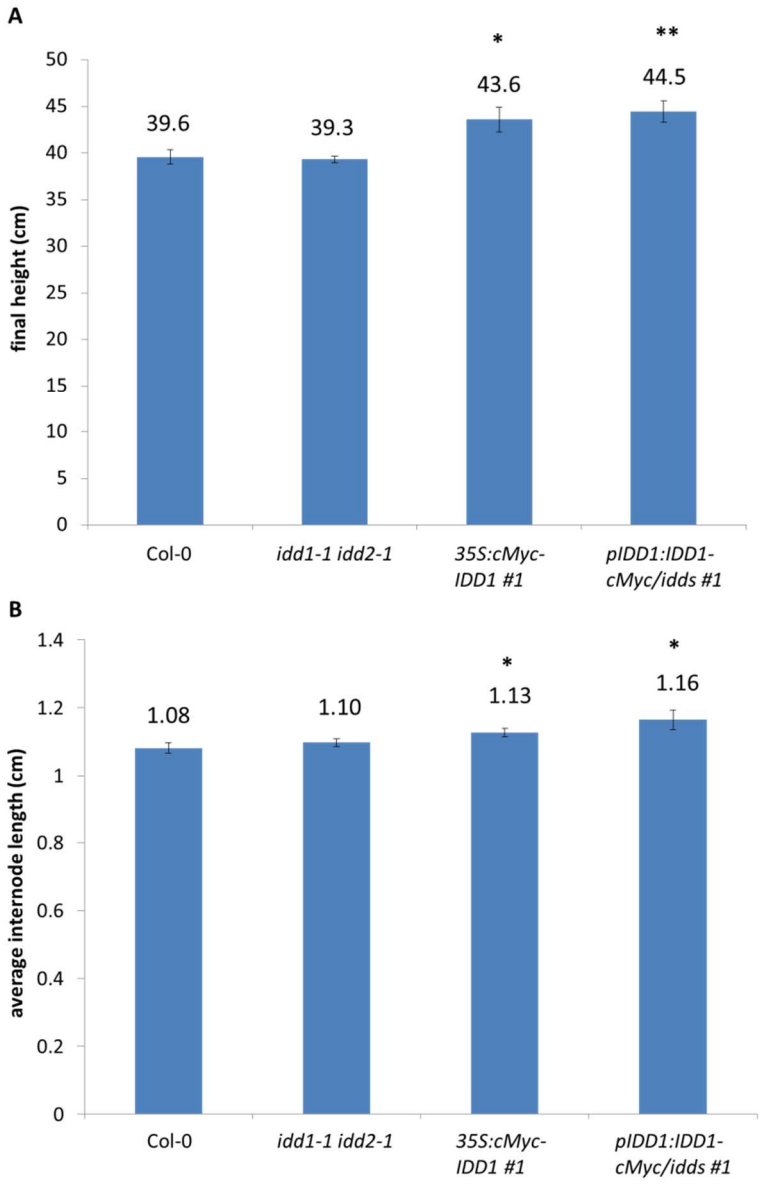

Figure 2.13 IDD1 overexpression promotes stem elongation in Col-0.

A. Final heights of *idd1-1 idd2-1*, *35S:cMyc-IDD1* #1, *pIDD1:IDD1-cMyc/idds* #1 and Col-0 plants. At least 11 plants were measured for each line. The numbers above bars represent the mean of measurements for each line. *: $p < 0.05$. **: $p < 0.01$.

B. Average internode lengths of *idd1-1 idd2-1*, *35S:cMyc-IDD1* #1, *pIDD1:IDD1-cMyc/idds* #1 and Col-0 plants. The internode length was obtained by dividing the length between 1st silique and 20th silique on the primary inflorescence stem by 19. At least 11 plants were measured for each line. The numbers above bars represent the mean of measurements for each line. *: $p < 0.05$.

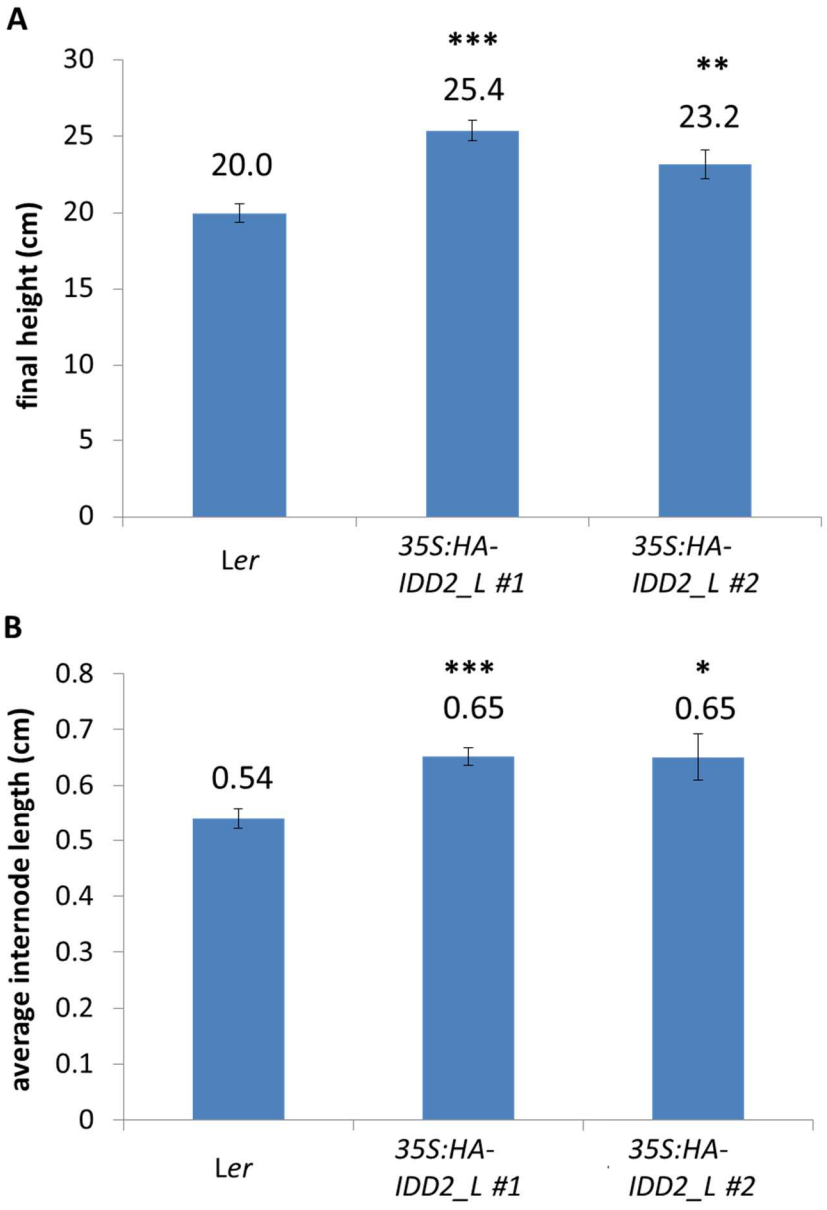

Figure 2.14 IDD2 overexpression promotes stem elongation in L*er*.

A. Final heights of *35S:HA-IDD2_L* #1, #2 and L*er* plants. At least 12 plants were measured for each line. The numbers above bars represent the mean of measurements for each line. **: $p < 0.01$. ***: $p < 0.001$.

B. Average internode lengths of *35S:HA-IDD2_L* #1, #2 and L*er* plants. The internode length was obtained by dividing the length between 1st silique and 20th silique on the primary inflorescence stem by 19. At least 12 plants were measured for each line. The numbers above bars represent the mean of measurements for each line. **: $p < 0.01$. ***: $p < 0.001$.

2.3.4 IDD2 antagonizes the role of GAI in flowering and stem growth.

We see that IDD1 and IDD2 positively regulate flowering and stem elongation, but whether this regulation has any connection with DELLAs is not sure. As a first step to answer this question, we tested the genetic interaction between DELLA and IDDs with respect to adult phenotypes. Since endogenous DELLA protein levels are already pretty low (Silverstone et al., 2001), we crossed *35S:HA-IDD2_L* lines with the gain-of-function *gai-1* in L*er* in hope of achieving more obvious phenotypic differences. *gai-1* is a semidominant allele of *GAI*, whose protein product lacks 17 amino acids in DELLA domain and is thus constitutively resistant to GA-induced degradation (Peng et al., 1997; Willige et al., 2007). As a result, *gai-1* confers plants GA-insensitive late flowering and dwarfism (Koornneef et al., 1985; Willige et al., 2007). By Y2H assays, the truncated RGA (RG52) missing 185 amino acids in N terminal (including the DELLA domain) still strongly interacts with IDD1 and IDD2 (Zhong-Lin Zhang, unpublished data). This finding suggests that proteins encoded by *gai-1* should interact with IDD1 and IDD2 as well, so *gai-1* is a valid mutant for epistasis analysis. Different from the similar germination time between *35S:HA-IDD2_L* and L*er*, *gai-1 35S:HA-IDD2_L* lines have a delay in seed germination vs. *gai-1*, by around half a day when grown on half-strength MS plates, which could be due to defects in seed development caused by IDD2 ectopic expression as shown in the case of IDD1 before (Feurtado et al., 2011). Nonetheless, the digenic dominant plants display a slight but consistent earlier-flowering phenotype

compared to *gai-1*, both chronologically and developmentally (Figure 2.15). Moreover, the main stem in *gai-1 35S:HA-IDD2_L* grew strikingly faster than that in *gai-1* during the early bolting stage, rendering the former plants higher than the latter plants (Figure 2.16). The pedicles, a modified stem, seemed to grow longer in *gai-1 35S:HA-IDD2_L* plants than in *gai-1* plants, too (Figure 2.16B). These results suggest that IDD2 overexpression can partially rescue the flowering and stem growth defects in *gai-1*, giving further evidence for an antagonistic role of IDD1 and IDD2 against DELLAs in GA signaling.

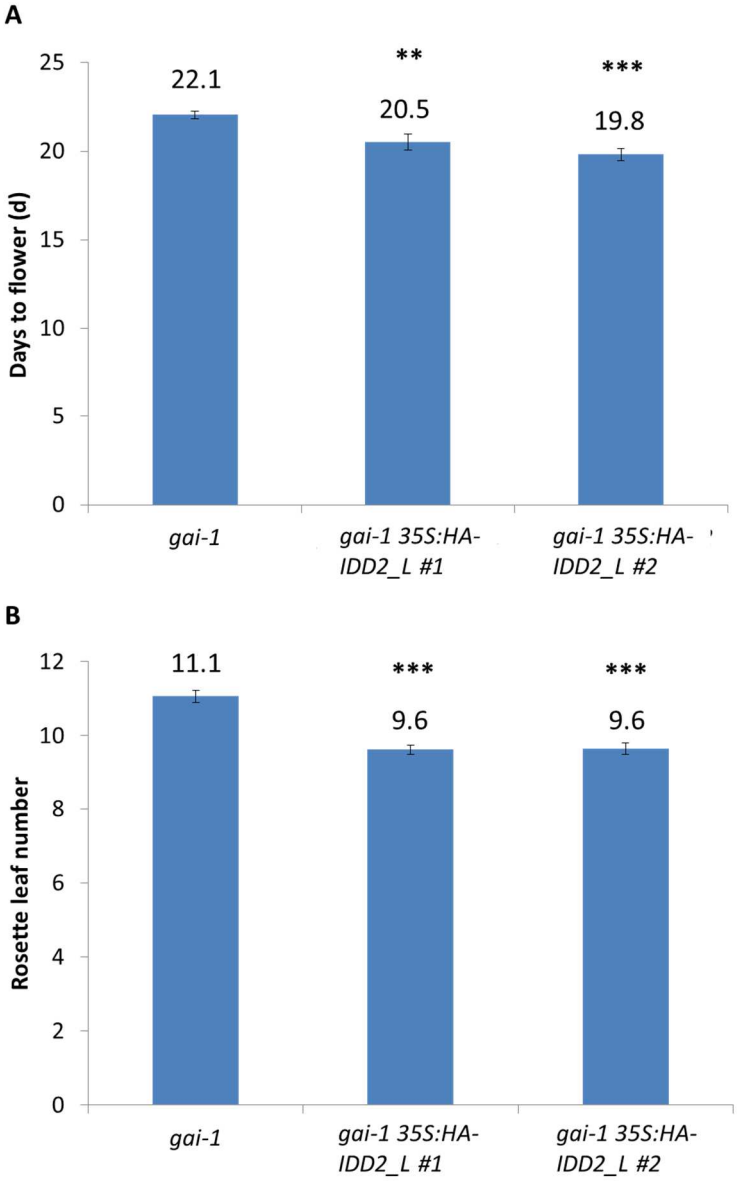

Figure 2.15 ***35S:HA-IDD2_L*** **partially rescues the late-flowering phenotype in** ***gai-1*** **mutant.**

A. Flowering time of *gai-1 35S:HA-IDD2_L* #1, #2 and *gai-1* measured by days to flower. 16 plants were scored for each line. The numbers above bars represent the mean of measurements for each line. **: $p < 0.01$. ***: $p < 0.001$.

B. Flowering time of *gai-1 35S:HA-IDD2_L* #1, #2 and *gai-1* plants measured by the rosette leaf number when bolting stem reaches ~ 1cm high. 16 plants were scored for each line. The numbers above bars represent the mean of measurements for each line. ***: $p < 0.001$.

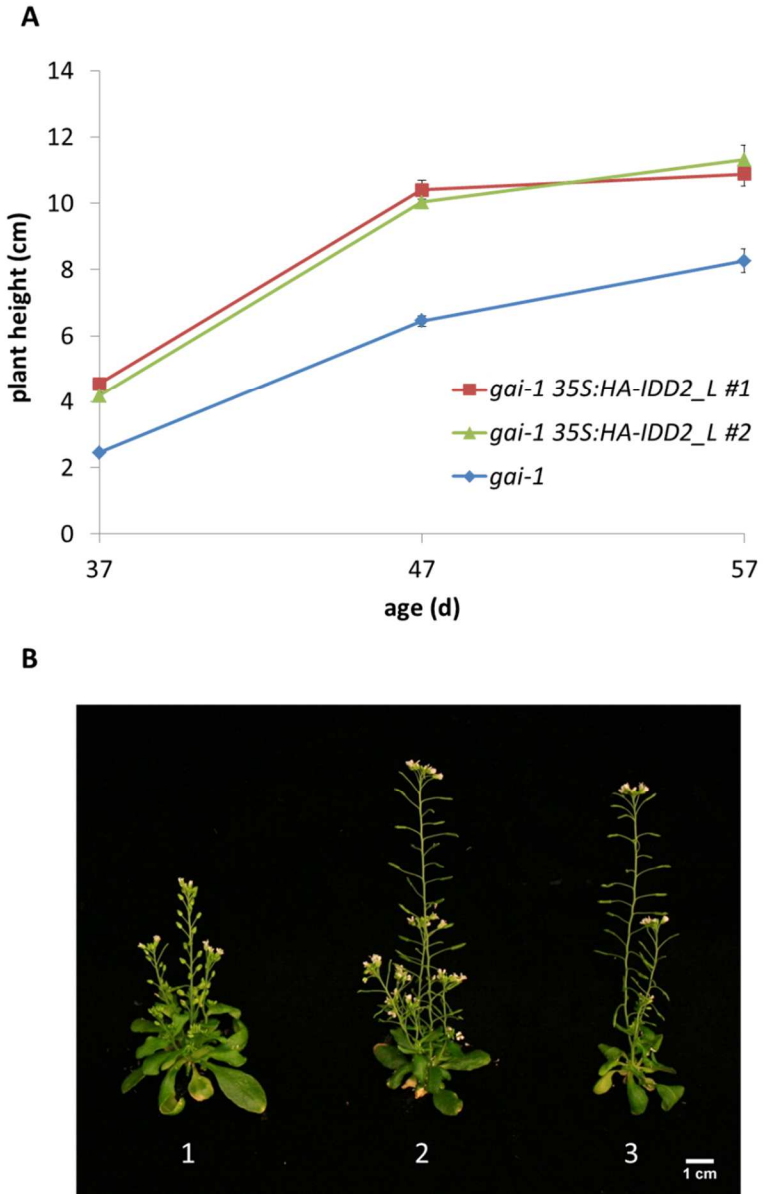

Figure 2.16 ***35S:HA-IDD2_L*** **partially rescues the dwarf phenotype of** ***gai-1*** **mutant.**

A. The growth curve of *gai-1 35S:HA-IDD2_L* #1, #2 and *gai-1* plants in terms of plant height. Plants are grown under LD conditions at 22°C. At least 16 plants were measured for each line at 37, 47 and 57 days old, respectively. At all the three ages, both *gai-1 35S:HA-IDD2_L* #1 plants and *gai-1 35S:HA-IDD2_L* #1 plants are significantly higher than *gai-1* plants ($p < 0.001$).

B. The picture of 47-day-old plants representative of *gai-1 35S:HA-IDD2_L* #1, #2 and *gai-1*. 1: *gai-1*. 2: *gai-1 35S:HA-IDD2_L* #1. 3: *gai-1 35S:HA-IDD2_L #2*. Scale bar: 1cm

2.4 Discussion

In this chapter, we showed that IDD1 and IDD2 positively regulate GA-responsive hypocotyl elongation in an additive manner and DELLAs antagonize IDD1 and IDD2 in this process through direct protein-protein interaction. Although IDD1 and IDD2 share a high homology, *idd2-1* showed a less obvious hypocotyl phenotype than *idd1-1*. This minor role of IDD2 as opposed to IDD1 is possibly due to lower expression levels of IDD2 than IDD1 in WT plants. It is also noteworthy that in this study, *35S:HA-IDD2* lines generally have a much stronger hypocotyl phenotype than *35S:cMyc-IDD1* lines. This is probably caused by differential levels of transgene expression between *35S:HA-IDD2* and *35S:cMycIDD1* plants. In general, *pCAMBIA1300*, the backbone of *35S:HA-IDD2* constructs, tend to produce more transgene products in plants than *pGWB418*, the backbone of *35S:cMyc-IDD1* constructs (Rodolfo Zentella, personal communication). As such, for a more exaggerated phenotype, *pCAMBIA1300* and its variants (Broothaerts et al., 2005) should be considered over *pGWB* series (Nakagawa et al., 2007) in future transgenic research.

Recent genetic analyses in our lab also identified a positive and synergistic role of IDD1 and IDD2 in GA-regulated root hair cell patterning, which is antagonized by RGA (Zhong-Lin Zhang, unpublished data). In analogy to their relation in hypocotyl growth, IDD1 has a primary role, and IDD2 a secondary role, in regulation of root hair development. These findings, combined with the high similarity in their protein

sequences and expression patterns (Feurtado et al., 2011; Fukazawa et al., 2014), reveal that IDD1 and IDD2 play largely redundant roles in a range of plant growth events.

A difference between hypocotyl elongation and root hair development is, *rga* mutation only can partially rescue defects of *idd1-1 idd2-1* in former but not in latter. This difference might be owing to distinct contexts between hypocotyl cells and root epidermal cells. In hypocotyl, there exists near-redundancy of GAI and RGA function. With a low concentration of exogenous GA (<0.01 μM GA_3), *ga1-3 gai-t6* and *ga1-3 rga-24* mutants have short hypocotyls whose lengths are closer to those of *ga1-3*, whereas *ga1-3 rga-24 gai-t6* seedlings have hypocotyls as long as L*er* ones (King et al., 2001). On the other hand, it is possible that RGA plays a more critical role in root hair development than other DELLAs, as suggested in trichome development (Qi et al., 2014), a plant epidermal cell developmental process related to root hair development (Schiefelbein, 2003).

Concerns arise when *rga-29 gai-t6* seedlings did not reach the same height as Col-0 ($p < 0.05$) at a high GA concentration (> 0.1 μM GA_4) in hypocotyl elongation assays. This phenomenon cannot be explained by the current model of DELLA function. Neither is it consistent with previous case where hypocotyl lengths are similar between *ga1-3 rga-24 gai-t6* and L*er* at high GA concentrations (King et al., 2001). The inconsistency could be attributed to differences in days of growth, since their seedlings grew for 7 days, a period that guarantee hypocotyls to finish their growth under white light

(Gendreau et al., 1997), while our seedlings were 4 days old. Another possibility is that the T-DNA mutation *rga-29* may cause some unexpected effects other than knocking out RGA. For example, the T-DNA insertion interferes with neighboring genes of RGA, or there exists close-linked background mutations that inhibit hypocotyl growth.

Many DELLA-interacting and -antagonizing transcription factors are also known to be positive regulators in GA-responsive hypocotyl elongation, such as PIFs, SCL3, BZR1 and ARF6 (Bai et al., 2012b; de Lucas et al., 2008; Oh et al., 2014; Zhang et al., 2011). Our work lays the foundation for placement of IDD1 and IDD2 in the big picture of transcription factor circuits underlying GA-mediated hypocotyl growth. What is the relationship between IDDs and other DELLA interactors with a similar role in hypocotyl growth? Do they function in the same pathway, in parallel or in a competitive manner? What is the significance of DELLA controlling a single process via interacting with different proteins? These are examples of interesting questions to be addressed by future studies, which shall shed light on a more detailed framework of how DELLAs integrate and coordinate multiple branches of regulatory modules in modifying hypocotyl growth.

In addition to their functions in hypocotyl growth, IDD1 and IDD2 seem to also promote flowering and stem elongation by opposing the function of DELLAs. These roles, however, should be examined with caution, because only those IDD transgenic lines with high-level transgene expression showed some consistent phenotypes, whereas

idd1-1 idd2-1 was phenotypically indistinguishable from WT. Further experiments need to be conducted to confirm whether the phenotypes of IDD overexpressors truly reflect the physiological functions of IDD1 and IDD2 or are actually artifacts caused by ectopic overexpression.

The reason why *idd* mutants did not exhibit obvious adult phenotypes could be that IDD1 and IDD2 are involved in a redundant transcription network, such that the losses of their functions are buffered by the whole system. The redundancy could derive from other IDD homologs, because many of them have also been found to interact with DELLAs (Zhong-Lin Zhang, unpublished data). A well-characterized example for this type of functional redundancy in *Arabidopsis* is the PIF gene family (Leivar and Quail, 2011). At least four members (PIF1, PIF3, PIF4 and PIF5) play important and cooperative roles in repressing photomorphogenesis and plants will not be fully constitutively photomorphogenic without removal of all four PIF genes (Leivar et al., 2008). An alternative type of redundancy could stem from feedback mechanisms. It has been shown that induction of IDD1 downregulates GA biosynthesis genes including members of *GA20oxes* and *GA3oxes*, whereas upregulates GA catabolic genes, i.e. members of *GA2oxes* (Feurtado et al., 2011). Coincidentally, we noticed that *35S:cMyc-IDD1 #1* and *35S:HA-IDD2 #1*, two lines expressing high levels of IDD1 and IDD2 protein, respectively, have an obvious increase in abundance of RGA protein compared with Col-0, a possible outcome of feedback regulation (data not shown). These data suggest,

while IDD1 and IDD2 promote GA signaling, they exert negative feedback to balance the enhancement in GA signaling and restore a steady state.

Surprisingly, Fukazawa et al. recently identified a significantly delayed flowering defect in their *idd1 idd2* double mutant, especially under SD conditions (Fukazawa et al., 2014), a phenotype that cannot be repeated using our *idd1-1 idd2-1* mutant (Jeongmoo Park, unpublished data). Although they used a different *idd1* mutant (SALK_022425) from ours, it is unlikely that their allele could confer such a severe phenotype. Side-by-side comparison between their *idd1 idd2* mutants and ours should be done to address this inconsistency.

Chapter 3 IDD1 and IDD2 function antagonistically with DELLAs in transcriptional regulation of DELLA target genes

3.1 Introduction

3.1.1 Canonical DELLA targets and the potential role of IDD1 and IDD2 in transcriptional regulation of these genes.

Since the discovery of DELLAs, the molecular mechanisms of how they act as master growth repressors have been a focus of GA signaling research. Previous microarray studies reveal that DELLAs are involved in the majority of GA-regulated global transcription (Cao et al., 2006; Gallego-Bartolome et al., 2011; Hou et al., 2008; Zentella et al., 2007), suggesting DELLAs were transcription factors. Without any canonical DNA-binding domain, however, the nuclear-localized DELLAs are believed to function as transcriptional regulators by interacting with transcription factors (Zentella et al., 2007). To date, a number of transcription factors have been identified as DELLA interactors in *Arabidopsis*, among which PIFs and BZR1 are examples of the best studied DELLA-binding transcriptional factors (Bai et al., 2012b; de Lucas et al., 2008; Feng et al., 2008; Gallego-Bartolome et al., 2012). PIFs and BZR1 interact with each other and synergistically promote hypocotyl elongation (Oh et al., 2012). Through interacting with both BZR1 and PIFs, DELLAs block their DNA-binding activities and thus inhibit BZR1-PIFs-induced hypocotyl elongation (Bai et al., 2012b; de Lucas et al., 2008). GA-triggered degradation of DELLAs, on the other hand, releases PIFs and BZR1 to activate their

common targets (Bai et al., 2012b; Oh et al., 2012). This demonstrates one mechanism of DELLA-mediated GA-dependent transcription: repressing transcription activators by sequestration. Given that IDDs are zinc-finger transcription factors and play an opposite role to DELLAs in GA-regulated hypocotyl elongation due to DELLA-IDD interaction, we hypothesize that in analogy to PIFs and BZR1, DELLAs inhibit IDDs' function by antagonizing their transactivity. To test this hypothesis, one approach is to test whether some of IDD direct target genes are regulated antagonistically by DELLAs vs. IDDs. A direct target of DELLA interactors BZR1 and PIF4, *PACLOBUTRAZOL RESISTANCE 1* (*PRE1*) serves as a good candidate of IDD target genes (Bai et al., 2012b; Oh et al., 2012). PRE family members are helix-loop-helix factors in a core transcription network that promote cell elongation in response to GA, BL and light signaling (Bai et al., 2012a; Bai et al., 2012b; Ikeda et al., 2012; Oh et al., 2012). Specifically, PRE1 has been shown to be a positive regulator in hypocotyl elongation, whose expression is induced by GA and repressed by DELLAs (Bai et al., 2012b; Lee et al., 2006; Oh et al., 2012). To test the possibility that PRE1 is activated by IDD1 and/or IDD2, we analyzed the transcript levels of PRE1 by qRT-PCR in transgenic lines overexpressing IDD1 or IDD2, as well as in *idd1-1 idd2-1* double mutant. To further test the roles of RGA and IDD1 (IDD1 and IDD2 are highly conserved in sequence and in function) in regulating PRE1 transcription, we also characterized the effects of RGA and/or IDD1 on PRE1 promoter

activity using transient expression assays in *Nicotiana benthamiana* (*N. benthamiana*, or tobacco).

DELLAs do not function only as transcriptional repressors. They have been found to also participate in maintaining GA homeostasis partly by feedback upregulating genes encoding GA biosynthetic enzymes GA3ox1 and GA20ox2, GA receptors GID1a and GID1b, and GA signaling positive regulator SCL3 (Zentella et al., 2007). These genes are likely direct targets of DELLA, since their transcription showed a rapid decrease and an abrupt increase, right after destruction and accumulation of DELLA proteins, respectively (Zentella et al., 2007). The mechanisms how DELLAs activate the expression of these genes, however, remain elusive. By contrast, it has been shown that induction of IDD1 causes reduced transcription of positive components in GA biosynthesis and signaling, including *GA20ox2*, *GA3ox1*, *GID1b* and *SCL3* (Feurtado et al., 2011). These results indicate that DELLA targets *GA20ox2*, *GA3ox1*, *GID1b* and *SCL3* are also candidates of IDD1 direct targets. Importantly, promoters (3000 bp) of these DELLA targets also contain various numbers of known cis-elements for homologous IDD proteins (Table 3.1). There are four different cis-regulatory sequences that have been identified for IDD homologs in various species. The maize ID1 (ZmID1) protein has been found to target a TTTGTCGTTTT or TTTTGTCG/C motif (Kozaki et al., 2004). The rice IDD10 protein (OsIDD10) binds to a contiguous 7-bp GGACAAA sequence (Xuan et al., 2013). In *Arabidopsis*, IDD3 and IDD8 proteins bind to cis-elements

TTGTCT and CTTTTGTCC, respectively (Seo et al., 2011b; Yoshida et al., 2014). Among these target sequences, the ZmID1 target motif TTTTGTCG has also been shown to be bound to by IDD2 through a gel retardation assay (Fukazawa et al., 2014), raising a possibility that IDD1 might also share this binding motif with ZmID1 and IDD2. Strikingly, *GA20ox2*, *GA3ox1*, *GID1b* and *SCL3* 3000-bp promoter regions each contains at least two ZmID1 binding sites (Table 3.1), supporting a hypothesis that these genes are directly regulated by IDD1 and IDD2. To verify the effects of IDD1 and IDD2 on transcription of abovementioned DELLA targets, *GA20ox2*, *GA3ox1*, *GID1b* and *SCL3* were included in the list of genes for expression analyses in *Arabidopsis* seedlings with manipulated amounts of IDD1 and/or IDD2 proteins. Then, similar to PRE1, promoters of these genes were fused to firefly luciferase (fLUC) for transient expression assays in *N. benthamiana*, in order to elucidate the relationship between IDD1 and RGA in the control of their downstream targets. These experiments helped shed light on a molecular mechanism for fine tuning GA homeostasis by feedback regulation with IDDs and DELLAs.

In addition to IDD1 and IDD2, other AtIDD family members have also been shown to be involved in transcription regulation. Recently, it was reported that AtIDD3, -4, -5, -9 and -10 interact with DELLAs while bound to the *SCL3* promoter to mediate the activation of *SCL3* by DELLAs (Yoshida et al., 2014). The five newly characterized IDD family members apparently differ from IDD1 and IDD2 in their relationship with

DELLAs and their regulatory roles in *SCL3* gene expression, which might be due to the presence of a putative repression motif in IDD1 and IDD2, but not in the other IDD homologs (Feurtado et al., 2011; Mitsuda et al., 2011; Yoshida et al., 2014). To explore the mechanisms underlying the differences between the two groups of DELLA-interacting IDDs, wild-type IDD1, a mutant version of IDD1 whose putative repression motif is mutated (IDD1-m), a translational fusion of IDD1 with the transcriptional activation domain from viral protein 16 (VP16) (IDD1-VP16) (Triezenberg et al., 1988) and wild-type IDD3 were respectively included as the effector with or without RGA in transient expression assays, for a comparison in their regulatory activities over the *SCL3* promoter.

Table 3.1: Frequency of binding sites of known IDD homologs in promoters of promising AtIDD1 and AtIDD2 targets

The 3kb promoters of canonical DELLA targets *GA3ox1*, *GA20ox2*, *GID1b*, *SCL3*, *PRE1* and essential root-hair growth regulators *GL2* and *CPC* were searched for the binding cis-elements of AtIDD3 (Yoshida et al., 2014), ZmID1 (Kozaki et al., 2004), AtIDD8 (Seo et al., 2011b) and OsIDD10 (Xuan et al., 2013), respectively, using the Patmatch tool (http://www.arabidopsis.org/cgi-bin/patmatch/nph-patmatch.pl). Note that among the known binding motifs of IDD proteins, one version of the ZmID1 binding motif (5′-TTTTGTCG-3′) was also claimed to be a cis-element for AtIDD2 (Fukazawa et al., 2014). The average frequency of each cis element in 3kb promoters throughout *Arabidopsis* genome ("random") is included as a comparison.

Gene name	Gene ID	Number of cis-elements contained in both DNA strands of 3000-bp upstream sequences			
		AtIDD3 binding motif (5′-TTGTCT-3′)	ZmID1 binding motif (5′-TTTGTCGTTTT-3′ or 5′-TTTTGTCG/C-3′)	AtIDD8 binding motif (5′-CTTTTGTCC-3′)	OsIDD10 binding motif (5′-GGACAAA-3′)
GA3ox1	AT1G15550	7	5	1	3
GA20ox2	AT5G51810	0	2	0	2
GID1b	AT3G63010	1	10	0	2
SCL3	AT1G50420	8	3	0	2
PRE1	AT5G39860	1	0	0	0
GL2	AT1G79840	1	0	0	0
CPC	AT2G46410	1	2	0	0
random	–	2.75	0.36	0.04	0.47

3.1.2 Signaling network underlying root epidermal cell patterning and the role of IDD1 and IDD2 in GA-regulated root-hair development

Plant root hairs are hair-like outgrowths of certain root epidermal cells that extend cell surface areas to promote the uptake of water and nutrient from soil (Libault et al., 2010). In *Arabidopsis* root epidermis, the distribution of hair (H) and non-hair (N) cell types follows a position-dependent pattern. H cells arise from root epidermal cells that overlie outside two cortical cell files (H position), whereas N cells originate from those placed outside a single cortical cell file (N position) (Duckett et al., 1994; Galway et al., 1994). At the molecular level, this epidermal cell-fate specification is determined by an intercellular gene network among different cell types (Figure 3.1) (Libault et al., 2010). In N cells, the MYB transcription factor WEREWOLF (WER) binds to the bHLH transcription factors GLABRA3 (GL3), ENHANCER OF GLABRA3 (EGL3) and the WD40-repeat protein TRANSPARENT TESTA GLABRA (TTG), forming a protein complex that induces the expression of the homeodomain leucine zipper protein GLABRA2 (GL2) and the MYB-like protein CAPRICE (CPC). GL2 is a key regulator that specifies and maintains the hairless cell fate of N cells. On the other hand, CPC expressed in N cells is transported laterally to the neighboring H cells and competes with WER for interaction with the GL3/EGL3/TTG complex. The CPC/GL3/EGL3/TTG complex represses the expression of GL2, thus releasing the inhibition of root hair development in H cells. From this, it can be seen that CPC plays a positive role in specification of hair-cell fate.

Under normal conditions, the formation of either H cells or N cells in ectopic positions is fairly rare (Wada et al., 2002). However, it was discovered in our lab that with PAC treatment, the frequency of H cells in the N position of wild-type root epidermis rises, an effect that can be reversed by addition of GA_4 (Zhong-Lin Zhang, unpublished data). This GA-mediated inhibition of root-hair cell fate in N files is a novel GA-related phenotype. Importantly, the PAC-induced increase in ectopic growth of root hairs in the N position is even more significant in *idd1-1 idd2-1* double mutant, a defect that could be complemented by introduction of IDD1 transgene driven by IDD1 native promoter (*pIDD1:IDD1-cMyc*/*idds* #1) (Zhong-Lin Zhang, unpublished data). These findings support a hypothesis that IDD1 and IDD2 boost the repressive effect of GA on root hair differentiation in the N position, consistent with the positive role of the two IDDs in GA signaling in general.

Based on their roles as transcription regulators, we propose that IDDs and DELLAs may affect root hair differentiation through modulating the transcription of known genes underlying root epidermal cell fate determination. As mentioned above, CPC and GL2 are essential positive and negative regulators of root hair development, respectively. Notably, *CPC* promoter (3kb) bears two ZmID1 binding sites, or putative IDD2 binding motifs (Table 3.1), suggesting *CPC* might be targeted by IDDs and DELLAs. Although *GL2* promoter (3kb) does not contain any IDD2 binding motifs, *GL2* transcription has been shown to be negatively regulated by DELLAs in L*er* seedlings (Qi

et al., 2014) and the expression pattern of *GL2* in root epidermis was interfered with by PAC treatment (Figure 3.2; Zhong-Lin Zhang, unpublished data), revealing that IDDs may be involved in GL2 expression regulation by antagonizing the function of DELLAs. Hence, *CPC* and *GL2* are both candidate targets of IDDs. To test whether the two important root epidermal patterning genes are truly regulated by IDDs, we performed transient expression assays in *N. benthamiana* and *A. thaliana*. These assays aimed to assess the individual and combinatorial effects of RGA and IDD1, respectively on *CPC* and *GL2* promoter activities, which would shed some light on the association of IDDs with the root epidermal patterning network, if any.

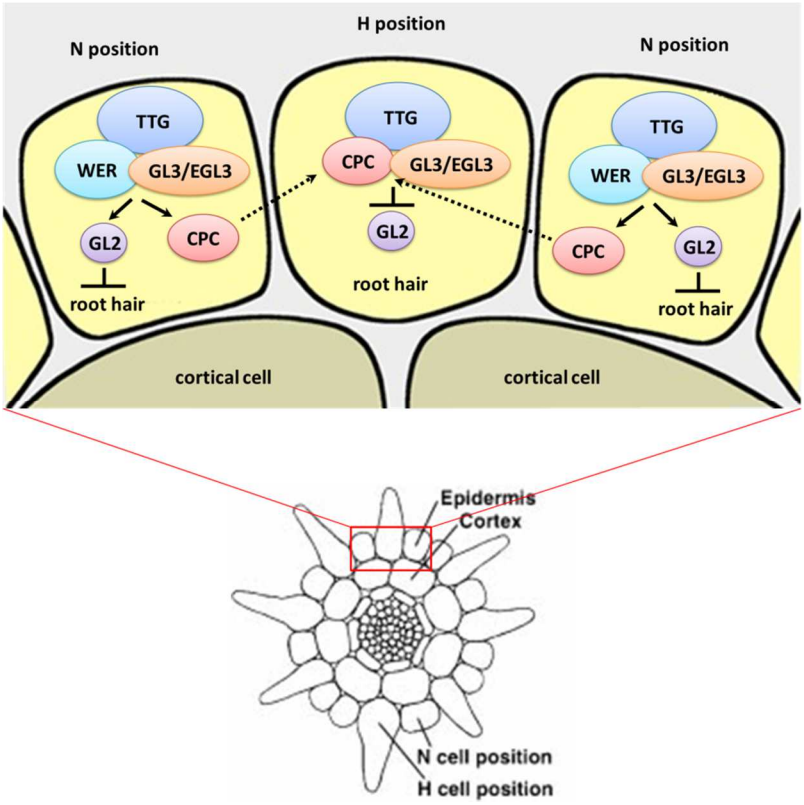

Figure 3.1 Current model of intercellular signaling network controlling the root epidermal cell patterning in *Arabidopsis*.

As shown in the schematic cross section of *Arabidopsis* root hair zone (bottom), the outermost cell layer is the epidermis and the cell layer inside epidermis is the cortex. In root epidermis, an H position is a cleft between two underlying cortical cells, whereas an N position is a place over a single cortical cell.

The top figure shows the molecular signaling network involved in root epidermal cell patterning. In epidermal cells in the N position, WER, GL3 or EGL3, and TTG form a transcriptional activator complex, which induces the expression of GL2 and CPC (Koshino-Kimura et al., 2005). GL2 promote a hairless fate in cells in the N position (Masucci et al., 1996). By contrast, CPC protein moves to the neighboring cells in the H position and competes with WER for binding to the GL3/EGL3/TTG complex (Kurata et al., 2005). The CPC/GL3/EGL3/TTG complex represses GL2 expression and cells in the H position consequently adopt a hair fate (Bernhardt et al., 2005). Diagram modified from http://labs.mcdb.lsa.umich.edu/labs/schiefel/research/.

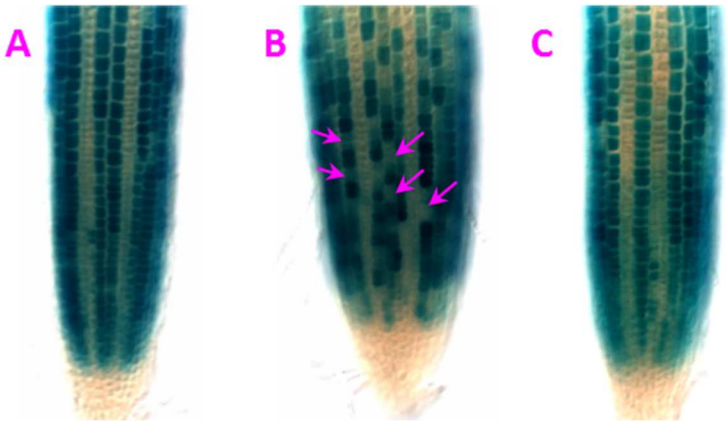

Figure 3.2 PAC treatment caused a mosaic pattern of *pGL2:GUS* expression (Zhong-Lin Zhang, unpublished data)

GUS staining in the primary root of *pGL2:GUS* seedlings grown vertically on 1/2 MS plates with no treatment, PAC (1.0 μM) treatment or GA_4 (0.1 μM) treatment. Note PAC treatment caused mosaic spots in the N position of epidermis in primary roots of the *pGL2:GUS* transgenic plants, whereas GA_4 treatment almost make no difference from no treatment. Some representative mosaic spots are pointed at by arrows.

3.2 Materials and Methods

3.2.1 Plant materials

The mutants and transgenic lines for all experiments were derived from *Arabidopsis thaliana* ecotype Col-0. The homozygous mutants *idd1-1 idd2-1* and *ga1-3 idd1-1 idd2-1* and the transgenic lines *35S:cMyc-IDD1* #1 and *35S:HA-IDD2* #1 have been described in Chapter 2. The digenic line *ga1-3 35S:HA-IDD2* #1 was obtained by crossing *ga1-3* to *35S:HA-IDD2* #1. *ga1-3 35S:cMyc-IDD1* lines were obtained by *Agrobacterium*-mediated transformation of *ga1-3* plants with *35S:cMyc-IDD1* constructs as mentioned in Chapter 2.

3.2.2 Plant tissue growth and RNA analysis.

Seeds were sterilized in 10% Clorox and 0.5% SDS for 20 minutes and rinsed five times. After sterilization, seeds in WT background were directly plated on 1× MS media with 1% sucrose and 0.8% agar in petri dishes, whereas seeds in *ga1-3* background were treated with 50 μM GA_4 for 3 days at 4°C in the dark before plating. The plates were placed horizontally in continuous light at 22°C. 9-day seedlings in Col-0 background, or 8-day seedlings in *ga1-3* background, were harvested and frozen in liquid nitrogen. Total RNA was isolated from frozen whole seedlings using the RNeasy plant mini kit (Qiagen, Valencia, CA) and then treated with DNaseI using the DNA-free kit (Life Technologies), according to manufacturers' instructions. 0.5 μg of DNaseI-treated RNA was used to synthesize cDNA using Transcriptor First Strand cDNA Synthesis kit (Roche

Diagnostics). qRT-PCR was performed using Faststart universal SYBR Green Master (Rox) (Roche Diagnostics) with 50 ng cDNA and 0.5 μM primers (see Appendix A for primer sequences) in a Roche LightCycler (Roche Diagnostics). The housekeeping gene *Exp-PT* (At4g33380) was used as the normalization control of data from qRT-PCR. The relative mRNA level of tested genes is the mean ± SEM (the standard error of the mean) of two biological repeats including two technical repeats in each. A Student's t test was performed with the significance cutoff set to be 0.05.

3.2.3 Plasmid constructs for transient expression assays

All the PCR amplifications were conducted with Phusion High-Fidelity DNA polymerase (New England Biolabs, Ipswich, MA) unless otherwise noted. The PCR-amplified fragments in all constructs were verified by DNA sequencing to ensure that the cloned inserts are error-free. Sequences of primers used are listed in Appendix A.

3.2.3.1 Effector constructs for tobacco and *Arabidopsis* transient expression

The plasmids *p35S:HA-RGA* and *p35S:HA-GAI* were constructed before in our lab (Rodolfo Zentella, unpublished data).

The plasmid *p35S:cMyc-IDD1* was constructed as follows (Zhong-Lin Zhang and Yuanjie Jin, unpublished data). The ORF of IDD1 was PCR amplified with oligos IDD1-CDS-5 and IDD1-CDS-3 using the full-length cDNA clone U25708 from ABRC. The amplified DNA was cloned into *pCR8* (Life Technologies, Grand Island, NY), which is referred to as pCR8-IDD1_CDS hereafter. LR recombination (Life Technologies) between

pCR8-IDD1_CDS and *pEarleyGate 203* (*pEG203*) (Earley et al., 2006) was performed to create *p35S:cMyc-IDD1*.

The plasmid *p35S:cMyc-IDD2* was constructed as follows (Zhong-Lin Zhang and Yuanjie Jin, unpublished data). The ORF of IDD2 was PCR amplified with oligos IDD2-CDS 5-1 and IDD2-CDS 3-1 using the full-length cDNA clone U67269 from ABRC. The amplified DNA was cloned into *pENTR/D-TOPO* (Life Technologies, Grand Island, NY) to create *pENTR/D-IDD2 FL*. *pENTR/D-IDD2 FL* was linearized with PvuI, followed by LR recombination (Life Technologies) with *pEG203* (Earley et al., 2006) to form *p35S:cMyc-IDD2*.

The plasmid *p35S:cMyc-IDD3* was made through the following process. The ORF of MGP was PCR amplified with oligos MGP_CDS_FW and MGP_CDS_RV using cDNA of *Arabidopsis* whole seedlings. The amplified DNA was first A-tailed with Choice Taq polymerase (Denville Scientific, Metuchen, NJ) and then cloned into *pCR8* (Life Technologies, Grand Island, NY) by TA-cloning. LR recombination of *pCR8-MGP* with *pEG203* (Earley et al., 2006) was performed to obtain *p35S:cMyc-IDD3*.

The plasmid *p35S:cMyc-IDD1_m* was made as follows. An *IDD1* coding sequence fragment (*IDD1* CDS 777~1266bp) containing the desired mutations (IDD1 417-422aa: GLGLGL -> AAAAAA) at the end of it was PCR amplified using pCR8-IDD1_CDS as template and pCR8-IDD1m_F2 and pCR8-IDD1_m2_R2 as primers. A second *IDD1* coding sequence fragment (*IDD1* CDS 1249~1497bp) with the same mutations (IDD1

417-422aa: GLGLGL -> AAAAAA) introduced to the beginning of it was amplified using pCR8-IDD1_CDS as template and pCR8-IDD1_m2_F1 and pCR8-IDD1m_R1 as primers. The two primary PCR products were purified by Zymoclean Gel DNA Recovery Kit (Zymo Research, Irvine, CA) and combined as template to amplify an integrate piece by their overlapping region, using primers pCR8-IDD1m_R1 and pCR8-IDD1m_F2. This secondary PCR product was first digested by restriction enzymes HindIII and SacI, and then cloned into HindIII-SacI site in pCR8-IDD1_CDS to obtain pCR8-IDD1_m. LR recombination of pCR8-IDD1_m with pEG203 (Earley et al., 2006) was performed to create *p35S:cMyc-IDD1_m*.

The plasmid *p35S:cMyc-IDD1-VP16* was made by the following procedure. The full-length IDD1 ORF with part of VP16 (Triezenberg et al., 1988) beginning sequence attached to its end was PCR amplified using pCR8-IDD1_CDS as template and pCR8-IDD1-VP16_F1 and pCR8-IDD1-VP16_R1 as primers. In parallel, the full-length VP16 coding sequence with part of IDD1 ending sequence (without stop codon) attached to its beginning was PCR amplified using *pTA7001* (Aoyama and Chua, 1997) as template and pCR8-IDD1-VP16_F2 and pCR8-IDD1-VP16_R2 as primers. The two primary PCR products were purified by Zymoclean Gel DNA Recovery Kit (Zymo Research) and combined as template to create a fused piece IDD1-VP16 by PCR through their overlapping region, using primers pCR8-IDD1-VP16_F1 and pCR8-IDD1-VP16_R2. The amplified IDD1-VP16 fragment was purified and TA-cloned into *pCR8* (Life

Technologies, Grand Island, NY) to obtain pCR8-IDD1-VP16. LR recombination between *pCR8-IDD1-VP16* and *pEG203* (Earley et al., 2006) was performed to create *p35S:cMyc-IDD1-VP16*.

3.2.3.2 Reporter constructs for tobacco and *Arabidopsis* transient expression

The construct *p35S:Renilla-luciferase* (*p35S:rLUC*) as internal control has been described before (Zhang et al., 2011). The reporter construct *pSCL3:fLUC* is *pRZ502* previously made in our lab (Zhang et al., 2011). The plasmids *pGA3ox1:fLUC*, *pGA20ox2:fLUC*, *pGID1b:fLUC*, *pPRE1:fLUC*, *pPRE5:fLUC*, *pCPC:fLUC* and *pGL2:fLUC* were all derived from *pRZ502* with the following procedure. A DNA fragment of a promoter of interest (generally ~3000 bp) was PCR amplified from Col-0 genomic DNA with its corresponding primer pair (Table 3.2). After purification by Zymoclean Gel DNA Recovery Kit (Zymo Research), the amplified promoter was restriction digested with designated enzymes and then cloned into specific restriction sites in *pRZ502* as indicated in Table 3.2, replacing the *SCL3* promoter to generate a desired plasmid. All final constructs were transformed into *Agrobacterium tumefaciens* strains GV3101 and C58C1 for transient expression assays in *N. benthamiana* and *A. thaliana*, respectively.

Table 3.2: Primers and restriction enzymes invovled in cloing of reporter constructs for transient expression.

Note in some cases, restriction enzyme MfeI was used in place of EcoRI, and SalI in place of XhoI. This is feasible because MfeI and EcoRI generate compatible cohesive ends, and so do SalI and XhoI.

Plasmid to make	Primer pair used in promoter amplification	Restriction enzymes	Involved restriction sites in pRZ502
pGA3ox1:fLUC	GA3ox1pro-FW + GA3ox1pro-RV1	EcoRI + XhoI	EcoRI-XhoI
pGA20ox2:fLUC	GA20ox2pro-FW + GA20ox2pro-RV	MfeI + XhoI	EcoRI-XhoI
pGID1b:fLUC	GID1bpro-FW1 + GID1bpro-RV1	SwaI + XhoI	SwaI-XhoI
pPRE1:fLUC	PRE1pro-FW + PRE1pro-RV	EcoRI + SalI	EcoRI-XhoI
pPRE5:fLUC	PRE5pro-FW + PRE5pro-RV	EcoRI + SalI	EcoRI-XhoI
pCPC:fLUC	CPCpro-FW + CPCpro-RV2	MfeI + SalI	EcoRI-XhoI
pGL2:fLUC	GL2_promoter_FW + GL2_promoter_RV1	SwaI + XhoI	SwaI-XhoI

3.2.4 Transient expression assays in *Nicotiana benthamiana* by Agro-Infiltration

The procedure of transient expression assays in tobacco was modified from a previously published protocol (Zhang et al., 2011). After overnight growth, *Agrobacterium* cells were incubated in induction media (60 mM K_2HPO_4, 33 mM KH_2PO_4, 7.6 mM $(NH_4)_2SO_4$, 2 mM sodium citrate, 1 mM $MgSO_4$, 0.2% glucose, 0.4% glycerol, 10 mM MES, 50 μg/mL acetosyringone, pH 5.6) without antibiotics for 3 to 4 hours. Cells were then resuspended in infiltration media (0.5× MS, 10 mM MES, 150 μg/mL acetosyringone, pH 5.6) without antibiotics. *Agrobactium* strains carrying different constructs were mixed to make final OD_{600} ~ 0.6 (and 0.2 for Renilla luciferase) for each strain and infiltrated into 3 to 4-week-old *N. benthamiana* leaves by needle-less syringe. Four *N. benthamiana* leaves transiently transformed with the same combination of *Agrobactium* cultures for 48 hours were collected and piled up, where four strips of about 1 cm^2 were cut. These four-layer strips were distributed into individual microfuge tubes on ice and ground by blue pestles in 250 μl ice-cold Grinding Buffer (100 mM pH 7.0 Sodium Phosphate, 5 mM DTT, 20 ug/mL Leupeptin, 20% glycerol). The homogenate was centrifuged at top speed for 10 minutes at 4°C. 15 μl supernatant of each sample was transferred to a well of a white 96-well microtiter plate on ice. A dual-luciferase reporter assay (DLRA) system (Promega, Madison, WI) was used to quantify fLUC and rLUC activities in *N. benthamiana* leaf extract following the manufacturer's protocol with slight modifications. The measurements of luciferase activities were taken by a

VICTOR™ X5 Multilabel Plate Reader (PerkinElmer, Waltham, MA), with 0.5-second measurement time and one-second delay between repeats. First, 75 μl LAR II Reagent was dispensed to individual extract samples, followed by mixing and four-round fLUC activity reading. Secondly, 75 μl Stop & Glo® Reagent (freshly prepared by adding 50× Stop & Glo® Substrate to the required amount of Stop & Glo® Buffer to make a final 1× concentration) was dispensed to individual samples, followed by mixing and four-round rLUC activity reading. The average of the four repeats was used for further data analyses.

3.2.5 Transient expression assays in *Arabidopsis* Seedlings.

The *Agrobacterium*-mediated enhanced seedling transformation (AGROBEST) method (Wu et al., 2014) was employed with some modifications for transient expression assays in *Arabidopsis* seedlings. *Arabidopsis* seeds were sterilized in 10% Clorox and 0.5% SDS for 20 minutes prior to germination. 13~17 seeds were germinated in each well of a 6-well plate. Cells of *Agrobacterium tumefaciens* strain C58C1 transformed with plasmids of interest were used for infection. Single colonies were inoculated in 5 ml LB liquid medium containing 10 μg/mL Rifampicin, 10 μg/mL Tetracycline and 50 μg/mL Kanamycin for growth and *vir* gene pre-induction. Each sample was repeated for three wells. *Agrobacterium-Arabidopsis* were co-cultured under LD photoperiods (16-hour light/8-hour dark) at 22°C for 2-3 days prior to gene expression analysis.

The luciferase assay procedure was largely the same as mentioned in *N. benthamiana* transient expression assays, except the following steps: 1) instead of four detached *N. benthamiana* leaves, ten whole *Arabidopsis* seedlings with similar growth were picked from each well and ground in 100 μl ice-cold Grinding Buffer. 2) the VICTOR™ X5 Multilabel Plate Reader (PerkinElmer) was set to have one-second measurement time in measuring luciferase activities.

3.2.6 Immunoblotting.

The immunoblot analysis was performed as described in Section 2.2.5 except that tobacco leaves were used for protein extraction.

3.3 Results

3.3.1 IDDs and DELLAs act antagonistically on transcriptional regulation of several GA pathway feedback genes

It was reported that IDD1 acts as a repressor for GA biosynthesis and signaling genes, including DELLA targets *GA20ox2*, *GA3ox1*, *GID1b* and *SCL3*, whose transcription is all subject to GA feedback regulation (Feurtado et al., 2011; Zentella et al., 2007). To verify the results and test whether it also applies to IDD2, we compared the mRNA levels of *GA20ox2*, *GA3ox1*, *GID1b* and *SCL3* by qRT-PCR in 9-day-old whole seedlings of the wild type (Col-0), *idd1-1 idd2-1* double mutant and transgenic plants overexpressing IDD1 or IDD2. As mentioned in Chapter 2, *35S:cMyc-IDD1 #1* and *35S:HA-IDD2 #1* are the two lines that have a high level of transgene expression and exhibited prominent GA hypersensitive phenotypes, respectively among the isolated IDD1- and IDD2-overexpressing transgenic lines. Hence, *35S:cMyc-IDD1 #1* and *35S:HA-IDD2 #1* were used for the qRT-PCR assays here.

Among tested genes, *GA20ox2* and *GID1b* were both transcriptionally upregulated in *idd1-1 idd2-1* mutant than in the wild type (Figure 3.3). In contrast, transcript levels of *GA3ox1*, *GID1b* and *SCL3* in *35S:HA-IDD2 #1* seedlings were all significantly reduced compared with the wild-type counterparts (Figure 3.3). Consistent with previously published findings (Feurtado et al., 2011), these results indicate that IDD1 and IDD2 function as transcriptional repressors of important GA biosynthetic genes and positive signaling transducers. Note that none of these genes displayed a

significantly altered expression level in *35S:cMyc-IDD1 #1* seedlings (Figure 3.3). A possible reason for this is that the degree of IDD1 overexpression in *35S:cMyc-IDD1 #1* is not high enough to repress the genes whose transcription is already pretty low due to abundant endogenous GA (Zentella et al., 2007). In order to circumvent this issue, the same assays were carried out in IDD mutant and transgenic lines in *ga1-3* background, because the amounts of *GA20ox2*, *GA3ox1*, *GID1b* and *SCL3* transcripts are known to be higher under GA-deficient background (Zentella et al., 2007). The results are largely similar to what happened in the wild-type background (Figure 3.4). Notably, however, the transcription of *GA20ox2* was significantly reduced in IDD overexpressors in *ga1-3* but not in Col-0 background (Figure 3.4). The general trend of gene upregulation owing to *idd* mutations, and even more obvious inhibitory effects of IDD overexpression on GA feedback genes like *GA20ox2*, further support that IDDs act as transcriptional repressors of above genes. Taken together, these expression analyses confirmed the contribution of IDD1 and IDD2 to GA feedback regulation in plants, and also indicated there must exist other regulators involved in GA feedback process, based on the minor change in mRNA levels of tested genes in *idd1-1 idd2-1* double mutant.

Since DELLAs and IDDs function oppositely in transcriptional regulation of DELLA targets *GA20ox2*, *GA3ox1*, *GID1b* and *SCL3*, chances are that DELLAs and IDDs antagonize each other's transactivity through direct protein-protein interaction. To test such a possibility, we conducted transient expression assays using *N. benthamiana*

(Zhong-Lin Zhang and Yuanjie Jin, unpublished data). ~3kb promoters of *GA20ox2*, *GA3ox1*, *GID1b* and *SCL3* were each cloned into the reporter constructs, where they were fused with a fLUC gene (*pGA20ox2:fLUC, pGA3ox1:fLUC*, *pGID1b:fLUC* and *pSCL3:fLUC*; also see Figure 3.5A). *p35S:cMyc-IDD1* and *p35S:HA-RGA* were used as effectors, and the *p35S:rLUC* was incorporated as an internal control (Figure 3.5A). As expected, overexpression of IDD1 alone caused a drastic decrease in reporter activities of all four promoters (Figure 3.5B). Overexpression of RGA alone, on the other hand, resulted in universal upregulation of tested promoter activities by at least two fold (Figure 3.5B). For reporters *pGA20ox2:fLUC, pGID1b:fLUC* and *pSCL3:fLUC*, coexpression of RGA and IDD1 showed an intermediate effect on their activities between RGA and IDD1 alone (Figure 3.5B), suggesting that RGA and IDD1 interact and interfere with each other in regulating the corresponding genes. *pGA3ox1:fLUC* is exceptional, though, in that the repression of *pGA3ox1:fLUC* by IDD1 was totally masked by RGA when IDD1 and RGA were coexpressed (Figure 3.5B). To sum up, these transient expression studies recapitulated the respective transregulatory effects of IDDs and DELLAs on a few canonical DELLA direct targets, and also elucidated the antagonistic relationship of IDDs and DELLAs in regulation of all the target genes but GA3ox1.

Although *GA20ox2*, *GA3ox1*, *GID1b* and *SCL3* are negatively regulated by IDDs and their promoters contain various numbers of IDD2 cis-elements (Table 3.1), ChIP-qPCR experiments using transgenic plants expressing IDD1-4×cMyc under the control

of *IDD1* native promoter (*pIDD1:IDD1-cMyc/idds* #1) could not detect binding of IDD1 protein to any of their promoters (Zhong-Lin Zhang, unpublished data). However, it may be too early to conclude that none of these genes are direct targets of IDDs (see Section 3.3.2).

The inhibition of above GA biosynthetic and signaling genes by IDDs, whether direct or not, is more like part of GA feedback, which does not explain the positive role of IDDs in cell elongation as shown by their mutant and transgenic phenotypes. To explore the mechanism of how IDDs promote GA-induced cell elongation, we tested if *PRE1*, a putative DELLA target boosting cell elongation (Bai et al., 2012b; Lee et al., 2006; Oh et al., 2012), is regulated by IDDs. Expression assays showed that *PRE1* mRNA level is reduced almost by a half in *idd1-1 idd2-1* mutant, while it is elevated by around 2 fold in *35S:HA-IDD2* #1 plants (Figure 3.3). However, in *35S:cMyc-IDD1 #1* plants, transcription of *PRE1* was slightly lowered, inconsistent with the observations in *idd1-1 idd2-1* and *35S:HA-IDD2* #1 plants (Figure 3.3). We also performed transient expression assays using *N. benthamiana*, with *pPRE1:fLUC* as the reporter (Figure 3.5A). To our surprise, *pPRE1:fLUC* activity was significantly suppressed and upregulated by IDD1 and RGA alone, respectively (Figure 3.5B), a pattern contradictory to what occurred in expression assays in *idd1-1 idd2-1* and *35S:HA-IDD2* #1 plants (Figure 3.3). Thus, the role of IDDs in transcriptional control of *PRE1* is still illusive.

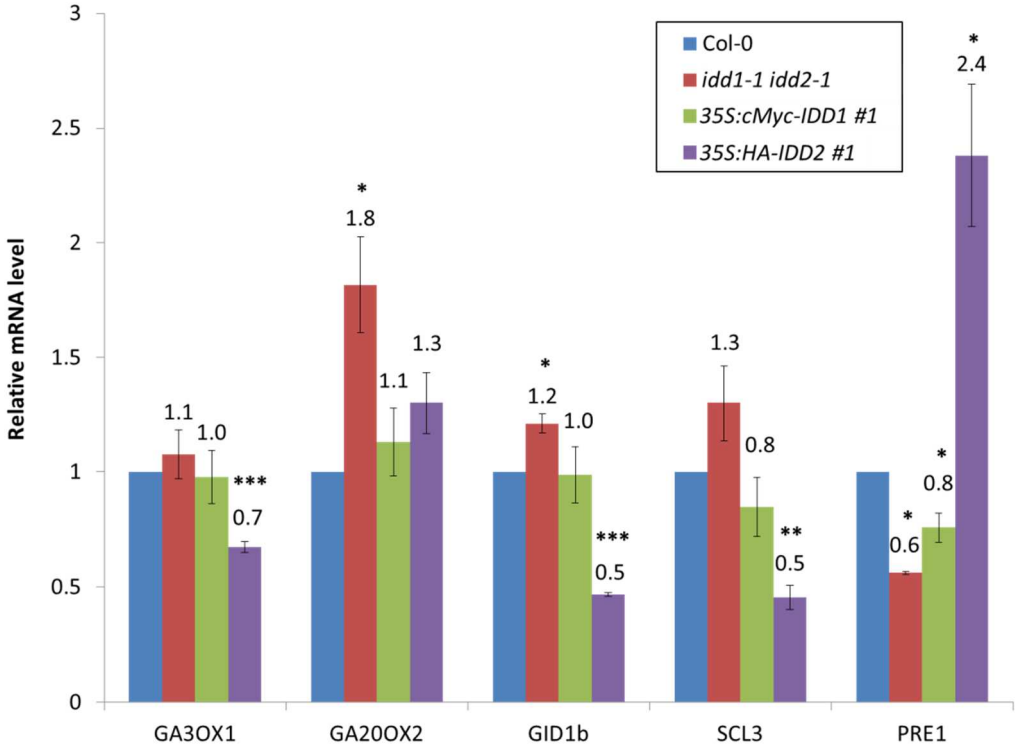

Figure 3.3 Relative mRNA levels of DELLA targets in 9-day-old seedlings in the Col-0 background.

The housekeeping gene *Exp-PT* (At4g33380) was used to normalize different samples. The mRNA level of each gene in Col-0 was arbitrarily set to 1. Data represent the average of four qRT-PCR measurements ± SE. *: $p < 0.05$. **: $p < 0.01$. ***: $p < 0.001$.

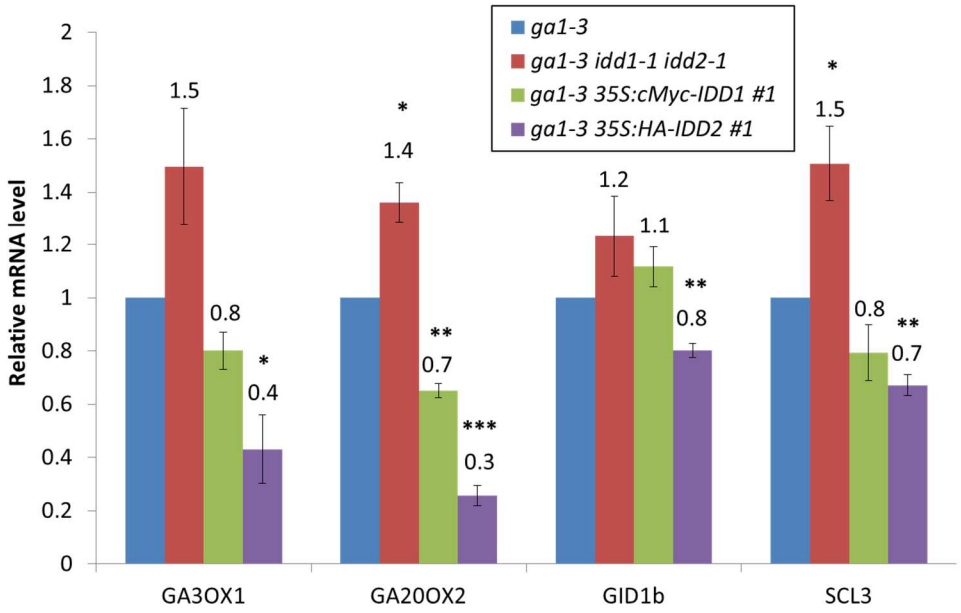

Figure 3.4 Relative mRNA levels of DELLA targets in 8-day-old seedlings in the *ga1-3* background.

The housekeeping gene *Exp-PT* (At4g33380) was used to normalize different samples. The mRNA level of each gene in Col-0 was arbitrarily set to 1. Data represent the average of four qRT-PCR measurements ± SE. *: $p < 0.05$. **: $p < 0.01$. ***: $p < 0.001$.

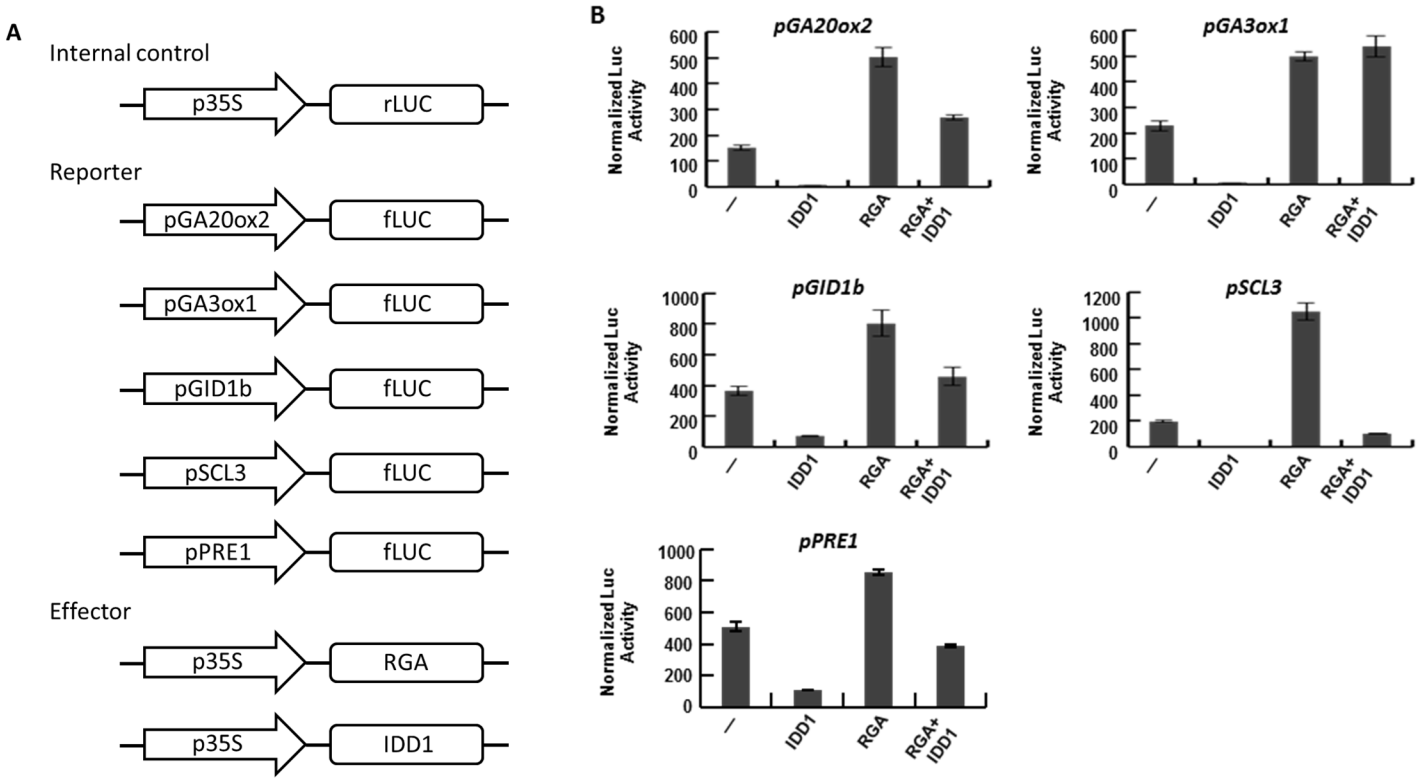

Figure 3.5 IDD1 and RGA antagonize each other in regulation of canonical DELLA targets from tobacco transient expression studies

(A) Schematic representations of the internal control, reporter and effector constructs.

(B) The reporter activities of *pGA20ox2:fLUC*, *pGA3ox1:fLUC*, *pGID1b:fLUC*, *pSCL3:fLUC* and *pPRE1:fLUC*, respectively with different combinations of effectors (most data were generated by Zhong-Lin Zhang, except assays with *pPRE1:fLUC*). Bars marked — correspond to control experiments in which no effectors were transformed. Data represent the average value ± SE of four replicates.

3.3.2 The inhibitory effect of IDD1 and IDD2 is not conferred by the putative repression motif GLGLGL

In addition to IDD1 and IDD2, AtIDD homologs IDD3, -4, -5, -9 and -10 have also been identified as DELLA interactors and more interestingly, they cooperate with DELLAs to activate their common target *SCL3* (Fukazawa et al., 2014). The distinct functions of these IDD proteins as opposed to IDD1 and IDD2 likely stem from differences in their structures. As reflected by the sequence alignment, IDD1 and IDD2 share a potential repression motif (GLGLGL) near their C termini (at 416aa/500aa in IDD1, and at 368aa/452aa in IDD2), which does not exist in other DELLA-interacting IDDs (Figure 3.6) (Mitsuda et al., 2011). This putative repression motif resembles the so-called EAR-like motif XLXLXL, a plant-specific repression motif where X represents a non-hydrophobic A, R, N, D, C, Q, E, G, H, K, M, S or T residue (Hiratsu et al., 2004; Mitsuda et al., 2011).

To verify if the hexapeptide GLGLGL is required for the repressive activity of IDD1 and IDD2 in transcription, we created a mutant version of IDD1 by replacing all the residues of the EAR-like motif with Ala residues, designated as IDD1-m (Figure 3.6), and tested the effects of IDD1-m with or without RGA on *SCL3* promoter activity in comparison with IDD1 using transient expression assays (Figure 3.7). In the same assays, we also included effectors expressing IDD3 and a chimeric protein IDD1-VP16 (*p35S:cMyc-IDD1-VP16*; see Figure 3.7A), in which the VP16 activation domain is fused to the C terminal of IDD1 (Triezenberg et al., 1988). We found that IDD1-m showed a

repressive activity similar to that of IDD1, either with or without RGA, indicating that the EAR-like motif is not essential to IDD1 function (Figure 3.7B). In contrast to a dramatically reduced reporter activity caused by overexpression of IDD1, the transient expression of IDD1-VP16 resulted in 2.2-fold stimulation of the *SCL3* reporter activity (Figure 3.7B). Similarly, coexpression of IDD1-VP16 and RGA enhanced *pSCL3:fLUC* much more than coexpression of IDD1 and RGA (Figure 3.7B). These results suggest that the strong repressive activity of IDD1 can be overridden by VP16 and also provide evidence that *SCL3* is a direct target of IDD1 and that the IDD1/RGA complex does not dissociate from *SCL3* promoter.

It has been reported that the IDD3/RGA complex induced *SCL3* promoter activity by around 40 fold in transient expression assays using *Arabidopsis* protoplasts (Yoshida et al., 2014). However, this result was not repeatable in our transient expression assays using tobacco leaves. Coexpression of IDD3 and RGA only increased the reporter gene expression by around 10 fold, similar to what overexpression of RGA alone did (Figure 3.7B). This discrepancy might be attributed to the difference in the experimental system. We also noted that IDD3 had a much lower protein level than IDD1 did in our system (Figure 3.8), which may lead to insufficient amounts of the IDD3/RGA complex. In an attempt to avoid these potential issues and better mimic *Arabidopsis* physiology, we tested transient expression assays in *Arabidopsis* seedlings with the above-described reporter and effectors following a recently published protocol

AGROBEST (Wu et al., 2014). The results exhibited some inconsistencies with data from tobacco transient assays. For instance, in the new system, IDD1 did not show any inhibitory effect on *SCL3* promoter activity, and the inductive effect of RGA was less dramatic than in tobacco (Figure 3.7C). There were common patterns, though. IDD1-m showed almost the same effects as wild-type IDD1, and IDD1-VP16 significantly promoted *pSCL3:fLUC* activity again, to name a few (Figure 3.7C). Although this time the IDD3/RGA complex appeared to confer a slightly higher induction of the reporter activity than RGA itself (Figure 3.7C), the extent was still not as substantial as published data (Yoshida et al., 2014). Together, these observations provide some insights into the possible roles of IDD1, IDD3 and RGA in regulating downstream genes. However, it remains to be determined which transient expression system can reveal the true functions of IDDs. Our initial results indicate that the AGROBEST protocol for transforming whole *Arabidopsis* seedlings is not as efficient as the tobacco system, but tobacco is a heterologous system for testing *Arabidopsis* protein functions. Based on our results, however, the hexapeptide GLGLGL alone in IDD1 and IDD2 is unlikely to be the transcription repression motif.

Figure 3.6 Putative repression motifs in IDD1 and IDD2, and the mutations introduced in IDD1-m

The amino acid sequence of the putative EAR-like motifs (in red) and their positions in IDD1 and IDD2 proteins are shown. Also shown are the mutations (in red) introduced into the putative EAR-like motif in IDD1-m.

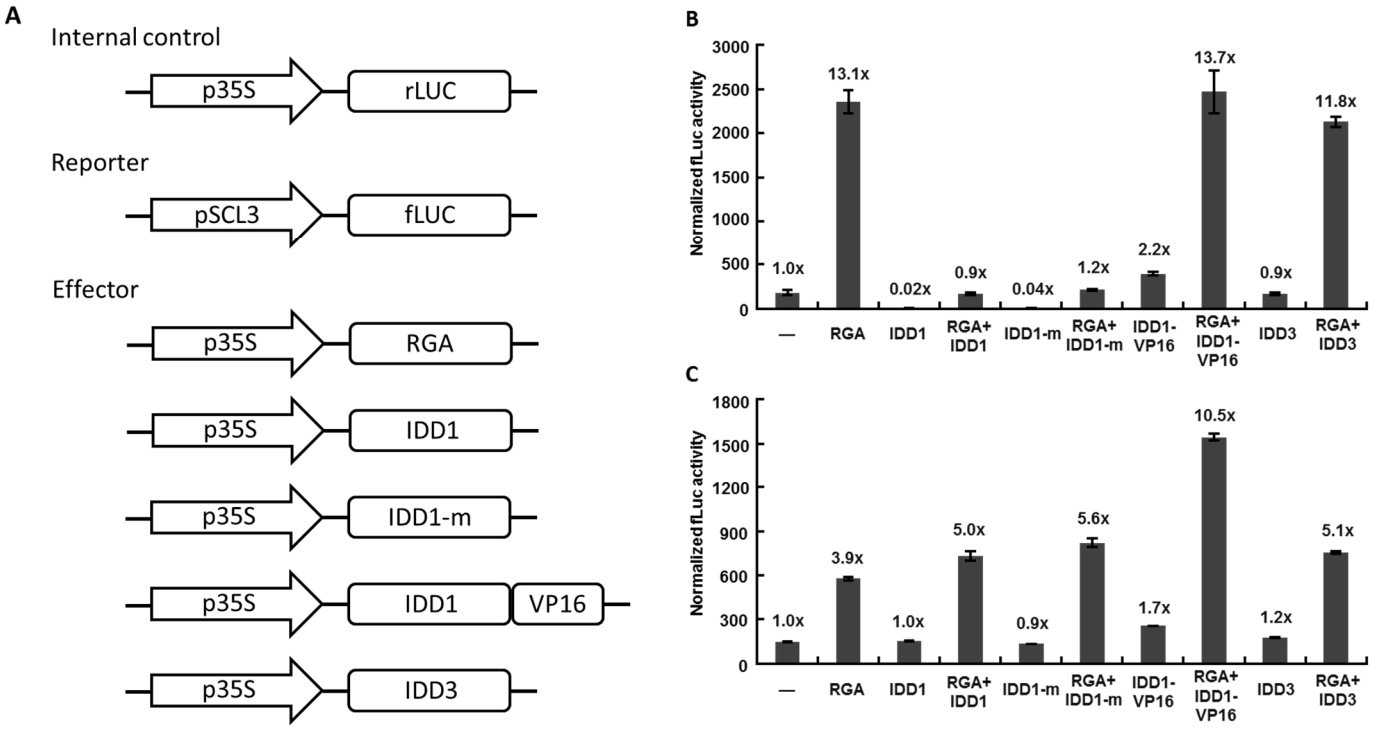

Figure 3.7 The effects of IDD1, IDD1-m, IDD1-VP16 and IDD3 with or without RGA on SCL3 promoter activity in tobacco and *Arabidopsis* transient expression assays.

(A) Schematic representations of the internal control, reporter and effector constructs.

(B) and (C) show the reporter activities of *pSCL3:fLUC* with different combinations of effectors in tobacco and *Arabidopsis* transient expression assays, respectively. Bars marked — correspond to control experiments in which no effectors were transformed. Data represent the average value ± SE of four replicates.

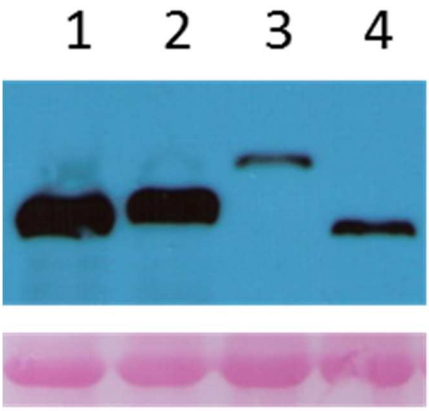

Figure 3.8 The protein levels of IDD3 and IDD1-VP16 are much lower than those of IDD1 and IDD1-m in tobacco transient expression assays

Western blot analysis comparing expression levels of effectors (1) IDD1, (2) IDD1-m, (3) IDD1-VP16 and (4) IDD3 without RGA using tissues from tobacco transient expression assays whose results are shown in Figure 3.8B. Bottom: Ponceau Staining to check for equal loading of protein samples.

3.3.3 IDD1 and IDD2 antagonize DELLA activity in transcriptional regulation of CPC and GL2

Our recent findings showed that under GA-deficient condition (PAC treatment or *ga1-3* background), more root hairs were formed in the N position of *Arabidopsis* root epidermis, whereas GA treatment or mutation(s) in major DELLA genes rescued these phenotypes in varying degrees, suggesting that ectopic formation of root hairs is inhibited by GA-mediated removal of DELLAs (Zhong-Lin Zhang, unpublished data). The positive effect of PAC on N-position root hair growth was enhanced in *idd1-1 idd2-1* double mutant and suppressed by overexpression of IDD1, from which we see IDD1 and IDD2 promote GA action in this process (Zhong-Lin Zhang, unpublished data). Epistasis studies in *ga1-3* background revealed that the root hair phenotype of *idd1-1 idd2-1* was greatly diminished by *rga-28* single mutation, indicating that IDDs and DELLAs antagonistically regulate root hair differentiation through physical interaction (Zhong-Lin Zhang, unpublished data).

It is unclear how IDDs and DELLAs get involved in root epidermal cell patterning. Given that IDDs and DELLAs are transcription regulators, it is possible that they modulate the expression of genes important for root hair cell fate specification. CPC and GL2, the crucial positive and negative regulator of hair-cell differentiation, respectively (Libault et al., 2010), are two such candidates based on following observations: (1) In *Arabidopsis* root, *CPC* and *GL2* are both preferentially transcribed in N cells of root epidermis, and CPC protein is then translocated to H cells (Masucci et al.,

1996; Wada et al., 2002). These expression patterns overlap with those of IDD1 and RGA, since IDD1 and RGA are expressed universally in all root-cell types (Zhong-Lin Zhang, unpublished data). (2) In the presence or absence of PAC, *cpc-1 idd1-1 idd2-1* triple mutant was indistinguishable from *idd1-1 idd2-1* plants in root hair numbers in the N position, suggesting that CPC acts downstream of IDDs (Zhong-Lin Zhang, unpublished data). (3) *CPC* promoter contains two ZmID1 cis-elements (Table 3.1), one of which sits between −2330 and −2323 and is also an IDD2 cis-element (5′-TTTTGTCG-3′) (Fukazawa et al., 2014). Moreover, binding of IDD1 and RGA proteins to a region close to the IDD2 cis-element in *CPC* promoter was confirmed by ChIP experiments (Zhong-Lin Zhang, unpublished data). (4) PAC treatment abolished GL2 expression in some cells in the N position, which could be caused by accumulation of DELLA proteins in those cells (Zhong-Lin Zhang, unpublished data; Figure 3.3). In agreement with this, evidence shows that DELLAs inhibit GL2 expression by repressing the GL1/GL3/EGL3/TTG complex to regulate trichome initiation, a differentiation process of shoot epidermal cells analogous to root hair formation (Qi et al., 2014; Schiefelbein, 2003). As DELLA interactors, IDDs might also participate in modulating the expression of GL2.

In order to investigate the roles of IDDs and DELLAs in transcriptional regulation of *CPC* and *GL2* in detail, *CPC* and *GL2* transcript levels were measured by qRT-PCR using whole-root tissues from wild type, *idd1-1 idd2-1* mutant, and transgenic plants expressing IDD1 (Zhong-Lin Zhang, unpublished data). No significant difference

was detected. These results may not accurately reflect the truth, however. As a result of the restrictive expression of *CPC* and *GL2* in N cells, mRNA amounts of the two genes are diluted in whole-root lysate and the changes could be too subtle to be detectable.

As an alternative approach, transient expression assays were conducted in *N. benthamiana*. Since DELLAs repress transactivity of the GL1/GL3/EGL3/TTG1 complex through interaction with its components GL3, EGL3 and the MYB transcription factor GL1 that is related to WER (Qi et al., 2014; Schiefelbein, 2003), we propose that DELLAs also interact with the WER/GL3/EGL3/TTG1 complex to regulate their targets *CPC* and *GL2* (Koshino-Kimura et al., 2005; Ryu et al., 2005). To test this hypothesis, we included WER and GL3 as effectors (Figure 3.9A), as EGL3 is functionally redundant with GL3 (Bernhardt et al., 2003; Bernhardt et al., 2005; Zhang et al., 2003) and a previous study demonstrated that GL1 and GL3 are required and sufficient to activate the transcription of GL2 (Wang and Chen, 2008). *pCPC:fLUC* and *pGL2:fLUC* served as reporters, and the internal control was *p35S:rLUC*, again (Figure 3.9A). As we expected, WER/GL3 complex greatly enhanced the expression of *pGL2:fLUC* and *pCPC:fLUC* (Zhong-Lin Zhang and Yuanjie Jin, unpublished data). In the presence of the WER/GL3 complex, *pGL2:fLUC* activity was induced by RGA, was significantly repressed by IDD1, and was intermediate when RGA and IDD1 were coexpressed (Rodolfo Zentella and Yuanjie Jin, unpublished data; Figure 3.9B). A similar pattern was seen for *pCPC:fLUC* activity, except that the inductive effect of RGA appeared less dramatic (Rodolfo Zentella and

Yuanjie Jin, unpublished data; Figure 3.9C). Taken together, we may conclude that DELLAs and IDDs likely function as transcription activators and repressors, repressively, and antagonize each other's transactivity, in regulation of *CPC* and *GL2*.

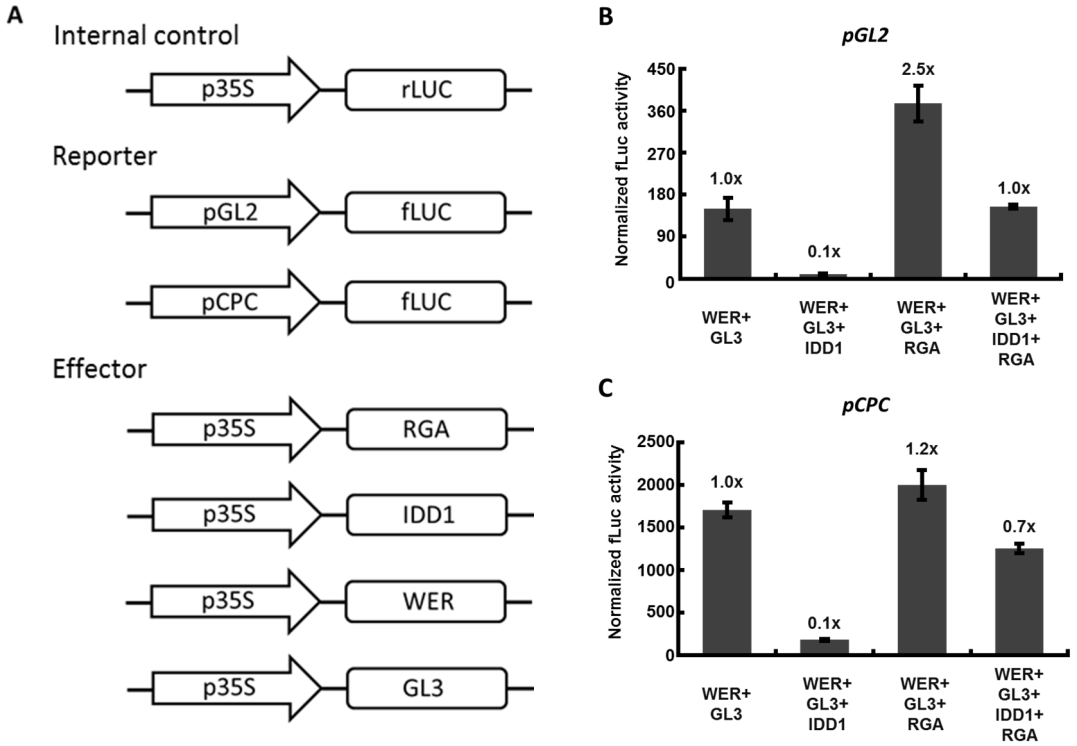

Figure 3.9 The effects of IDD1 and RGA on the expression of GL2 and CPC in the presence of WER and GL3.

(A) Schematic representations of the internal control, reporter and effector constructs.

(B) and (C) show the reporter activities of *pGL2:fLUC* and *pCPC:fLUC*, respectively, with indicated combinations of effectors. The normalized fLUC activity when effectors *p35S:cMyc-WER* and *p35S:cMyc-GL3* were cotransformed was set to 1.0× for both reporters. Data represent the average value ± SE of four replicates.

3.4 Discussion

In this chapter, we confirmed the negative role of IDD1 and IDD2 in transcription regulation of canonical DELLA targets *GA20ox2*, *GA3ox1*, *GID1b* and *SCL3 in planta* (Feurtado et al., 2011). It is noteworthy that the decrease in transcript levels of these DELLA targets in *35S:cMyc-IDD1* #1 appeared not so dramatic as in *35S:HA-IDD2* #1, whether under GA-deficient conditions or not. Most likely, this is attributed to a lower magnitude of transgene expression in *35S:cMyc-IDD1* #1 than in *35S:HA-IDD2* #1, as discussed in Chapter 2. In agreement with this possibility, IDD1 and IDD2 showed almost the same effects on expression of above DELLA targets in tobacco transient expression assays (Zhong-Lin Zhang, unpublished data). Thus, IDD1 and IDD2 function redundantly as transcriptional repressors of above-described DELLA targets.

From our tobacco transient expression assays, we also found that IDD1 and RGA oppose each other through interaction in regulating the DELLA targets *GA20ox2*, *GID1b* and *SCL3*. GAI played a similar role as RGA when it was substituted for RGA (Data not shown). In contrast, in transient expression assays by Fukazawa et al. using *Arabidopsis* protoplast, neither GAI nor IDD2 alone affects the expression of *GA20ox2*, *GA3ox1* and *GID1b*, whereas coexpression of GAI and IDD2 strongly activates the expression of these genes (Fukazawa et al., 2014), from which they concluded that IDD1 and IDD2 function as transcriptional scaffolds that do not regulate gene expression by themselves. Their observations are different from our results. However, some of their data do not seem to

support their conclusion. First of all, in their study, despite the marginal effect IDD2 alone had on target gene expression, IDD1 alone exerts an obvious inhibitory effect comparable to our results. This discrepancy is confusing, given the fact that IDD1 and IDD2 share a high homology. Secondly, their *idd1 idd2* double mutant and IDD2 overexpressors exhibited strikingly late- and early-flowering phenotypes, respectively under SD condition, phenotypes relevant to altered GA signaling. It would be surprising that the elevated GA signaling resulted from IDD2 overexpression does not cause a feedback downregulation of *GA20ox2*. Thirdly, the effect of GAI alone in their transient assays was not shown in the paper, making it impossible to verify whether GAI alone has any inductive activity in their experiment and how this inductive activity compares with that of the IDD2/GAI complex. Together, more convincing evidence is needed to resolve the disagreement between their claim and ours.

Although IDD2 has been shown to associate with the promoters of *GA20ox2* and *GID1b* by gel retardation assays and ChIP assays (Fukazawa et al., 2014), our ChIP-qPCR assays failed to detect binding of IDD1-4×cMyc proteins to those promoters. Since we used transgenic plants expressing IDD1-4×cMyc driven by the endogenous promoter of IDD1, our results are supposed to be more reliable than the published data obtained using an ectopic misexpression line (*p35S:Myc-IDD2*). However, this might not be the case in reality. For instance, we did not detect binding of IDD1-4×cMyc to *SCL3* promoter, either, but IDD1 probably associate with *SCL3* promoter based on the results

of transient assays with IDD1-VP16. It is possible that our ChIP-qPCR assays did not work well due to technical issues, or the binding sites of IDD1 in the promoters were not covered by the region amplified by our qPCR primers. Hence, before we conclude that IDD1 and IDD2 have differences in their direct targets, a more extensive promoter scanning by ChIP-qPCR needs to be performed to double check if any of the genes *GA20ox2*, *GA3ox1*, *GID1b* and *SCL3* subject to IDD1 repression are IDD1 direct targets.

As shown in our tobacco and *Arabidopsis* transient expression experiments, the repressive activity of IDD1 and IDD2 is not conferred by their putative EAR-like motif GLGLGL (Mitsuda et al., 2011). It is possible that GLGLGL is not a real repression motif. An alternative possibility is that there exists more repression motifs other than the EAR-like motif and different repression motifs share some redundancy in transcriptional function of IDD1 and IDD2. For example, WUSCHEL, an *Arabidopsis* transcription factor that contains two repression motifs, the WUS box and the EAR-like motif, maintained its original repressive activity when either domain was mutated, whereas lost the repressive activity when both domains were mutated (Ikeda et al., 2009).

Interestingly, our ChIP assays showed the association of IDD1 with a region of *CPC* promoter containing the IDD2 target sequence, which implies that IDD1 and IDD2 likely share the same cis-element at least in *CPC* promoter. Further, the concurrent binding of RGA and IDD1 to the same region of CPC promoter reveals that RGA associates with CPC promoter by forming a complex with IDD1 instead of blocking the

DNA-binding ability of IDD1. These results, together with data from corresponding transient expression assays, unveil that IDD1 and RGA directly repress and promote *CPC* expression, respectively. Although *GL2* also seems to be transcriptionally inhibited by IDD1 while activated by RGA in transient expression experiments, it is not sure whether GL2 is a direct target of IDD1 and RGA. Neither is known how to fit above transregulatory roles of IDD1 and RGA in the big picture of root hair cell patterning. For the increased ectopic root hair growth in the N position under GA-deficient condition, one explanation could be accumulation of DELLAs derepresses CPC expression in N cells partly by inhibiting IDDs and the extra CPC proteins are not able to be transported to neighboring H cells in time, leading to interference with the WER/GL3/EGL3/TTG complex and a consequent reduction in net amounts of GL2 proteins. In order to elucidate the real mechanisms underlying the involvement of IDDs and DELLAs in root hair development, more studies are yet to be done.

Contradictory to the repressive activity of RGA in GL1/GL3-induced GL2 expression (Qi et al., 2014), we observed a slight positive effect of RGA on GL2 expression with GL1/GL3 in our tobacco transient expression system (data not shown; Rodolfo Zentella, unpublished). We repeated these assays in *Arabidopsis* seedlings following the AGROBEST method (Wu et al., 2014), but the results are hard to interpret (data not shown). To avoid potential systematic issues and address the inconsistency,

future experiments should adopt an *Arabidopsis* transient expression system with an improved AGROBEST method or a more reliable approach.

Chapter 4 Conclusions and Implications

4.1 IDD1 and IDD2 antagonize DELLA function in GA-responsive phenotypes and transcriptional regulation of DELLA targets

My thesis project identified the positive roles of IDD1 and IDD2 in GA relevant phenotypes, including hypocotyl elongation, stem elongation and floral initiation. IDD1 and IDD2 promote GA signaling in root elongation and root hair development, too (Zhong-Lin Zhang, unpublished data). Using hypocotyl growth and root epidermal cell patterning as models, we unraveled the antagonistic relationship between IDDs and DELLAs in the two physiological processes. With respect to the function of IDDs in transcription regulation, we found that IDDs repress transcription of a few canonical DELLA-induced target genes, such as *GA20ox2*, *GA3ox1*, *GID1b* and *SCL3*. Further, IDDs and DELLAs antagonize each other's transactivity in regulating these genes except *GA3ox1*. The inhibition of these genes subject to GA feedback regulation also indicates that IDDs are involved in GA feedback. In addition, IDDs inhibit and DELLAs elevate the expression of root hair growth regulators CPC and GL2. When IDDs and DELLAs are coexpressed in our transient expression system, they counteract each other's effects in regulation of CPC and GL2, an observation that sheds light on the molecular mechanisms underlying the opposing roles of IDDs and DELLAs in root epidermal cell patterning. Taken together, our data are consistent with a model where IDD1 and IDD2 antagonize DELLA function in GA responses as well as GA feedback regulation (Figure 4.1).

4.2 Insights into DELLA function and GA feedback

DELLAs have been shown to mediate GA feedback by upregulating GA biosynthesis, receptor and signaling genes (Zentella et al., 2007). However, it is not well understood how DELLAs achieve this regulation without a DNA binding domain. Based on our study, IDD1 and IDD2 likely serve as two intermediate proteins that connect DELLAs with promoters of downstream GA feedback genes. The relationship between IDDs and DELLAs exemplify the complex and robust transcriptional circuit surrounding DELLAs. In the presence of GA, IDDs promote GA-responsive growth, while inhibit expression of genes in GA biosynthesis and signaling as a negative feedback; in the absence of GA, DELLAs interact with IDDs and antagonize their function in growth, but also release their repression on GA biosynthesis and signaling for a new balance. Consequently, the relevant plant growth is always coordinated and autoregulated, rendering it robust against disturbance.

4.3 Mechanisms of repressive activity in IDD1 and IDD2

It seems that IDD1 and IDD2 act as transcriptional repressors for almost all the DELLA targets tested. We have shown by transient expression assays that the repressive activity of the two IDDs is not conferred by their putative EAR-like motif GLGLGL. It remains an open question whether there exists a real repression motif for IDDs or not. Given that the target sequences of IDD2 and IDD3 are very close (Table 3.1), IDD1, IDD2 and IDD3 likely share many common target genes, such as SCL3. Hence, overexpressed

IDD1 might compete IDD3 for binding to the promoters of their common targets and by blocking the inductive activity of the IDD3/DELLA complex. If that is the case, then IDD1 and IDD2 are not transcriptional repressors *per se*, but show repressive activity by interfering with transcriptional activator complex.

Interestingly, VP16 transactivation domain is able to override the repressive activity of IDD1, making it a useful tool for further dissection of molecular mechanisms underlying IDD function. For example, transgenic plants expressing IDD1-VP16 fusion protein under the control of IDD1 native promoter can be made to circumvent the potential functional redundancy of other IDD genes and exaggerate the phenotypes of *idd1-1 idd2-1* mutant.

4.4 Potential future directions

Analogous to IDD1 and IDD2, SCL3 and PIF4 are two known DELLA interactors and also play a positive role in GA-regulated hypocotyl elongation (de Lucas et al., 2008; Zhang et al., 2011). Some preliminary data suggest that SCL3 and PIF4 share overlapping expression patterns in the hypocotyl with IDDs (data not shown), raising questions about how DELLAs control hypocotyl elongation via interacting with different proteins. It would be interesting to identify the genetic interaction between IDDs and SCL3 or PIF4 by epistasis analyses, and characterize the underlying molecular mechanisms. Also, according to previous studies, GA promotes development of stomata in hypocotyl and initiation of trichome in shoot epidermis (Chien and Sussex, 1996;

Perazza et al., 1998; Saibo et al., 2003). Because stomata and trichome patterning shares many common regulators as root hair cell patterning (Berger et al., 1998; Schiefelbein, 2003), and IDD1 was shown to be expressed in trichome and hypocotyl epidermis based on preliminary data (data not shown), it would be interesting to explore if IDDs are also involved in GA-regulated stomata and trichome patterning.

4.5 Some inconsistencies with published studies

There are several inconsistencies between our observations and previously published findings. For instance, the substantial activation of SCL3 expression by the IDD3/RGA complex was not reproducible in our transient expression assays (Yoshida et al., 2014). Another example is, Fukazawa et al. identified a drastically delayed floral initiation in their *idd1 idd2* mutant under short day conditions (Fukazawa et al., 2014), a defect not seen in our *idd1-1 idd2-1* mutant. A third case is that we failed to reproduce the repressive activity of RGA in GL1/GL3-induced GL2 expression (Qi et al., 2014), using our tobacco transient expression assays (Rodolfo Zentella, unpublished data). These discrepancies could be caused by different experimental systems (e.g., tobacco vs. Arabidopsis transient expression assay), different mutations (e.g., *idd1 idd2* used by Fukazawa et al. vs. *idd1-2 idd2-2*), different conditions, etc. Some of the inconsistent results have a tremendous impact on the validity of our model. Therefore, future experiments are needed to resolve these inconsistencies through side-by-side comparisons with published mutants and conditions.

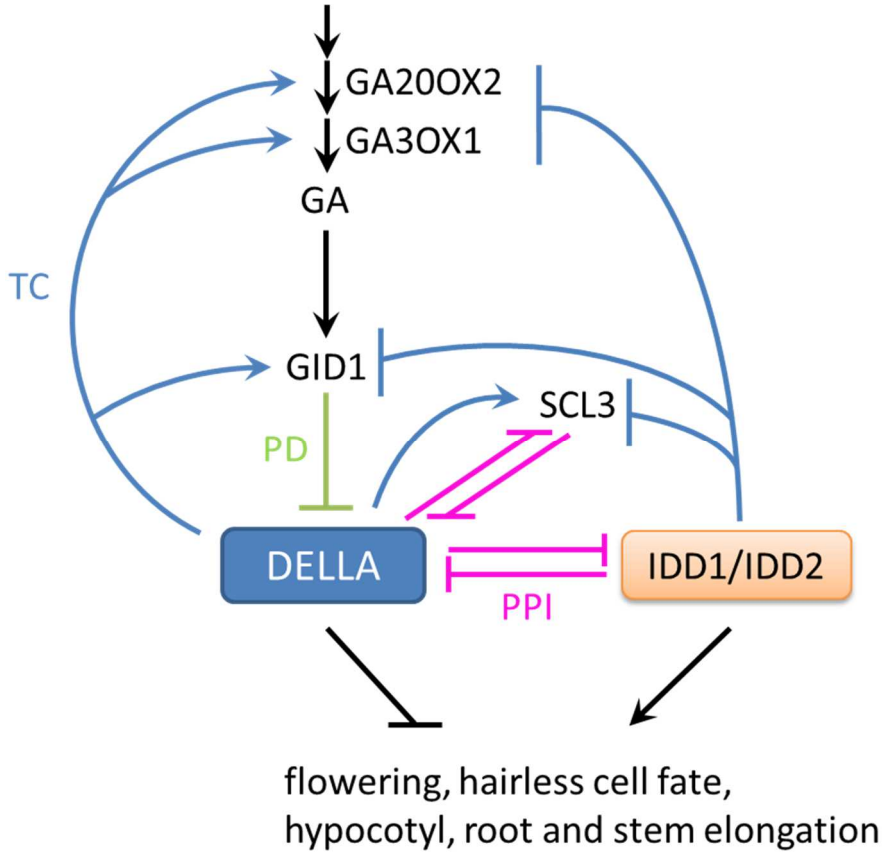

Figure 4.1 A proposed model for antagonistic interaction between IDD1, IDD2 and DELLA in regulation of GA responses and GA feedback.

Similar to another DELLA interactor SCL3, IDD1 and IDD2 antagonize DELLA function through protein-protein interaction. The two IDDs promote GA-responsive flowering, hairless cell development, hypocotyl, root and stem elongation, while repress the transcription of GA biosynthetic genes GA20ox2 and GA3ox1, GA receptor GID1b, and DELLA attenuator SCL3. PPI, protein-protein interaction (pink lines); PD, protein degradation (green lines); TC, transcription (blue lines).

Appendix A: Sequences of PCR primers

Primers	Sequences	Used for	Notes
PRE1pro-FW	ATATGAATTCgctaaatccagagaaacatttcgcag	cloning PRE1 promoter (from 3458bp upstream of start codon till the start codon)	forward primer. EcoRI site. Primers PRE1pro-FW + PRE1pro-RV generate a 3478 bp PCR product from genomic DNA
PRE1pro-RV	ATATGTCGACgttcaacaatgtggcaagaaaagacc	cloning PRE1 promoter (from 3458bp upstream of start codon till the start codon)	reverse primer. SalI site
PRE1pro-FW_seq1	TGTAAAATCTCCCTTTGCAATTT	sequencing PRE1 promoter	forward primer
PRE1pro-FW_seq2	gagggataatgagggatttcgaaa	sequencing PRE1 promoter	forward primer
PRE1pro-FW_seq3	TTTGGTTTCCTTTTCACGTTTT	sequencing PRE1 promoter	forward primer
PRE1pro-FW_seq4	TTTACAGATAAATATACAAACTGTACC	sequencing PRE1 promoter	forward primer
PRE1pro-RV_seq1	TGCCCTTAAACCACAAAACTT	sequencing PRE1 promoter	reverse primer
PRE5pro-FW	ATATGAATTCgcatactgtcaaggaaactgagat	cloning PRE5 promoter (from 4834bp upstream of start codon till start codon)	forward primer. EcoRI site. Primers PRE5pro-FW + PRE5pro-RV generate a 4854 bp PCR product from genomic DNA
PRE5pro-RV	ATATGTCGACtttcttgtttttactttgtgattaggtg	cloning PRE5 promoter (from 4834bp upstream of start codon till start codon)	reverse primer. SalI site
PRE5pro-FW_seq1	TAACCGCGAACTTTCAAAT	sequencing PRE5 promoter	forward primer
PRE5pro-FW_seq2	ATGAATATCCCAATGCCGAG	sequencing PRE5 promoter	forward primer
PRE5pro-FW_seq3	CATAAAAACATCGTGGAGCCT	sequencing PRE5 promoter	forward primer
PRE5pro-FW_seq4	TTCCGAATATGAGAACGAACC	sequencing PRE5 promoter	forward primer
PRE5pro-FW_seq5	CATTTATGCTATGTAGTATTGTTCTTG	sequencing PRE5 promoter	forward primer
PRE5pro-FW_seq6	GATGCGAAGCTAAGGCAAAC	sequencing PRE5 promoter	forward primer
PRE5pro-FW_seq7	AATCTGAGATCTGAAGCAACCA	sequencing PRE5 promoter	forward primer

PRE5pro-FW_seq8	GTAATGAAATGAAAATAGAAAGTCAA	sequencing PRE5 promoter	forward primer
CPCpro-FW	CATGCAATTGtagccaatacctttttactttcatagc	cloning CPC promoter (from 3159bp upstream of start codon till start codon)	forward primer. MfeI site. Primers CPCpro-FW + CPCpro-RV2 generate a 3179 bp PCR product from genomic DNA
CPCpro-RV2	ATATGTCGACcgaactaatctgaagacacgaaac	cloning CPC promoter (from 3159bp upstream of start codon till start codon)	reverse primer. SalI site
CPCpro-seq1	aaactctgaatgcttctatttt	sequencing CPC promoter	forward primer
CPCpro-seq2	agcccatattgttttgaataggccc	sequencing CPC promoter	forward primer
CPCpro-seq3	ttcccgttttgctgttctcttc	sequencing CPC promoter	forward primer
CPCpro-seq1_RV	aaaatagaagcattcagagttt	sequencing CPC promoter	reverse primer
GL2_CDS_FW	atgtcaatggccgtcgacatgt	cloning GL2 (GL2.1) coding sequence from cDNA	forward primer. Primers GL2_CDS_FW + GL2_CDS_RV generate a 2244 bp PCR product
GL2_CDS_RV	tcagcaatcttcgattgtagacttc	cloning GL2 (GL2.1) coding sequence from cDNA	reverse primer
GL2_CDS_seq1	TCAAAGAGACACCACATCCG	sequencing GL2 (GL2.1) coding sequence	forward primer
GL2_CDS_seq2	CTCGAGAAGTCCCGTATTGC	sequencing GL2 (GL2.1) coding sequence	forward primer
GL2_CDS_seq3	GAAGTGTACTTCGTGAGAAGCTG	sequencing GL2 (GL2.1) coding sequence	forward primer
GL2_CDS_seq4	TGACACAAAGCTTCTACCGC	sequencing GL2 (GL2.1) coding sequence	forward primer
GL2_promoter_FW	CGCGATTTAAATctctacttgagagatatatctgg	cloning GL2 promoters, either including or excluding a short ORF in 5' UTR	forward primer. SwaI site.
GL2_promoter_RV1	ATCGCTCGAGtttttcttcttaatattcgattttaata	cloning GL2 promoter (from 3584bp upstream of start codon till the start codon, including a short ORF in 5' UTR)	reverse primer. XhoI site. Primers GL2_promoter_FW + GL2_promoter_RV1 generate a 3606 bp PCR product from genomic DNA
GL2_promoter_RV2	GCATCTCGAGatatatatgatgagcaaaattcaaattt	cloning GL2 promoter (from 3584bp upstream of start codon till 35bp upstream of start codon, excluding a short	reverse primer. XhoI site. Primers GL2_promoter_FW + GL2_promoter_RV2 generate a 3571 bp PCR product from

		ORF in 5' UTR)	genomic DNA
GL2_promoter_seq1_rv	AGGGTGCCTTGGTTTGCT	sequencing GL2 promoter	reverse primer
GL2_promoter_seq2_rv	AACCGCAAAACAAAAGATGG	sequencing GL2 promoter	reverse primer
GL2_promoter_seq3_rv	TTACCCGTGTTGGCAAACTT	sequencing GL2 promoter	reverse primer
GL2_promoter_seq4	GGATCGTCGTCACTTGTTGA	sequencing GL2 promoter	forward primer
GL2_promoter_seq5	TTTAAGAGCATGTGGTGAATG	sequencing GL2 promoter	forward primer
GL2_promoter_seq6	TTGTCAAATATTAAAACAACATACACA	sequencing GL2 promoter	forward primer
GL2_promoter_seq7	ACTGTTAGTAACTCTCTCTTACCCAT	sequencing GL2 promoter	forward primer
GL3pro-FW	CGCGCAATTGaatattaatttataaaatattttgttttt	cloning GL3 promoter (from 3003bp upstream of start codon till start codon)	forward primer. MfeI site. Primers GL3pro-FW + GL3pro-RV2 generate a 3023 bp PCR product from genomic DNA
GL3pro-RV2	ATATGTCGACtgtttcttcatccctatatccc	cloning GL3 promoter (from 3003bp upstream of start codon till start codon)	reverse primer. SalI site
GL3pro-seq1	catagcattgaatctctcacatc	sequencing GL3 promoter	forward primer
GL3pro-seq2	gactatagggagaatcaacgtcg	sequencing GL3 promoter	forward primer
GL3pro-seq3	aggttgttcttcccaaatgagg	sequencing GL3 promoter	forward primer
GL3pro-seq1_RV	gatgtgagagattcaatgctatg	sequencing GL3 promoter	reverse primer
GA3ox1pro-FW	CGCGGAATTCgattaataccaaacgataccattttg	cloning GA3ox1 promoter (from 3088bp upstream of start codon till start codon)	forward primer. EcoRI site. Primers GA3ox1pro-FW + GA3ox1pro-RV1 generate a 3108 bp PCR product from genomic DNA
GA3ox1pro-RV1	CGATCTCGAGcttgctctttttaattagt	cloning GA3ox1 promoter (from 3088bp upstream of	reverse primer. XhoI site

	ttt	start codon till start codon)	
GA3ox1pro-seq1	tcgggagtgattatcatcacac	sequencing GA3ox1 promoter	forward primer
GA3ox1pro-seq2	agacgtattcatatagtttatctc	sequencing GA3ox1 promoter	forward primer
GA3ox1pro-seq3	ctactgttgtgtataataactttc	sequencing GA3ox1 promoter	forward primer
GA3ox1pro-seq1_RV	gtgtgatgataatcactcccga	sequencing GA3ox1 promoter	reverse primer
GA20ox2pro-FW	CATGCAATTGttacgttttgaaaatgtgattccgc	cloning GA20ox2 promoter (from 3063bp upstream of start codon till start codon)	forward primer. MfeI site. Primers GA20ox2pro-FW + GA20ox2pro-RV generate a 3083 bp PCR product from genomic DNA
GA20ox2pro-RV1	ATATCTCGAGttcttttctttttttttcttgagagttttg	cloning GA20ox2 promoter (from 3063bp upstream of start codon till start codon)	reverse primer. XhoI site
GA20ox2pro-seq1	GGGTAAAAGGCAATGGAATCGG	sequencing GA20ox2 promoter	forward primer
GA20ox2pro-seq2	CCTGCCTAGAACACAAGTACTC	sequencing GA20ox2 promoter	forward primer
GA20ox2pro-seq3	TGCGATCCAATAGAAAATCGAC	sequencing GA20ox2 promoter	forward primer
GID1bpro-FW1	CGCGATTTAAATaacaattaatgtgcgaaagttttattc	cloning GID1b promoter (from 3295bp upstream of start codon till start codon)	forward primer. SwaI site. Primers GID1bpro-FW1 + GID1bpro-RV1 generate a 3317 bp PCR product from genomic DNA
GID1bpro-RV1	ATATCTCGAGagtctccaaaacccagcaaaaaa	cloning GID1b promoter (from 3295bp upstream of start codon till start codon)	reverse primer. XhoI site
GID1bpro-seq1	ctaacattataggacctatcttg	sequencing GID1b promoter	forward primer
GID1bpro-seq2	catatgataagtaaagtcgtac	sequencing GID1b promoter	forward primer
GID1bpro-seq3	gctaaagatttagatggaattattg	sequencing GID1b promoter	forward primer
GID1bpro-seq4	CACAAGTTGTATGGGGACAAAA	sequencing GID1b promoter	forward primer
GID1bpro-seq5	AGCCATATTTTCTTCCAAAAG	sequencing GID1b promoter	forward primer
GID1bpro-seq6	TAATAAAACAAACCAAAAACCAAA	sequencing GID1b promoter	forward primer

	A		
GID1bpro-seq1_RV	caagataggtcctataatgttag	sequencing GID1b promoter	reverse primer
GID1bpro-seq7	CGACACAACAAAAGAGTTAATAG	sequencing GID1b promoter	forward primer
GID1bpro-seq8_rv	CATTAGTGCTCCTTTTGACCAC	sequencing GID1b promoter	reverse primer
GID1bpro-seq9_rv	CTCCCCCCCTTTTTCTTTTCTA	sequencing GID1b promoter	reverse primer
pRZ502-seqFW	gccatgtcctacacgccgaaat	sequencing insert in pRZ502	forward primer. 101bp upstream of EcoRI site in pRZ502
pCR8-IDD1_m1_F1	ggtGCTggaGCAggaGCTccttgtagcagcggtggtag	cloning part of IDD1_m1 (from 1249bp to 1497bp). Mutate GLGLGL to GAGAGA in IDD1 coding sequence.	forward primer. Primers pCR8-IDD1_m1_F1 + pCR8-IDD1m_R1 generate a 249 bp PCR product
pCR8-IDD1_m1_R2	AGCtccTGCtccAGCaccaggagctaatgacaatgcatca	cloning part of IDD1_m1 (from 777bp to 1266bp). Mutate GLGLGL to GAGAGA in IDD1 coding sequence.	reverse primer. Primers pCR8-IDD1_m1_R2 + pCR8-IDD1m_F2 generate a 490 bp PCR product
pCR8-IDD1_m2_F1	GCTGCAGCTGCAGCTGCAccttgtagcagcggtggtag	cloning part of IDD1_m2 (from 1249bp to 1497bp). Mutate GLGLGL to AAAAAA in IDD1 coding sequence.	forward primer. Primers pCR8-IDD1_m2_F1 + pCR8-IDD1m_R1 generate a 249 bp PCR product
pCR8-IDD1_m2_R2	TGCAGCTGCAGCTGCAGCaggagctaatgacaatgcatca	cloning part of IDD1_m2 (from 777bp to 1266bp). Mutate GLGLGL to AAAAAA in IDD1 coding sequence.	reverse primer. Primers pCR8-IDD1_m2_R2 + pCR8-IDD1m_F2 generate a 490 bp PCR product
pCR8-IDD1m_R1	acttcttccaatgtcttgcc	cloning IDD1-m1 and IDD1-m2	reverse primer
pCR8-IDD1m_F2	gccgattcagaattctccag	cloning IDD1-m1 and IDD1-m2	forward primer. Primers pCR8-IDD1m_R1 + pCR8-IDD1m_F2 generate a 721 bp PCR product
MGP_CDS_FW	atgacaactgaagatcagacaat	cloning MGP coding sequence from cDNA	forward primer. Primers MGP_CDS_FW + MGP_CDS_RV generate a 1521 bp PCR product
MGP_CDS_RV	tcaaatccatccattgatagagg	cloning MGP coding sequence from cDNA	reverse primer
MGP_CDS_seq1	GTTGCGTCCACCACCATC	sequencing MGP coding sequence	forward primer
MGP_CD	CACCACCAATTC	sequencing MGP coding	forward primer

S_seq2	CCAATCAC	sequence	
MGP_CDS_seq3	CAGATGGGAGCGACTTCTTC	sequencing MGP coding sequence	forward primer
pCR8-IDD1-VP16_R2(VP16-3')	ctacccaccgtactcgtcaattc	cloning VP16 part of IDD1-VP16 from pTA7001.	reverse primer. Primers pCR8-IDD1-VP16_F1 + pCR8-IDD1-VP16_R2 generate a 1755 bp PCR product.
pCR8-IDD1-VP16_F1(IDD1-5')	ATGCCGGTTGATTTAGATAATTCC	cloning IDD1 part of IDD1-VP16 from pCR8-IDD1.	forward primer. Primers pCR8-IDD1-VP16_F1 + pCR8-IDD1-VP16_R1 generate a 1518 bp PCR product.
pCR8-IDD1-VP16_F2	AAAGACATTGGAAGAAGTTCGgcccaccgaccgatgtc	cloning VP16 part of IDD1-VP16 from pTA7001.	forward primer. Primers pCR8-IDD1-VP16_F2 + pCR8-IDD1-VP16_R2 generate a 258 bp PCR product.
pCR8-IDD1-VP16_R1	gacatcggtcggtgggcCGAACTTCTTCCAATGTCTTTG	cloning IDD1 part of IDD1-VP16 from pCR8-IDD1.	reverse primer. Introduce a synonymous mutation (c to a) at 6th bp in VP16 coding sequence.
IDD1-VP16_seq1	TCTTGGAGATCTTACTGGAATCAA	sequencing IDD1-VP16 coding sequence	forward primer
IDD1-VP16_seq2	ATATCTTCCTCTGTTTTGCCGA	sequencing IDD1-VP16 coding sequence	forward primer
IDD1-VP16_seq3	ATCAGGAGGTTCGTTGCTTC	sequencing IDD1-VP16 coding sequence	forward primer
IDD1-VP16_seq4_RV	TGATTGAACAGCATACTTCTTAGAACA	sequencing IDD1-VP16 coding sequence	reverse primer
LBb1.3	ATTTTGCCGATTTCGGAAC	genotyping SALK mutants	forward primer
rga-28 LP	GTTCGATTCTTGCTCAACCAC	genotyping RGA	forward primer. Primers rga-28 LP + rga-28 RP generate a 1062 bp PCR product for wild-type RGA allele.
rga-28 RP	ATGCTCTCTGAGCTTAATCCTC	genotyping RGA and the SALK mutant rga-28	reverse primer. Primers LBb1.3 + rga-28 RP generate a 648 bp PCR product for rga-28.
rga-29 LP	ATGAATGATGATTGAAGTGG	genotyping RGA	forward primer. Primers rga-29 LP + rga-29 RP generate a 870 bp PCR product for wild-type RGA allele.

rga-29 RP	CTAAACGAACACCGTTCTCT	genotyping RGA and the SALK mutant rga-29	reverse primer. Primers LBb1.3 + rga-29 RP generate a ~600 bp PCR product for rga-29.
GAI100-1	CATGAAGAGAGATCATCATCATC	genotyping GAI	forward primer. Primers GAI100-1 + gai-2RP generate a 649 bp PCR product for wild-type GAI allele.
gai-2RP	AGCTTCGGCGAAGTAAGTAGC	genotyping GAI and the SAIL mutant gai-2	reverse primer. Garlic LB3 + gai-2RP
Garlic LB3	TAGCATCTGAATTTCATAACCAATCTCGATACAC	genotyping the SAIL mutant gai-2	forward primer.
GAI 300	CTAGATCCGACATTGAAGGA	genotyping GAI, the Ds insertion mutant gai-t6 and the semi-dominant mutant gai-1	forward primer.
GAI 302	AGCATCAAGATCAGCTAAAG	genotyping GAI	reverse primer. Primers GAI 300 + GAI 302 generate a 1200 bp PCR product for wild-type GAI allele.
gai-t6 304	TCGGTACGGGATTTTCGCAT	genotyping the Ds insertion mutant gai-t6	reverse primer. Primers GAI 300 + gai-t6 304 generate a 600 bp PCR product for gai-t6.
gai-1 303	TCAAGCTGCTCGAGTTTCTG	genotyping GAI and the semi-dominant mutant gai-1	reverse primer. Primers GAI 300 + gai-1 303 generate a 214 bp PCR product for wild-type GAI allele and a 165 bp PCR product for gai-1
idd1-1 LP	CGGCAAAACAGAGGAAGATATG	genotyping IDD1	forward primer. Primers idd1-1 LP + idd1-1 RP generate a 955 bp PCR product for wild-type IDD1 allele.
idd1-1 RP	ATGCCGGTTGATTTAGATAATTC	genotyping IDD1 and the SALK mutant idd1-1	reverse primer. Primers LBb1.3 + idd1-1 RP generate a 645 bp PCR product for idd1-1.
idd1-1 LP-3	TTGACAGACTCAGTCTCAACCGA	alternative primers for genotyping IDD1	forward primer. Primers idd1-1 LP-3 + idd1-1 RP-2 generate a 1005 bp PCR product for wild-type IDD1 allele.
idd1-1 RP-2	ACCCTAGATTGAGCTGAGCTGAG	alternative primers for genotyping IDD1 and the SALK mutant idd1-1	reverse primer. Primers LBb1.3 + idd1-1 RP-2 generate a 740 bp PCR product for idd1-1.
idd2-1 LP	ACTTTTGTCGGAAACATGGTG	genotyping IDD2	forward primer. Primers idd2-1 LP + idd2-1 RP generate a 1224

			bp PCR product for wild-type IDD2 allele.
idd2-1 RP	AGCTCTTTTAAA CCCGAGCTG	genotyping IDD2 and the SALK mutant idd2-1	reverse primer. Primers LBb1.3 + idd2-1 RP generate a 824 bp PCR product for idd2-1.
35S promoter FW	TTCGCAAGACCC TTCC	genotyping the 35S promoter	forward primer. 54bp upstream of the end of 35S promoter
Exp-PT-qFW	TAGAAACGTGG CGCAA	Exp-PT qPCR (cDNA as template)	forward primer. Primers Exp-PT-qFW + Exp-PT-qRV generate a 239 bp PCR product from cDNA, and the same 486 bp PCR product from genomic DNA.
Exp-PT-qRV	TGGTCTGCCTGC CAATA	Exp-PT qPCR (cDNA as template)	reverse primer
GID1b-qFW	GCTGGTGGTAA CGAAG	GID1b qPCR (cDNA as template)	forward primer. Primers GID1b-qFW + GID1b-qRV generate a 247 bp PCR product from cDNA, and a 452 bp PCR product from genomic DNA.
GID1b-qRV	ACGCAGGTTGG TAGAT	GID1b qPCR (cDNA as template)	reverse primer
GA3ox1-qFW	CCATTCACCTCC CACACTCT	GA3ox1 qPCR (cDNA as template)	forward primer. Primers GA3ox1-qFW + GA3ox1-qRV generate a 401 bp PCR product from cDNA, and the same 401 bp PCR product from genomic DNA.
GA3ox1-qRV	GCCAGTGATGG TGAAACCTT	GA3ox1 qPCR (cDNA as template)	reverse primer
GA20ox2-qFW	TCCAACGATAAT AGTGGCT	GA20ox2 qPCR (cDNA as template)	forward primer. Primers GA20ox2-qFW + GA20ox2-qRV generate a 234 bp PCR product from cDNA, and a 377 bp PCR product from genomic DNA.
GA20ox2-qRV	TTGGCATGGAG GATAATGA	GA20ox2 qPCR (cDNA as template)	reverse primer
SCL3-qFW	GAACTGCGCTTT ACGG	SCL3 qPCR (cDNA as template)	forward primer. Primers SCL3-qFW + SCL3-qRV generate a 228 bp PCR product from cDNA, and the same 228 bp PCR product from genomic DNA.
SCL3-qRV	GTGACCACCATG	SCL3 qPCR (cDNA as	reverse primer

	ACCT	template)	
RGA qPCR 254	AGAAGCAATCC AGCAGA	RGA qPCR (cDNA as template)	forward primer. Primers RGA qPCR 254 + RGA qPCR 255 generate a 286 bp PCR product from cDNA, and the same 286 bp PCR product from genomic DNA.
RGA qPCR 255	GTGTACTCTCTT CTTACCTTC	RGA qPCR (cDNA as template)	reverse primer
GAI qPCR 305	CACACGACCGCT CATAG	GAI qPCR (cDNA as template)	forward primer. Primers GAI qPCR 305 + GAI qPCR 306 generate a 250 bp PCR product from cDNA, and the same 250 bp PCR product from genomic DNA.
GAI qPCR 306	TGCCTATCCAAT TTACCCTC	GAI qPCR (cDNA as template)	reverse primer
IDD1-qFW1	TAACTCCTAAAT CCGTCGGG	IDD1 qPCR (cDNA as template)	forward primer. Primers IDD1-qFW1 + IDD1-qRV1 generate a 263 bp PCR product from cDNA, and a 354 bp PCR product from genomic DNA.
IDD1-qRV1	ATGATGAACACA GCCAGA	IDD1 qPCR (cDNA as template)	reverse primer
IDD1-qFW2	TCCGTCATTACC GCCT	alternative primers for IDD1 qPCR (cDNA as template)	forward primer. Primers IDD1-qFW1 + IDD1-qRV1 generate a 323 bp PCR product from cDNA, and a 615 bp PCR product from genomic DNA.
IDD1-qRV2	ACGATGGTGCG AATAG	alternative primers for IDD1 qPCR (cDNA as template)	reverse primer
IDD2-qFW	GGTGGATACTG AGTCTGCT	IDD2 qPCR (cDNA as template)	forward primer. Primers IDD2-qFW + IDD2-qRV generate a 323 bp PCR product from cDNA, and a 689 bp PCR product from genomic DNA.
IDD2-qRV	CGGTTGCTGACA TCGC	IDD2 qPCR (cDNA as template)	reverse primer
rt_fp_IDD 2-1	TGCCTGATCCAG AGTCAGAA	alternative primers for IDD2 qPCR (cDNA as template)	forward primer. Span the junction between Exon 1 and Exon 2. Primers rt_fp_IDD2-1 + rt_rp_IDD2-1 generate a 285 bp PCR product from cDNA, and none from genomic DNA.

rt_rp_IDD2-1	TCTCACCATGTTTCCGACAA	alternative primers for IDD2 qPCR (cDNA as template)	reverse primer
PRE1_qF	CAGCCTCGAAAGTATTGCAAG	PRE1 qPCR (cDNA as template)	forward primer. Primers PRE1_qF + PRE1_qR generate a 135 bp PCR product from cDNA, and the same 135 bp PCR product from genomic DNA.
PRE1_qR	TTCTAATAACGGCGGCTTCAG	PRE1 qPCR (cDNA as template)	reverse primer
PRE1-qFW	GTTCTGATAAGGCATCAGCCTCG	alternative primers for PRE1 qPCR (cDNA as template)	forward primer. Span the junction between Exon 1 and Exon 2. Primers PRE1-qFW + PRE1-qRV generate a 161 bp PCR product from cDNA, and none from genomic DNA.
PRE1-qRV	CATGAGTAGGCTTCTAATAACGG	alternative primers for PRE1 qPCR (cDNA as template)	reverse primer

Appendix B: Plasmids made by Yuanjie Jin

plasmid	vector	insert	description	construction	selection for bacteria*	selection for plants*
pEG203-IDD2	pEG203	IDD2 CDS (AT3G50700.1)	p35S:Myc-IDD2	LR recombination of pENTR/D-IDD2 FL (Zhong-Lin, linearized with PvuI) with pEG203	Kan^{50}	Basta^{10}
pEG201-IDD2	pEG201	IDD2 CDS (AT3G50700.1)	p35S:HA-IDD2	LR recombination of pENTR/D-IDD2 FL (Zhong-Lin, linearized with PvuI) with pEG201	Kan^{50}	Basta^{10}
pRZ502-GA3ox1 promoter	pRZ502 backbone	GA3ox1 promoter	pGA3ox1:fLUC	Amplification of 3088bp GA3ox1 promoter fragment from whole-seedling genomic DNA extract using Phusion High-Fidelity DNA polymerase (New England Biolabs) and primers GA3ox1pro-FW + GA3ox1pro-RV1; cloned into the EcoRI and XhoI sites of pRZ502 backbone; insert was verified to be error-free by sequencing.	Kan^{50}	Basta^{10}
pRZ502-CPC promoter	pRZ502 backbone	CPC promoter	pCPC:fLUC	Amplification of 3159bp CPC promoter fragment from whole-seedling genomic DNA extract using Phusion High-Fidelity DNA polymerase (New England Biolabs) and primers CPCpro-FW + CPCpro-RV2; cloned into the	Kan^{50}	Basta^{10}

				EcoRI and XhoI sites of pRZ502 backbone; insert was verified to be error-free by sequencing.		
pRZ502-GL3 promoter	pRZ502 backbone	GL3 promoter	pGL3:fLUC	Amplification of 3003bp GL3 promoter fragment from whole-seedling genomic DNA extract using Phusion High-Fidelity DNA polymerase (New England Biolabs) and primers GL3pro-FW + GL3pro-RV2; cloned into the EcoRI and XhoI sites of pRZ502 backbone; insert was verified to be error-free by sequencing.	Kan[50]	Basta[10]
pRZ502-GID1b promoter	pRZ502 backbone	GID1b promoter	pGID1b:fLUC	Amplification of 3295bp GID1b promoter fragment from whole-seedling genomic DNA extract using Phusion High-Fidelity DNA polymerase (New England Biolabs) and primers GID1bpro-FW1 + GID1bpro-RV1; cloned into the SwaI and XhoI sites of pRZ502 backbone; insert was verified to be error-free by sequencing.	Kan[50]	Basta[10]
pRZ502-GA20ox2 promoter	pRZ502 backbone	GA20ox2 promoter	pGA20ox2:fLUC	Amplification of 3063bp GA20ox2 promoter fragment from whole-seedling genomic DNA extract using Phusion High-Fidelity DNA polymerase (New England Biolabs) and primers	Kan[50]	Basta[10]

				GA20ox2pro-FW + GA20ox2pro-RV; cloned into the EcoRI and XhoI sites of pRZ502 backbone; insert was verified to be error-free by sequencing.		
pEG201-IDD1	pEG201	IDD1 CDS (AT5G66730.1)	p35S:HA-IDD1	LR recombination of pCR8-IDD1 CDS (Zhong-Lin) with pEG201	Kan^{50}	$Basta^{10}$
pEG203-IDD1	pEG203	IDD1 CDS (AT5G66730.1)	p35S:Myc-IDD1	LR recombination of pCR8-IDD1 CDS (Zhong-Lin) with pEG203	Kan^{50}	$Basta^{10}$
pEG201-IDD1 (1-222)	pEG201	IDD1 1-222aa	p35S:HA-IDD1(1-222aa)	LR recombination of pCR8-IDD1 aa 1-222 (Zhong-Lin) with pEG201	Kan^{50}	$Basta^{10}$
pEG203-IDD1 (1-222)	pEG203	IDD1 1-222aa	p35S:Myc-IDD1(1-222aa)	LR recombination of pCR8-IDD1 aa 1-222 (Zhong-Lin) with pEG203	Kan^{50}	$Basta^{10}$
pRZ502-PRE1 promoter	pRZ502 backbone	PRE1 promoter	pPRE1:fLUC	Amplification of 3458bp PRE1 promoter fragment from whole-seedling genomic DNA extract using Phusion High-Fidelity DNA polymerase (New England Biolabs) and primers PRE1pro-FW + PRE1pro-RV; cloned into the EcoRI and XhoI sites of pRZ502 backbone; insert was verified to be error-free by sequencing.	Kan^{50}	$Basta^{10}$
pRZ502-PRE5 promoter	pRZ502 backbone	PRE5 promoter	pPRE5:fLUC	Amplification of 4834bp PRE5 promoter fragment from whole-seedling genomic DNA extract using Phusion High-Fidelity DNA	Kan^{50}	$Basta^{10}$

				polymerase (New England Biolabs) and primers PRE5pro-FW + PRE5pro-RV; cloned into the EcoRI and XhoI sites of pRZ502 backbone; insert was verified to be error-free by sequencing.		
pCR8-GL2_CDS	pCR8	GL2 CDS (AT1G79840.1)	GL2 CDS ENTRY clone	PCR amplification from cDNA library of whole seedlings, followed by A-tailing and TOPO reaction; used Phusion High-Fidelity DNA polymerase (New England Biolabs) and primers GL2_CDS_FW + GL2_CDS_RV for PCR; insert was checked by sequencing.	$Spec^{100}$	N/A
pDEST22(FLAG tag)-GL2_CDS	pDEST22 (FLAG tag)	GL2 CDS (AT1G79840.1)	GL2 CDS Y2H Prey	LR recombination of pCR8-GL2_CDS with pDEST22 (FLAG tag) (Jianhong)	Amp^{100} ($Carb^{100}$)	N/A
pRZ502-GL2 promoter (RV1)	pRZ502 backbone	GL2 promoter	pGL2(RV1):fLUC	Amplification of 3584bp GL2 promoter fragment (including a short ORF in 5' UTR) from whole-seedling genomic DNA extract using Phusion High-Fidelity DNA polymerase (New England Biolabs) and primers GL2_promoter_FW + GL2_promoter_RV1; cloned into the SwaI and XhoI sites of pRZ502 backbone; insert was	Kan^{50}	$Basta^{10}$

				verified to be error-free by sequencing.		
pRZ502-GL2 promoter (RV2)	pRZ502 backbone	GL3 promoter	pGL2(RV2):LUC	Amplification of 3549bp GL2 promoter fragment (excluding a short ORF in 5' UTR) from whole-seedling genomic DNA extract using Phusion High-Fidelity DNA polymerase (New England Biolabs) and primers GL2_promoter_FW + GL2_promoter_RV2; cloned into the SwaI and XhoI sites of pRZ502 backbone; insert was verified to be error-free by sequencing.	Kan[50]	Basta[10]
pCR8-IDD1_CDS	pCR8	IDD1 CDS (AT5G66730.1)	IDD1 CDS ENTRY clone	by Zhong-Lin Zhang	Spec[100]	N/A
pCR8-MGP_CDS	pCR8	MGP CDS (AT1G03840.1)	MGP CDS ENTRY clone	PCR amplification from cDNA library of whole seedlings, followed by A-tailing and TOPO reaction; used Phusion High-Fidelity DNA polymerase (New England Biolabs) and primers MGP_CDS_FW + MGP_CDS_RV for PCR; insert was checked by sequencing.	Spec[100]	N/A
pCR8-IDD1-m	pCR8	IDD1 CDS with 417-422aa mutated to AAAAAA	IDD1-m CDS ENTRY clone	Using primer pairs pCR8-IDD1_m2_F1 + pCR8-IDD1m_R1 and pCR8-IDD1_m2_R2 + pCR8-IDD1m_F2, amplify two	Spec[100]	N/A

				separate DNA fragments of IDD1 coding sequence that contain the desired mutations (GLGLGL -> AAAAAA) as overlapping regions at the beginning and end of its sequence, respectively. The two purified primary PCR products are combined and used as template, together with pCR8-IDD1m_R1 + pCR8-IDD1m_F2 as primers, to create an integrate piece by PCR, which is then cloned into HindIII-SacI site in pCR8-IDD1_CDS. The introduced mutations are confirmed by sequencing.		
pCR8-IDD1-VP16	pCR8	IDD1 CDS (-STOP) + VP16	IDD1-VP16 CDS ENTRY clone	Amplify IDD1 coding sequence (without stop codon) with part of VP16 beginning sequence attached to the end, using primers pCR8-IDD1-VP16_F1 + pCR8-IDD1-VP16_R1 and template pCR8-IDD1_CDS. Amplify VP16 coding sequence (with stop codon) with part of IDD1 ending sequence attached to its beginning, using primers pCR8-IDD1-VP16_F2 + pCR8-IDD1-VP16_R2 and template	$Spec^{100}$	N/A

				pTA7001. The two purified primary PCR products are combined and used as template, together with pCR8-IDD1-VP16_F1 + pCR8-IDD1-VP16_R2 as primers, to create a fused piece IDD1-VP16 by PCR, which is then purified and TA-cloned into pCR8. The insert is verified to be error-free by sequencing.		
pEG203-MGP	pEG203	MGP CDS (AT1G03840.1)	p35S:Myc-MGP	LR recombination of pCR8-MGP_CDS with pEG203	Kan^{50}	$Basta^{10}$
pEG203-IDD1-m	pEG203	IDD1 CDS with 417-422aa mutated to AAAAAA	p35S:Myc-IDD1-m	LR recombination of pCR8-IDD1-m with pEG203	Kan^{50}	$Basta^{10}$
pEG203-IDD1-VP16	pEG203	IDD1 CDS (-STOP) + VP16	p35S:Myc-IDD1-VP16	LR recombination of pCR8-IDD1-VP16 with pEG203	Kan^{50}	$Basta^{10}$
pDEST22(FLAG tag)-MGP	pDEST22 (FLAG tag)	MGP CDS (AT1G03840.1)	MGP CDS Y2H Prey	LR recombination of pCR8-MGP_CDS with pDEST22(FLAG tag)	Amp^{100} ($Carb^{100}$)	N/A
pDEST32(HA tag)-MGP	pDEST32 (HA tag)	MGP CDS (AT1G03840.1)	MGP CDS Y2H Bait	LR recombination of pCR8-MGP_CDS with pDEST32(HA tag)	Gm^{40}	N/A
pDONR207-RG52	pDONR207	RGA 186-587aa CDS	RG52 CDS ENTRY clone	BP recombination of pDEST22-RG52 with pDONR207	Gm^{40}	N/A

*Kan: kanamycin; Spec: spectinomycin; Amp: ampicillin; Carb: carbenicillin; Gm: gentamicin; Basta: glufosinate-ammonium. The superscript that follows indicates the concentration of each compound, in μg/ml, used for selection on plates.

References

Achard, P., Baghour, M., Chapple, A., Hedden, P., Van Der Straeten, D., Genschik, P., Moritz, T., and Harberd, N.P. (2007a). The plant stress hormone ethylene controls floral transition via DELLA-dependent regulation of floral meristem-identity genes. Proc Natl Acad Sci U S A *104*, 6484-6489.

Achard, P., Gong, F., Cheminant, S., Alioua, M., Hedden, P., and Genschik, P. (2008). The cold-inducible CBF1 factor-dependent signaling pathway modulates the accumulation of the growth-repressing DELLA proteins via its effect on gibberellin metabolism. Plant Cell *20*, 2117-2129.

Achard, P., Liao, L., Jiang, C., Desnos, T., Bartlett, J., Fu, X., and Harberd, N.P. (2007b). DELLAs contribute to plant photomorphogenesis. Plant Physiol *143*, 1163-1172.

Alabadi, D., Gil, J., Blazquez, M.A., and Garcia-Martinez, J.L. (2004). Gibberellins repress photomorphogenesis in darkness. Plant Physiol *134*, 1050-1057.

An, F., Zhang, X., Zhu, Z., Ji, Y., He, W., Jiang, Z., Li, M., and Guo, H. (2012). Coordinated regulation of apical hook development by gibberellins and ethylene in etiolated Arabidopsis seedlings. Cell Research *22*, 915-927.

Aoyama, T., and Chua, N.-H. (1997). A glucocorticoid-mediated transcriptional induction system in transgenic plants. Plant Journal *11*, 605-612.

Arnaud, N., Girin, T., Sorefan, K., Fuentes, S., Wood, T.A., Lawrenson, T., Sablowski, R., and Ostergaard, L. (2010). Gibberellins control fruit patterning in Arabidopsis thaliana. Genes & Development *24*, 2127-2132.

Bai, M.Y., Fan, M., Oh, E., and Wang, Z.Y. (2012a). A triple helix-loop-helix/basic helix-loop-helix cascade controls cell elongation downstream of multiple hormonal and environmental signaling pathways in Arabidopsis. Plant Cell *24*, 4917-4929.

Bai, M.Y., Shang, J.X., Oh, E., Fan, M., Bai, Y., Zentella, R., Sun, T.P., and Wang, Z.Y. (2012b). Brassinosteroid, gibberellin and phytochrome impinge on a common transcription module in Arabidopsis. Nat Cell Biol.

Bailey, T.L., Boden, M., Buske, F.A., Frith, M., Grant, C.E., Clementi, L., Ren, J., Li, W.W., and Noble, W.S. (2009). MEME SUITE: tools for motif discovery and searching. Nucleic Acids Res *37*, W202-208.

Berger, F., Linstead, P., Dolan, L., and Haseloff, J. (1998). Stomata patterning on the hypocotyl of Arabidopsis thaliana is controlled by genes involved in the control of root epidermis patterning. Dev Biol *194*, 226-234.

Bernhardt, C., Lee, M.M., Gonzalez, A., Zhang, F., Lloyd, A., and Schiefelbein, J. (2003). The bHLH genes GLABRA3 (GL3) and ENHANCER OF GLABRA3 (EGL3) specify epidermal cell fate in the Arabidopsis root. Development *130*, 6431-6439.

Bernhardt, C., Zhao, M.Z., Gonzalez, A., Lloyd, A., and Schiefelbein, J. (2005). The bHLH genes GL3 and EGL3 participate in an intercellular regulatory circuit that controls cell patterning in the Arabidopsis root epidermis. Development *132*, 291-298.

Blazquez, M.A., Green, R., Nilsson, O., Sussman, M.R., and Weigel, D. (1998). Gibberellins promote flowering of Arabidopsis by activating the *LEAFY* promoter. Plant Cell *10*, 791-800.

Bolle, C. (2004). The role of GRAS proteins in plant signal transduction and development. Planta *218*, 683-692.

Broothaerts, W., Mitchell, H.J., Weir, B., Kaines, S., Smith, L.M., Yang, W., Mayer, J.E., Roa-Rodriguez, C., and Jefferson, R.A. (2005). Gene transfer to plants by diverse species of bacteria. Nature *433*, 629-633.

Cao, D., Cheng, H., Wu, W., Meng Soo, H., and Peng, J. (2006). Gibberellin mobilizes distinct DELLA-dependent transcriptomes to regulate seed germination and floral development in Arabidopsis. Plant Physiol *142*, 509-525.

Cheng, H., Qin, L., Lee, S., Fu, X., Richards, D.E., Cao, D., Luo, D., Harberd, N.P., and Peng, J. (2004). Gibberellin regulates Arabidopsis floral development via suppression of DELLA protein function. Development *131*, 1055-1064.

Chien, J.C., and Sussex, I.M. (1996). Differential regulation of trichome formation on the adaxial and abaxial leaf surfaces by gibberellins and photoperiod in *Arabidopsis thaliana* (L.) Heynh. Plant Physiol *111*, 1321-1328.

Clough, S.J., and Bent, A.F. (1998). Floral dip: a simplified method for *Agrobacterium*-mediated transformation of *Arabidopsis thaliana*. Plant Journal *16*, 735-743.

Colasanti, J., Yuan, Z., and Sundaresan, V. (1998). The indeterminate gene encodes a zinc finger protein and regulates a leaf-generated signal required for the transition to flowering in maize. Cell *93*, 593-603.

Conway, G. (1997). The doubly green revolution: Food for all in the twenty-first century. (Ithaca, Cornell University Press).

Cowling, R.J., and Harberd, N.P. (1999). Gibberellins control Arabidopsis hypocotyl growth via regulation of cellular elongation. Journal of Experimental Botany *50*, 1351-1357.

Cui, D., Zhao, J., Jing, Y., Fan, M., Liu, J., Wang, Z., Xin, W., and Hu, Y. (2013). The arabidopsis IDD14, IDD15, and IDD16 cooperatively regulate lateral organ morphogenesis and gravitropism by promoting auxin biosynthesis and transport. PLoS Genet *9*, e1003759.

Czechowski, T., Stitt, M., Altmann, T., Udvardi, M.K., and Scheible, W.R. (2005). Genome-wide identification and testing of superior reference genes for transcript normalization in Arabidopsis. Plant Physiol *139*, 5-17.

Daviere, J.-M., and Achard, P. (2013). Gibberellin signaling in plants. Development *140*, 1147-1151.

Davies, P.J., ed. (2004). Plant Hormones: Biosynthesis, Signal Transduction, Action! (Dordrecht, The Netherlands, Kluwer Academic Publishers).

de Lucas, M., Daviere, J.M., Rodriguez-Falcon, M., Pontin, M., Iglesias-Pedraz, J.M., Lorrain, S., Fankhauser, C., Blazquez, M.A., Titarenko, E., and Prat, S. (2008). A molecular framework for light and gibberellin control of cell elongation. Nature *451*, 480-484.

Dill, A., Jung, H.-S., and Sun, T.-p. (2001). The DELLA motif is essential for gibberellin-induced degradation of RGA. Proc Natl Acad Sci U S A *98*, 14162-14167.

Dill, A., and Sun, T.-p. (2001). Synergistic de-repression of gibberellin signaling by removing RGA and GAI function in *Arabidopsis thaliana*. Genetics *159*, 777-785.

Dill, A., Thomas, S.G., Hu, J., Steber, C.M., and Sun, T.-p. (2004). The Arabidopsis F-box protein SLEEPY1 targets GA signaling repressors for GA-induced degradation. Plant Cell *16*, 1392-1405.

Duckett, C.M., Grierson, C., Linstead, P., Schneider, K., Lawson, E., Dean, C., Poethig, S., and Roberts, K. (1994). Clonal relationships and cell patterning in the root epidermis of Arabidopsis. Development *120*, 2465-2474.

Earley, K.W., Haag, J.R., Pontes, O., Opper, K., Juehne, T., Song, K.M., and Pikaard, C.S. (2006). Gateway-compatible vectors for plant functional genomics and proteomics. Plant Journal *45*, 616-629.

Feng, S., Martinez, C., Gusmaroli, G., Wang, Y., Zhou, J., Wang, F., Chen, L., Yu, L., Iglesias-Pedraz, J.M., Kircher, S., *et al.* (2008). Coordinated regulation of *Arabidopsis thaliana* development by light and gibberellins. Nature *451*, 475-479.

Feurtado, J.A., Huang, D., Wicki-Stordeur, L., Hemstock, L.E., Potentier, M.S., Tsang, E.W.T., and Cutler, A.J. (2011). The Arabidopsis C2H2 Zinc Finger INDETERMINATE DOMAIN1/ENHYDROUS Promotes the Transition to Germination by Regulating Light and Hormonal Signaling during Seed Maturation. Plant Cell *23*, 1772-1794.

Fleet, C.M., and Sun, T.P. (2005). A DELLAcate balance: the role of gibberellin in plant morphogenesis. Current Opinion in Plant Biology *8*, 77-85.

Fu, X., Richards, D.E., Fleck, B., Xie, D., Burton, N., and Harberd, N.P. (2004). The Arabidopsis mutant sleepy1$^{gar2\text{-}1}$ protein promotes plant growth by increasing the affinity of the SCF^{SLY1} E3 ubiquitin ligase for DELLA protein substrates. Plant Cell *16*, 1406-1418.

Fukazawa, J., Teramura, H., Murakoshi, S., Nasuno, K., Nishida, N., Ito, T., Yoshida, M., Kamiya, Y., Yamaguchi, S., and Takahashi, Y. (2014). DELLAs function as coactivators of GAI-ASSOCIATED FACTOR1 in regulation of gibberellin homeostasis and signaling in Arabidopsis. Plant Cell *26*, 2920-2938.

Gallego-Bartolome, J., Alabadi, D., and Blazquez, M.A. (2011). DELLA-Induced Early Transcriptional Changes during Etiolated Development in Arabidopsis thaliana. Plos One *6*.

Gallego-Bartolome, J., Minguet, E.G., Grau-Enguix, F., Abbas, M., Locascio, A., Thomas, S.G., Alabadi, D., and Blazquez, M.A. (2012). Molecular mechanism for the interaction between gibberellin and brassinosteroid signaling pathways in Arabidopsis. Proceedings of the National Academy of Sciences of the United States of America *109*, 13446-13451.

Gallego-Bartolome, J., Minguet, E.G., Marin, J.A., Prat, S., Blazquez, M.A., and Alabadi, D. (2010). Transcriptional Diversification and Functional Conservation between DELLA Proteins in Arabidopsis. Molecular Biology and Evolution *27*, 1247-1256.

Galway, M.E., Masucci, J.D., Lloyd, A.M., Walbot, V., Davis, R.W., and Schiefelbein, J.W. (1994). THE TTG GENE IS REQUIRED TO SPECIFY EPIDERMAL-CELL FATE AND CELL PATTERNING IN THE ARABIDOPSIS ROOT. Dev Biol *166*, 740-754.

Gendreau, E., Traas, J., Desnos, T., Grandjean, O., Caboche, M., and Hofte, H. (1997). Cellular basis of hypocotyl growth in Arabidopsis thaliana. Plant Physiology *114*, 295-305.

Griffiths, J., Murase, K., Rieu, I., Zentella, R., Zhang, Z.L., Powers, S.J., Gong, F., Phillips, A.L., Hedden, P., Sun, T.-p., *et al.* (2006). Genetic Characterization and Functional Analysis of the GID1 Gibberellin Receptors in Arabidopsis. Plant Cell *18*, 3399-3414.

Hassan, H., Scheres, B., and Blilou, I. (2010). JACKDAW controls epidermal patterning in the Arabidopsis root meristem through a non-cell-autonomous mechanism. Development *137*, 1523-1529.

Hauvermale, A.L., Ariizumi, T., and Steber, C.M. (2012). Gibberellin signaling: a theme and variations on DELLA repression. Plant Physiol *160*, 83-92.

Hedden, P. (2003). The genes of the Green Revolution. Trends in Genetics *19*, 5-9.

Hedden, P., and Phillips, A.L. (2000). Gibberellin metabolism: new insights revealed by the genes. Trends Plant Sci *5*, 523-530.

Hedden, P., and Thomas, S.G. (2012). Gibberellin biosynthesis and its regulation. Biochem J *444*, 11-25.

Heo, J.-O., Chang, K.S., Kim, I.A., Lee, M.-H., Lee, S.A., Song, S.-K., Lee, M.M., and Lim, J. (2010). Funneling of gibberellin signaling by the GRAS transcription factor SCARECROW-LIKE 3 in the Arabidopsis root. submitted.

Hiratsu, K., Mitsuda, N., Matsui, K., and Ohme-Takagi, M. (2004). Identification of the minimal repression domain of SUPERMAN shows that the DLELRL hexapeptide is both necessary and sufficient for repression of transcription in Arabidopsis. Biochemical and Biophysical Research Communications *321*, 172-178.

Hou, X., Hu, W.-W., Shen, L., Lee, L.Y.C., Tao, Z., Han, J.-H., and Yu, H. (2008). Global identification of DELLA target genes during Arabidopsis flower development. Plant Physiology *147*, 1126-1142.

Hou, X., Lee, L.Y.C., Xia, K., Yen, Y., and Yu, H. (2010). DELLAs Modulate Jasmonate Signaling via Competitive Binding to JAZs. Developmental Cell *19*, 884-894.

Ikeda, M., Fujiwara, S., Mitsuda, N., and Ohme-Takagi, M. (2012). A triantagonistic basic helix-loop-helix system regulates cell elongation in Arabidopsis. Plant Cell *24*, 4483-4497.

Ikeda, M., Mitsuda, N., and Ohme-Takagi, M. (2009). Arabidopsis WUSCHEL Is a Bifunctional Transcription Factor That Acts as a Repressor in Stem Cell Regulation and as an Activator in Floral Patterning. Plant Cell *21*, 3493-3505.

Josse, E.M., Gan, Y.B., Bou-Torrent, J., Stewart, K.L., Gilday, A.D., Jeffree, C.E., Vaistij, F.E., Martinez-Garcia, J.F., Nagy, F., Graham, I.A., *et al.* (2011). A DELLA in Disguise: SPATULA Restrains the Growth of the Developing Arabidopsis Seedling. Plant Cell *23*, 1337-1351.

King, K., Moritz, T., and Harberd, N. (2001). Gibberellins are not required for normal stem growth in *Arabidopsis thaliana* in the absence of GAI and RGA. Genetics *159*, 767-776.

Koornneef, M., Elgersma, A., Hanhart, C.J., van Loenen, M.E.P., van Rijn, L., and Zeevaart, J.A.D. (1985). A gibberellin insensitive mutant of *Arabidopsis thaliana*. Physiologia Plantarum *65*, 33-39.

Koornneef, M., and van der Veen, J.H. (1980). Induction and analysis of gibberellin-sensitive mutants in *Arabidopsis thaliana* (L.) Heynh. Theor Applied Genetics *58*, 257-263.

Koshino-Kimura, Y., Wada, T., Tachibana, T., Tsugeki, R., Ishiguro, S., and Okada, K. (2005). Regulation of CAPRICE transcription by MYB proteins for root epidermis differentiation in Arabidopsis. Plant Cell Physiol *46*, 817-826.

Kozaki, A., Hake, S., and Colasanti, J. (2004). The maize ID1 flowering time regulator is a zinc finger protein with novel DNA binding properties. Nucleic Acids Research *32*, 1710-1720.

Kurata, T., Ishida, T., Kawabata-Awai, C., Noguchi, M., Hattori, S., Sano, R., Nagasaka, R., Tominaga, R., Koshino-Kimura, Y., Kato, T., *et al.* (2005). Cell-to-cell movement of the CAPRICE protein in Arabidopsis root epidermal cell differentiation. Development *132*, 5387-5398.

Lee, S., Cheng, H., King, K.E., Wang, W., He, Y., Hussain, A., Lo, J., Harberd, N.P., and Peng, J. (2002). Gibberellin regulates Arabidopsis seed germination via *RGL2*, a *GAI*/*RGA*-like gene whose expression is up-regulated following imbibition. Genes & Development *16*, 646-658.

Lee, S., Lee, S., Yang, K.-Y., Kim, Y.-M., Park, S.-Y., Kim, S.Y., and Soh, M.-S. (2006). Overexpression of PRE1 and its homologous genes activates gibberellin-dependent responses in Arabidopsis thaliana. Plant and Cell Physiology *47*, 591-600.

Leivar, P., Monte, E., Oka, Y., Liu, T., Carle, C., Castillon, A., Huq, E., and Quail, P.H. (2008). Multiple Phytochrome-Interacting bHLH Transcription Factors Repress Premature Seedling Photomorphogenesis in Darkness. Current Biology *18*, 1815-1823.

Leivar, P., and Quail, P.H. (2011). PIFs: pivotal components in a cellular signaling hub. Trends in Plant Science *16*, 19-28.

Li, Q.-F., Wang, C., Jiang, L., Li, S., Sun, S.S.M., and He, J.-X. (2012). An Interaction Between BZR1 and DELLAs Mediates Direct Signaling Crosstalk Between Brassinosteroids and Gibberellins in Arabidopsis. Science Signaling *5*.

Libault, M., Brechenmacher, L., Cheng, J.L., Xu, D., and Stacey, G. (2010). Root hair systems biology. Trends in Plant Science *15*, 641-650.

Masucci, J.D., Rerie, W.G., Foreman, D.R., Zhang, M., Galway, M.E., Marks, M.D., and Schiefelbein, J.W. (1996). The homeobox gene GLABRA2 is required for position-dependent cell differentiation in the root epidermis of Arabidopsis thaliana. Development *122*, 1253-1260.

Matsubara, K., Yamanouchi, U., Wang, Z.X., Minobe, Y., Izawa, T., and Yano, M. (2008). Ehd2, a rice ortholog of the maize INDETERMINATE1 gene, promotes flowering by up-regulating Ehd1. Plant Physiol *148*, 1425-1435.

McGinnis, K.M., Thomas, S.G., Soule, J.D., Strader, L.C., Zale, J.M., Sun, T.-p., and Steber, C.M. (2003). The Arabidopsis *SLEEPY1* gene encodes a putative F-box subunit of an SCF E3 ubiquitin ligase. Plant Cell *15*, 1120-1130.

Mitsuda, N., Takiguchi, Y., Shikata, M., Sage-Ono, K., Ono, M., Sasaki, K., Yamaguchi, H., Narumi, T., Tanaka, Y., Sugiyama, M., *et al.* (2011). The new FioreDB database provides comprehensive information on plant transcription factors and phenotypes induced by CRES-T in ornamental and model plants. Plant Biotechnology *28*, 123-130.

Morita, M.T., Sakaguchi, K., Kiyose, S.-i., Taira, K., Kato, T., Nakamura, M., and Tasaka, M. (2006). A C2H2-type zinc finger protein, SGR5, is involved in early events of gravitropism in Arabidopsis inflorescence stems. Plant Journal *47*, 619-628.

Murase, K., Hirano, Y., Sun, T.-p., and Hakoshima, T. (2008). Gibberellin-induced DELLA recognition by the gibberellin receptor GID1. Nature *456*, 459-463.

Nakagawa, T., Kurose, T., Hino, T., Tanaka, K., Kawamukai, M., Niwa, Y., Toyooka, K., Matsuoka, K., Jinbo, T., and Kimura, T. (2007). Development of series of gateway binary vectors, pGWBs, for realizing efficient construction of fusion genes for plant transformation. Journal of Bioscience and Bioengineering *104*, 34-41.

Nakajima, M., Shimada, A., Takashi, Y., Kim, Y.C., Park, S.H., Ueguchi-Tanaka, M., Suzuki, H., Katoh, E., Iuchi, S., Kobayashi, M., *et al.* (2006). Identification and characterization of Arabidopsis gibberellin receptors. Plant J *46*, 880-889.

Oh, E., Yamaguchi, S., Hu, J., Yusuke, J., Jung, B., Paik, I., Lee, H.-S., Sun, T.-p., Kamiya, Y., and Choi, G. (2007). PIL5, a phytochrome-interacting bHLH protein, regulates gibberellin responsiveness by binding directly to the *GAI* and *RGA* promoters in Arabidopsis seeds. Plant Cell *19*, 1192-1208.

Oh, E., Zhu, J.-Y., Bai, M.-Y., Arenhart, R.A., Sun, Y., and Wang, Z.-Y. (2014). Cell elongation is regulated through a central circuit of interacting transcription factors in the Arabidopsis hypocotyl. Elife *3*.

Oh, E., Zhu, J.Y., and Wang, Z.Y. (2012). Interaction between BZR1 and PIF4 integrates brassinosteroid and environmental responses. Nat Cell Biol.

Olszewski, N., Sun, T.-p., and Gubler, F. (2002). Gibberellin signaling:biosynthesis, catabolism, and response pathways. Plant Cell *14*, S61-S80.

Park, J., Khoa Thi, N., Park, E., Jeon, J.-S., and Choi, G. (2013). DELLA Proteins and Their Interacting RING Finger Proteins Repress Gibberellin Responses by Binding to the Promoters of a Subset of Gibberellin-Responsive Genes in Arabidopsis. Plant Cell *25*, 927-943.

Park, S.J., Kim, S.L., Lee, S., Je, B.I., Piao, H.L., Park, S.H., Kim, C.M., Ryu, C.H., Xuan, Y.H., Colasanti, J., *et al.* (2008). Rice Indeterminate 1 (OsId1) is necessary for the expression of Ehd1 (Early heading date 1) regardless of photoperiod. Plant J *56*, 1018-1029.

Penfield, S., Gilday, A.D., Halliday, K.J., and Graham, I.A. (2006). DELLA-mediated cotyledon expansion breaks coat-imposed seed dormancy. Current Biology *16*, 2366-2370.

Peng, J., Carol, P., Richards, D.E., King, K.E., Cowling, R.J., Murphy, G.P., and Harberd, N.P. (1997). The Arabidopsis *GAI* gene defines a signalling pathway that negatively regulates gibberellin responses. Genes Dev *11*, 3194-3205.

Peng, J., Richards, D.E., Hartley, N.M., Murphy, G.P., Devos, K.M., Flintham, J.E., Beales, J., Fish, L.J., Worland, A.J., Pelica, F., *et al.* (1999). 'Green Revolution' genes encode mutant gibberellin response modulators. Nature *400*, 256-261.

Perazza, D., Vachon, G., and Herzog, M. (1998). Gibberellins promote trichome formation by up-regulating GLABROUS1 in Arabidopsis. Plant Physiology *117*, 375-383.

Plackett, A.R., Ferguson, A.C., Powers, S.J., Wanchoo-Kohli, A., Phillips, A.L., Wilson, Z.A., Hedden, P., and Thomas, S.G. (2014). DELLA activity is required for successful pollen development in the Columbia ecotype of Arabidopsis. New Phytol *201*, 825-836.

Pysh, L.D., Wysocka-Diller, J.W., Camilleri, C., Bouchez, D., and Benfey, P.N. (1999). The GRAS gene family in Arabidopsis: sequence characterization and basic expression analysis of the *SCARECROW-LIKE* genes. Plant Journal *18*, 111-119.

Qi, T., Huang, H., Wu, D., Yan, J., Qi, Y., Song, S., and Xie, D. (2014). Arabidopsis DELLA and JAZ Proteins Bind the WD-Repeat/bHLH/MYB Complex to Modulate Gibberellin and Jasmonate Signaling Synergy. Plant Cell *26*, 1118-1133.

Rademacher, W. (2000). GROWTH RETARDANTS: Effects on Gibberellin Biosynthesis and Other Metabolic Pathways. Annu Rev Plant Physiol Plant Mol Biol *51*, 501-531.

Reid, J.B., Botwright, N.A., Smith, J.J., O'Neill, D.P., and Kerckhoffs, L.H.J. (2002). Control of gibberellin levels and gene expresion during de-etiolation in pea. Plant Physiology *128*, 734-741.

Ryu, K.H., Kang, Y.H., Park, Y.H., Hwang, I., Schiefelbein, J., and Lee, M.M. (2005). The WEREWOLF MYB protein directly regulates CAPRICE transcription during cell fate specification in the Arabidopsis root epidermis. Development *132*, 4765-4775.

Saibo, N.J., Vriezen, W.H., Beemster, G.T.S., and Van Der Straeten, D. (2003). Growth and stomata development of Arabidopsis hypocotyls are controlled by gibberellins and modulated by ethylene and auxins. Plant Journal *33*, 989-1000.

Sarnowska, E.A., Rolicka, A.T., Bucior, E., Cwiek, P., Tohge, T., Fernie, A.R., Jikumaru, Y., Kamiya, Y., Franzen, R., Schmelzer, E., *et al.* (2013). DELLA-Interacting SWI3C Core Subunit of Switch/Sucrose Nonfermenting Chromatin Remodeling Complex Modulates Gibberellin Responses and Hormonal Cross Talk in Arabidopsis. Plant Physiology *163*, 305-317.

Sasaki, A., Itoh, H., Gomi, K., Ueguchi-Tanaka, M., Ishiyama, K., Kobayashi, M., Jeong, D.-H., An, G., Kitano, J., Ashikari, M., *et al.* (2003). Accumulation of phosphorylated repressor for gibberellin signaling in an F-box mutant. Science *299*, 1896-1898.

Schiefelbein, J. (2003). Cell-fate specification in the epidermis: a common patterning mechanism in the root and shoot. Curr Opin Plant Biol *6*, 74-78.

Seo, P.J., Kim, M.J., Ryu, J.Y., Jeong, E.Y., and Park, C.M. (2011a). Two splice variants of the IDD14 transcription factor competitively form nonfunctional heterodimers which may regulate starch metabolism. Nat Commun *2*, 303.

Seo, P.J., Ryu, J., Kang, S.K., and Park, C.-M. (2011b). Modulation of sugar metabolism by an INDETERMINATE DOMAIN transcription factor contributes to photoperiodic flowering in Arabidopsis. Plant Journal *65*, 418-429.

Shimada, A., Ueguchi-Tanaka, M., Nakatsu, T., Nakajima, M., Naoe, Y., Ohmiya, H., Kato, H., and Matsuoka, M. (2008). Structural basis for gibberellin recognition by its receptor GID1. Nature *456*, 520-523.

Silverstone, A.L., Ciampaglio, C.N., and Sun, T.-p. (1998). The Arabidopsis *RGA* gene encodes a transcriptional regulator repressing the gibberellin signal transduction pathway. Plant Cell *10*, 155-169.

Silverstone, A.L., Jung, H.-S., Dill, A., Kawaide, H., Kamiya, Y., and Sun, T.-p. (2001). Repressing a repressor: gibberellin-induced rapid reduction of the RGA protein in Arabidopsis. Plant Cell *13*, 1555-1566.

Silverstone, A.L., and Sun, T.-p. (2000). Gibberellins and the green revolution. Trends in Plant Science *5*, 1-2.

Sun, T.-p. (2008). Gibberellin Metabolism, Perception and Signaling Pathways in Arabidopsis. In The Arabidopsis Book, R. Last, C. Chang, G. Jander, D. Kliebenstein, R. McClung, H. Millar, K. Torii, and D. Wagner, eds. (Rockville, MD, American Society of Plant Biologists), p. doi: 10.1199/tab.0103.

Sun, T.-p., Goodman, H.M., and Ausubel, F.M. (1992). Cloning the Arabidopsis *GA1* locus by genomic subtraction. Plant Cell *4*, 119-128.

Sun, T.P. (2010). Gibberellin-GID1-DELLA: a pivotal regulatory module for plant growth and development. Plant Physiol *154*, 567-570.

Triezenberg, S.J., Kingsbury, R.C., and McKnight, S.L. (1988). Functional dissection of VP16, the trans-activator of herpes simplex virus immediate early gene expression. Genes Dev *2*, 718-729.

Tyler, L., Thomas, S.G., Hu, J., Dill, A., Alonso, J.M., Ecker, J.R., and Sun, T.-p. (2004). DELLA proteins and gibberellin-regulated seed germination and floral development in Arabidopsis. Plant Physiol *135*, 1008-1019.

Ueguchi-Tanaka, M., Ashikari, M., Nakajima, M., Itoh, H., Katoh, E., Kobayashi, M., Chow, T.Y., Hsing, Y.I., Kitano, H., Yamaguchi, I., *et al.* (2005). *GIBBERELLIN INSENSITIVE DWARF1* encodes a soluble receptor for gibberellin. Nature *437*, 693-698.

Ueguchi-Tanaka, M., Nakajima, M., Katoh, E., Ohmiya, H., Asano, K., Saji, S., Hongyu, X., Ashikari, M., Kitano, H., Yamaguchi, I., *et al.* (2007). Molecular interactions of a soluble gibberellin receptor, GID1, with a rice DELLA protein, SLR1, and gibberellin. Plant Cell *19*, 2140-2155.

Vandenbussche, F., Verbelen, J.P., and Van der Straeten, D. (2005). Of light and length: regulation of hypocotyl growth in Arabidopsis. Bioessays *27*, 275-284.

Wada, T., Kurata, T., Tominaga, R., Koshino-Kimura, Y., Tachibana, T., Goto, K., Marks, M.D., Shimura, Y., and Okada, K. (2002). Role of a positive regulator of root hair development, CAPRICE, in Arabidopsis root epidermal cell differentiation. Development *129*, 5409-5419.

Wang, S., and Chen, J.G. (2008). Arabidopsis transient expression analysis reveals that activation of GLABRA2 may require concurrent binding of GLABRA1 and GLABRA3 to the promoter of GLABRA2. Plant Cell Physiol *49*, 1792-1804.

Welch, D., Hassan, H., Blilou, I., Immink, R., Heidstra, R., and Scheres, B. (2007). Arabidopsis JACKDAW and MAGPIE zinc finger proteins delimit asymmetric cell

division and stabilize tissue boundaries by restricting SHORT-ROOT action. Genes & Development *21*, 2196-2204.

Wild, M., Daviere, J.-M., Cheminant, S., Regnault, T., Baumberger, N., Heintz, D., Baltz, R., Genschik, P., and Achard, P. (2012). The Arabidopsis DELLA RGA-LIKE3 Is a Direct Target of MYC2 and Modulates Jasmonate Signaling Responses. Plant Cell *24*, 3307-3319.

Willige, B.C., Ghosh, S., Nill, C., Zourelidou, M., Dohmann, E.M.N., Maier, A., and Schwechheimer, C. (2007). The DELLA domain of GA INSENSITIVE mediates the interaction with the GA INSENSITIVE DWARF1A gibberellin receptor of Arabidopsis Plant Cell *19*, 1209-1220.

Wilson, R.N., Heckman, J.W., and Somerville, C.R. (1992). Gibberellin is required for flowering in *Arabidopsis thaliana* under short days. Plant Physiology *100*, 403-408.

Wong, A.Y.M., and Colasanti, J. (2007). Maize floral regulator protein INDETERMINATE1 is localized to developing leaves and is not altered by light or the sink/source transition. Journal of Experimental Botany *58*, 403-414.

Wu, C., You, C., Li, C., Long, T., Chen, G., Byrne, M.E., and Zhang, Q. (2008). RID1, encoding a Cys2/His2-type zinc finger transcription factor, acts as a master switch from vegetative to floral development in rice. Proc Natl Acad Sci U S A *105*, 12915-12920.

Wu, H.Y., Liu, K.H., Wang, Y.C., Wu, J.F., Chiu, W.L., Chen, C.Y., Wu, S.H., Sheen, J., and Lai, E.M. (2014). AGROBEST: an efficient Agrobacterium-mediated transient expression method for versatile gene function analyses in Arabidopsis seedlings. Plant Methods *10*.

Wu, X., Tang, D., Li, M., Wang, K., and Cheng, Z. (2013). Loose Plant Architecture1, an INDETERMINATE DOMAIN protein involved in shoot gravitropism, regulates plant architecture in rice. Plant Physiol *161*, 317-329.

Xu, H., Liu, Q., Yao, T., and Fu, X. (2014). Shedding light on integrative GA signaling. Curr Opin Plant Biol *21C*, 89-95.

Xuan, Y.H., Priatama, R.A., Huang, J., Je, B.I., Liu, J.M., Park, S.J., Piao, H.L., Son, D.Y., Lee, J.J., Park, S.H., *et al.* (2013). Indeterminate domain 10 regulates ammonium-mediated gene expression in rice roots. New Phytologist *197*, 791-804.

Yabuta, T., and Sumiki, Y. (1938). On the crystal of gibberellin, a substance to promote plant growth. J Agric Chem Soc Japan *14*, 1526.

Yamaguchi, S. (2008). Gibberellin metabolism and its regulation. Annu Rev Plant Biol *59*, 225-251.

Yang, D.-L., Yao, J., Mei, C.-S., Tong, X.-H., Zeng, L.-J., Li, Q., Xiao, L.-T., Sun, T.-p., Li, J., Deng, X.-W., *et al.* (2012). Plant hormone jasmonate prioritizes defense over growth by interfering with gibberellin signaling cascade. Proceedings of the National Academy of Sciences of the United States of America *109*, E1192-E1200.

Yoshida, H., Hirano, K., Sato, T., Mitsuda, N., Nomoto, M., Maeo, K., Koketsu, E., Mitani, R., Kawamura, M., Ishiguro, S., *et al.* (2014). DELLA protein functions as a transcriptional activator through the DNA binding of the INDETERMINATE DOMAIN family proteins. Proceedings of the National Academy of Sciences of the United States of America *111*, 7861-7866.

Yu, S., Galvao, V.C., Zhang, Y.-C., Horrer, D., Zhang, T.-Q., Hao, Y.-H., Feng, Y.-Q., Wang, S., Schmid, M., and Wang, J.-W. (2012). Gibberellin Regulates the Arabidopsis Floral Transition through miR156-Targeted SQUAMOSA PROMOTER BINDING-LIKE Transcription Factors. Plant Cell *24*, 3320-3332.

Zentella, R., Zhang, Z.L., Park, M., Thomas, S.G., Endo, A., Murase, K., Fleet, C.M., Jikumaru, Y., Nambara, E., Kamiya, Y., *et al.* (2007). Global analysis of DELLA direct targets in early gibberellin signaling in Arabidopsis. Plant Cell *19*, 3037-3057.

Zhang, F., Gonzalez, A., Zhao, M.Z., Payne, C.T., and Lloyd, A. (2003). A network of redundant bHLH proteins functions in all TTG1-dependent pathways of Arabidopsis. Development *130*, 4859-4869.

Zhang, Z.-L., Ogawa, M., Fleet, C.M., Zentella, R., Hu, J., Heo, J.-O., Lim, J., Kamiya, Y., Yamaguchi, S., and Sun, T.-p. (2011). SCARECROW-LIKE 3 promotes gibberellin signaling by antagonizing master growth repressor DELLA in Arabidopsis. Proceedings of the National Academy of Sciences of the United States of America *108*, 2160-2165.

Zhao, X.Y., Yu, X.H., Liu, X.M., and Lin, C.T. (2007). Light regulation of gibberellins metabolism in seedling development. J Integr Plant Biol *49*, 21-27.

Biography

Yuanjie Jin

Education:

2011-current: Graduate Research Assistant in Laboratory of Tai-Ping Sun, Ph.D

Department of Biology, Duke University

2009-2010: Graduate Research Assistant in Laboratory of Steve Haase, Ph.D

Department of Biology, Duke University

2008-current: Doctoral Program in Department of Biology, Duke University

2004-2008: Bachelors of Science (Biological Sciences), Fudan University